1000-MWe LMFBR ACCIDENT ANALYSIS AND SAFETY SYSTEM DESIGN STUDY

— Topical Report —

Accident Analysis Methods

by

J. H. Scott
M. G. Stevenson
R. W. Moore

Approved by: <u>M. W. Croft</u>
Project Manager

November 1970

DISCLAIMER

This report was prepared as an account of work sponsored by an agency of the United States Government. Neither the United States Government nor any agency Thereof, nor any of their employees, makes any warranty, express or implied, or assumes any legal liability or responsibility for the accuracy, completeness, or usefulness of any information, apparatus, product, or process disclosed, or represents that its use would not infringe privately owned rights. Reference herein to any specific commercial product, process, or service by trade name, trademark, manufacturer, or otherwise does not necessarily constitute or imply its endorsement, recommendation, or favoring by the United States Government or any agency thereof. The views and opinions of authors expressed herein do not necessarily state or reflect those of the United States Government or any agency thereof.

DISCLAIMER

Portions of this document may be illegible in electronic image products. Images are produced from the best available original document.

This report was originally prepared as a technical note to document the work performed in a specific contract activity as soon as the work was completed. The technical editing was limited in order to meet the objective of timely reporting. The report was issued for USAEC-ANL use only, and the intent was to update and consolidate the information from all technical notes in a comprehensive phase report before final publication for public distribution at the end of Phase II.

This plan was changed when the contract was terminated in October 1970 for the convenience of the government. Instead, a final summary report will be prepared, and the previously issued technical notes will be published as formal topical reports. In accordance with the modified plan, this technical note is being published in its original form without further editing or modification except for minor technical corrections and changes in the title and date of issue. Even without updating and technical editing, the report provides detailed information that should be helpful in evaluating and resolving LMFBR safety questions in related areas.

M. W. Croft
Lynchburg, Virginia
November 15, 1970

CONTENTS

List of Tables

List of Figures

1. INTRODUCTION

The Accident Analysis and Safety System Design Study will be conducted primarily to develop a better understanding of the influence of safety requirements on large LMFBR designs. To achieve this objective B&W will (1) analyze the accidents that determine the design bases for certain protective systems and safety features, and (2) perform conceptual designs for these protective systems and engineered safety features. The reference design[1] of B&W's 1000-MWe Follow-On Study will form the basis for this study. The work will be performed under ANL contract 31-109-38-2339. A summary flow chart for this work is included in Table 1 for convenience.

The success of any safety analysis depends to a great extent on the methods used in executing the analysis. This is particularly true in the analysis of fast reactor systems since there is relatively little operating experience or experimental data by which to bench-mark analyses. Therefore, it is necessary to select methods carefully and to exercise considerable care in their use.

The methods proposed for use in this study are discussed briefly in the related work plan, which is presented in report BAW-1339. This report expands the description of methods proposed in BAW-1339 and presents the rationale involved in selecting those methods.

A number of the methods specified in the work plan are used extensively in the nuclear industry today, but some are not in general use. Methods in the latter category are largely codes or models that have been developed or extensively modified at B&W. Since these methods are not widely used, they are described in some detail in the appendix. They include the following codes:

1. TART — a reactor transient analysis code.[2]
2. FIRE — a sodium fire code.
3. BANGO — a one-dimensional hydrodynamics code.

4. CLOUD — a dose calculation code for continuous release to the atmosphere.[3]

5. FARED — an all-purpose fast reactor design system code.[4]

6. DEFLECT — a bowing code, modified ELBOW.[5]

The better known codes are discussed in less detail at appropriate points in the text.

There are a number of areas in which our current understanding of phenomena and analytical modeling is inadequate for reliable application to safety analyses. These areas are discussed in a separate section devoted to analytical problems.

The technical approach to be followed in executing the Accident Analysis and Safety System Design Study is outlined in detail in BAW-1339; it may be necessary to repeat some of these descriptions in order to present a clear idea of the methods requirements and techniques of solution.

Table 1. Accident Analysis and Safety Design Study, Activity Flow Diagram
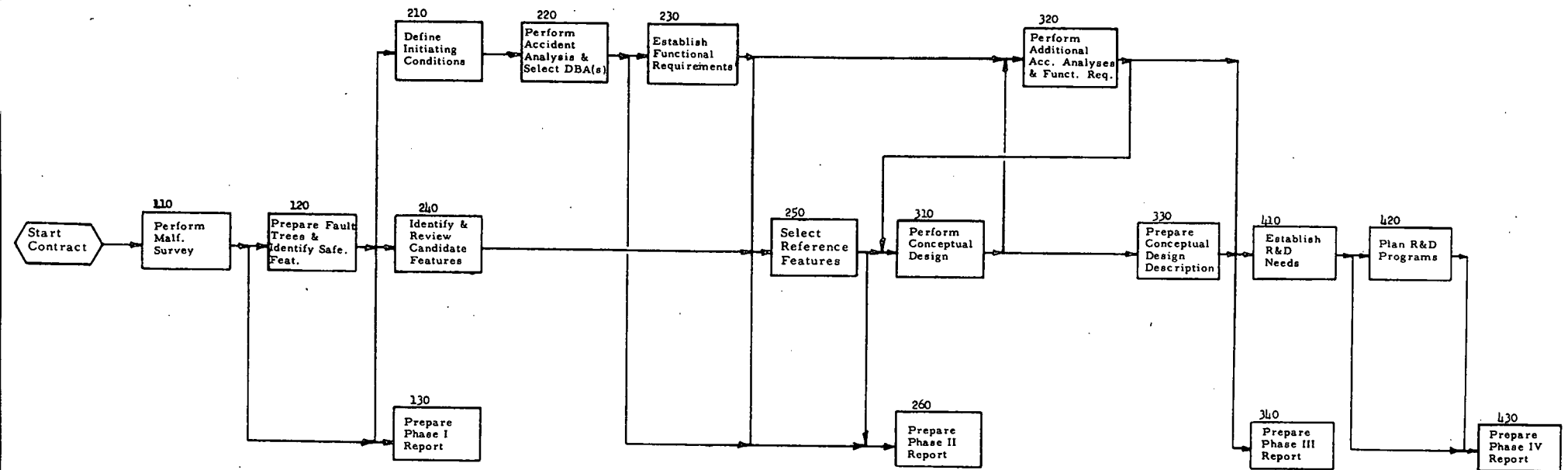
2. SUMMARY

This report describes the methods and models that will be used in the Accident Analysis and Safety System Design Study (AASSDS). In most cases the rationale for methods selection is given; in other cases, only a single model seemed adequate for a particular application, and this is stated in the text. Insofar as possible, the way that selected methods will be applied to the analysis is indicated.

In addition, significant problem areas in fast reactor safety are discussed along with their importance to accident analyses. In some cases, prospective solutions are discussed. The appendix provides detailed descriptions of the computer programs that will be used in the accident analyses but are not widely known in the nuclear industry.

For convenience in describing the methods proposed for use in the study, this report is organized according to major analytical activity; i.e., initiating conditions, accident analyses, and functional requirements. The types of calculations to be performed and the methods proposed for use are discussed in section 3 and outlined as follows:

Initiating Conditions

Effect of malfunctions arising within
the primary loop:

TART

SAS1A[6]

Analog[7]

Effect of malfunctions arising within
the secondary loop:

TART

SAS1A

Analog

Malfunctions affecting neutronic characteristics:

> SCRAM[8]
>
> FARED[9]
>
> 2DB-PERT IV[10]
>
> TART
>
> SAS1A
>
> DEFLECT

Accident Analyses

To fuel failure:

> TART
>
> SAS1A

Fuel failure to core compaction:

> MELT-1[11]

Nuclear disassembly:

> MARS/SAS
>
> VENUS[12]

Sodium fuel interaction:

> BANGO
>
> Thermodynamic calculation by hand

Hydrodynamics:

> BANG[13]

Functional Requirements

Fission product concentration:

> RIBD[14]
>
> BURP[15]

Environmental analysis:

> CLOUD (Direct dose and inhalation)

Sodium fire:

> FIRE

In addition to the foregoing methods, several standard engineering programs will be used to supplement or supply initial input to the safety analysis codes. These methods will include but not be limited to the following:

1. TIGER V.[16]
2. ARGUS.[17]
3. B&W flow analysis systems.
4. B&W stress analysis systems.

Several rather conspicuous gaps in the current safety methodology pose significant difficulties in the proposed safety analysis. The problem areas are discussed in detail in section 4 along with some prospective solutions. The problems to be considered are:

1. Fuel failure propagation.
2. Sodium fuel interaction.
3. Sodium boiling and superheat phenomena.

3. DESCRIPTION OF CALCULATIONS AND METHODS

3.1. General

The types of calculations to be performed in the AASSDS and the methods proposed for performing them are discussed in this section. The major accidents, or initiating events, within each analytical activity are described briefly along with the important variables to be determined. The prospective methods available for use are then identified, and their application to the analyses is discussed. Finally, the rationale involved in selecting the proposed methods is indicated along with a discussion of their major limitations and capabilities. Methods will be selected on the basis of currently available information; as more sophisticated and accurate methods or models become available, they will be included in the study if applicable. The division of information in this section is along the lines of the major analytical activities described in the work plan; i.e., initiating conditions, accident analyses, and functional requirements.

Perhaps the rather arbitrary split between initiating conditions and accident analysis should be mentioned. Most of the accident analysis codes, SAS1A, FORE-II,[18] etc., are not capable of directly computing the effects of malfunctions in the primary and intermediate systems. For example, the loss of flow, loss of heat sink and the like must be calculated separately and then input to the accident code in the form of changes in flow or inlet temperature.

TART, which includes a model for the primary system, is not so limited, since it can directly compute the changes in flow and core inlet temperature in addition to the transient that may result from these damages. Thus, there is no clear distinction between the analysis of initiating conditions and the resultant transient since the same method is used for both.

The work scope of the contract specifies an activity to develop initiating conditions and another to analyze accidents and to select the DBA(s). We therefore need to establish a criterion for categorizing analyses. The proposed criterion is that the analysis of transients resulting directly from a malfunction, e.g., the transient that follows the flow reduction resulting from a primary pump failure, are to be classed as initiating conditions. Other examples might be rod ejection, the introduction of gas bubbles, loss of access to heat sink, etc. If fuel failure criteria are exceeded or voiding begins during a transient, then the transient becomes an accident. Any further analysis would therefore be performed in the accident analysis activity. In effect, the initiating condition activity will serve to eliminate transients that need not be considered among the accidents that might lead to the DBA(s).

It should be strongly emphasized that it is both impossible and undesirable to definitively set forth the methods that will be used over the entire three-year duration of the study. Methods development in the fast breeder reactor industry is progressing rapidly, and better methods and models will continue to be developed. As such methods become available, they will be reviewed for application to the AASSDS. To some extent, then, the analytical schemes presented in this report are contingent and will be subject to revision depending on future developments in analytical methods.

3.2. Initiating Conditions

Several broad categories of initiating conditions will be investigated as described in the work plan. The major categories include abnormal changes in the primary coolant, abnormal changes in the secondary coolant, and abnormal changes in the neutronics characteristics.

3.2.1. Primary Coolant System Malfunctions

In the first category—malfunctions involving abnormalities in the behavior of the primary coolant—several broad groups of initiating conditions are important:

1. Failure of pumps.
2. Failure of couplings.
3. Failure of piping.

4. Flow blockage.

5. High flow at startup.

6. Entrained gas bubble.

In order to predict the effect of these initiating conditions on the core, several important parameters must be calculated. The minimum parameters to be calculated for any of the foregoing accidents are as follows:

1. Flow history.

2. Coolant inlet temperature history.

3. Time-dependent cladding temperature distributions.

4. Time-dependent fuel temperature distributions.

5. Time-dependent coolant temperature distributions.

The foregoing information will allow an assessment of the conditions imposed on the core by abnormalities in the primary loop and will provide initial conditions for the accident analysis. Sensitivity studies will be performed to determine how major parameters affect an event, such as pump inertia, effective mixing volumes, etc.

3.2.1.1. Methods

A number of methods are available for use in the area of primary loop malfunctions. Among those considered are FORE-II, SAS1A, TART, and the analog hybrid model. Any of these methods can be used to determine certain of the critical conditions impressed on the core by primary loop malfunctions. However, none of the methods by themselves can be used to determine all of the pertinent variables. In executing this portion of the study, TART, SAS1A, and the analog model will be used.

TART was selected for use in this segment of the analysis for several reasons:

1. It contains a primary loop model that allows direct calculation of the flow transients in the systems.

2. The primary loop model with its variable flow capability is directly coupled to the core thermal solutions.

3. The multichannel capability of TART allows a relatively accurate definition of the transient temperature distributions in core components and a more accurate determination of reactivity feedback.

However, a number of limitations in the TART program could lead to significant uncertainties in the result. For instance, the core outlet plenum, IHXs, and core inlet plenum are each represented by a single node in the thermal solutions. This representation is adequate for most of the transients possible in an integral pot system where transients tend to be slow and time constants long; however, it presents some difficulties in evaluating the degree of effective mixing. Mixing can be treated approximately by defining an equivalent perfect mixing volume for various conditions of channeling and imposing these volumes on the primary loop model.

Most of the faults in this category will affect the core through a reactivity perturbation. In order to determine the magnitude of these effects accurately, several parameters must be calculated. These include but are not necessarily limited to the following:

1. Reactivity worths of various core materials.
2. Irradiation history of components.
3. Thermal stress-strain relationships, both long term and transients, in various components.
4. Rates of deformation or deflection, where possible.

This information can be used to perform Δk calculations to determine rates of reactivity increase, which could be used as a driving function for the accident analyses.

Obviously, large uncertainties exist in many of the areas directly pertaining to this work, and many of the calculations are difficult. Analyses of this nature ordinarily require a rather detailed investigation over a reasonable range of parameters. In accidents of this type, sensitivity studies are likely to be very important. Such studies will be performed in conjunction with the calculations described above. In particular, the effects of temperature-dependent deflection-deformation rates will be investigated.

3.2.2.   Secondary Coolant Loop Malfunctions

In the second category—initiating conditions involving abnormalities in the secondary loop—a number of initiating events are possible, including partial malfunction of one IHX and loss of access to one or more IHXs.   Obviously, each of these events will produce much the same effect in the primary loop; however, care must be taken in analyzing these events because the time scales may be very different.

The consequences of secondary system malfunctions will be coupled to the primary systems principally through thermal effects; hence, it is important to be able to predict accurately the temperature historys of the various core components.   The minimum variables to be calculated are as follows:

1. Time-dependent coolant temperature distributions.

2. Time-dependent cladding temperature distributions.

3. Time-dependent fuel temperature distributions.

Again, sensitivity studies will be performed for important variables influencing the course of an event.   Among such variables are secondary flow rates and temperature rises and the degree of stratification or channeling in the "pot" and inlet plenum.

3.2.2.1.   Methods

There are fewer methods for investigating the influence of malfunctions in the secondary system because this problem tends to be strongly reactor specific.   Basically, one needs a method of describing the events in the secondary loop, coupling these to the primary loop and predicting the core response to the primary loop perturbations.

The analog model, along with the TART program, will be used to couple the secondary loop malfunctions to the primary loop.   Each of these models has relative advantages and disadvantages:

1. Both models have only a one-node representation of each IHX.

2. TART is capable of describing the time dependence of secondary coolant temperature or flows, but the analog can only treat steps or ramps in heat transferred through the tube wall. However, this capability is probably only of academic value in this study since it is currently planned to study only instantaneous loss of access to the heat sink. Preliminary calculations have indicated that, although this is the worst mode of failure, the transient developed is very slow and allows considerable time for protective action. If these preliminary results are verified, then less-severe transients will not be analyzed.

3. The analog model allows partial loss of heat transfer capability in any number of IHXs, but TART only allows complete loss of any integral number of IHXs.

Both methods will probably be used in this segment of the analysis. The response of the core to the thermal transients in the primary loop will be studied using SAS1A and TART. The TART program has the advantage of being able to treat the program integrally; that is, without external calculation of temperature transients. The multichannel capability of TART tends to be less important in these accidents. SAS1A, however, is capable of describing in some detail the important temperature response of the peak or average fuel pin and the relatively important (for this case) expansion feedbacks.

3.2.2.2. Application to Analyses

In this segment of the analyses, the TART program and the analog model will be used to simulate varying degrees of loss of access to the secondary loop. Fractional losses of an IHX will be investigated with the analog model by stepping the heat transfer to the secondary loop to the equivalent fraction. TART will be used for the loss of integral numbers of IHXs. In this way the results can be checked continuously. The thermal transients induced by a partial or a complete loss of access to the heat sink will be used as input to SAS1A. The SAS1A program will determine the response of the peak and/or average pins to the coolant temperature transients and the magnitude of the expansion feedback. The multichannel distribution will be determined from TART.

3.2.3. Malfunctions Affecting Core Neutronics Characteristics

The malfunctions that can affect the neutronic characteristics of the core include several thermal- and radiation-induced effects and several malfunctions of a statistical nature. Included among such events are:

1. Thermal bowing of components.
2. Swelling and restructuring of fuel.
3. Axial relocation of fuel.
4. Malfunction of control rod drives.
5. Unexpected change in control rod composition due to irradiation.
6. Changes in reactivity coefficients.

3.2.3.1. Methods

A number of excellent one- and two-dimensional static physics codes are available for determining the reactivity feedback coefficients and power and worth distributions, all of which are important in this portion of the analysis. Included among these codes are SIZZLE, FARED, 2DB, OPERT, PERT IV, and SCRAM. The programs available for dynamic analysis in this segment of the study are TART, SAS1A, and the analog hybrid model along with FORE-II.

In order to study incidents arising from fuel deformation, one needs some knowledge of the stresses in fuel and cladding and of the irradiation history of the components being studied. Fewer methods are available in this area because they are, for practical purposes, limited to the FUELDYN module of SAS1A and DEFLECT, a B&W modification of the GGA bowing code ELBOW.

The one-dimensional static physics calculations will be performed with FARED, a versatile fast reactor design code having criticality, depletion, fuel management, and first-order perturbation capabilities. FARED contains the REGA microscopic cross-section generation program, which includes both resolved and unresolved resonance treatment. FARED was chosen for the one-dimensional static physics calculations because it is specifically designed to perform rapid and accurate fast breeder reactor physics studies. It contains, in one

state-of-the-art package, all of the one-dimensional static physics methods that will be needed during the Accident Analysis and Safety System Design Study.

The two-dimensional static physics calculations will be performed with 2DB-PERT IV. 2DB is a diffusion theory code designed specifically for fast reactor analysis. PERT IV is a first-order perturbation theory code designed for use with 2DB. Early in the study the SCRAM program will probably be used extensively until the 2DB-PERT IV system has been thoroughly "debugged." 2 DB and PERT IV were chosen for the two-dimensional physics calculations because they constitute a rapid diffusion-depletion-perturbation code package designed solely for fast reactor analysis. In addition, 2DB has a hexagonal geometry option.

The dynamic segments of the analysis will be performed using TART and SAS1A for the reasons discussed earlier. SAS1A and DEFLECT will be used to determine the mechanics of states that could lead to deformation or bowing. Strain rates, on the fuel pin level, will be calculated with SAS1A, and DEFLECT will be used to determine fuel assembly bowing. SAS1A represents the current state of the art in fuel pin mechanics, and DEFLECT is one of the very few codes that adequately consider thermal, irradiation-induced, and creep-induced deflection in fuel assemblies.

3. 2. 3. 2. Application to Analyses

To perform the types of calculations indicated in 3. 2. 3, several parameters are needed. The FARED criticality calculations will provide flux, adjoint, and power distributions for the safety studies. Doppler, sodium density, and expansion reactivity feedback coefficients will be obtained from direct Δk criticality calculations. The perturbation edits will be used to obtain distributed self-worths or danger coefficients, distributed isotopic worths, including sodium, and distributed Doppler coefficients. The applicability of first-order perturbation theory will be verified with direct Δk criticality calculations. The depletion and fuel management capabilities of FARED will be utilized to determine fission concentrations during life. The 2DB program will be used for criticality and depletion calculations, and to determine flux, adjoint,

and power distributions. PERT IV will be used to obtain neutron generation times and effective delayed neutron fractions.

SAS1A and TART will be used to determine the dynamic response of the core to the various malfunctions to be treated in this portion of the analysis. The power histories and temperature distribution histories will be evaluated. One of the most difficult problems with these analyses will be the determination of rates, such as deformation or bow, relocation of fuel, and the like; determination of these rates will probably require a large parametric effort, since no methods of definitively treating them are available at this time. The magnitude of deflections will be determined from the stress-strain relationships from SAS1A and the DEFLECT code.

3.3. Accident Analysis

Once the initiating conditions for accident analysis have been defined, the analyses may be extended to determine the course of an accident. In the following discussion of proposed accident analysis methods, five major areas of investigation are defined, largely on the basis that separate, distinct treatments are required in each area. For the most part this requires the transfer of an analysis from one program to another at certain points during the investigation. The SAS1A program is a conspicuous exception because it is capable of integrally treating the accident through nuclear disassembly. The six categories that are discussed here are as follows:

1. Fuel failure criteria.
2. Transient analysis to fuel failure.
3. Fuel failure through core compaction.
4. Nuclear disassembly.
5. Sodium-fuel interaction.
6. Hydrodynamic response of the primary system.

Accidents may be terminated, of course, at nearly any level, but accidents that are terminated below fuel failure thresholds need not be considered further in these studies.

There are a number of calculations that cannot be performed now with an acceptable degree of reliability. Such calculations are mentioned

briefly in the following text; appropriate but detailed discussion is deferred until section 4.

3.3.1. Fuel Failure Mechanisms

The fuel pin failure mechanisms to be considered in failure analyses are fission gas and/or fuel vapor, and cladding melting. The mechanism of fuel expansion due to the change in density on melting is not considered to be operative for fuel pins having the smeared fuel density of the reference design. The mechanism of fuel thermal expansion may or may not be considered depending on forthcoming cladding ductility data.

3.3.1.1. Models and Applications

For the mechanisms to be considered, the initial or pretransient fuel pin conditions will be determined from the TAMPA computer program. This program will be used for initial thermal conditions and for the determination of fuel pin cross-sectional geometries. Transient temperature calculations can be made with the ARGS1 (modified ARGUS) computer program. Fuel vapor pressures will be considered as a function of maximum fuel temperatures only. Of course these calculated maximum fuel temperatures will vary with the extent of axial fuel movement. Simplified models for axial fuel movement will have to be formulated. This axial fuel movement will also have some influence on the calculated effects of the fission gas release mechanism. A simple computer program may have to be written to convert ARGS1 results to fuel pin pressures for both the fission gas and the fuel vapor failure mechanisms. The fuel pin pressures are easily converted to cladding hoop stresses; to properly account for cladding stresses and temperatures as functions of time (for determinations of failure points), a simple model of cladding creep behavior may be required. It is felt, however, that a sophisticated cladding mechanics model is not warranted at this time since material properties are inadequate.

As additional cladding ductility data become available, we will consider the fuel thermal expansion mechanisms for total elongation values of less than 2.0%. Proper treatment of this mechanism will require a simple modeling of the elastic and plastic deformation phenomena of the fuel in order to determine the values of effective

fuel thermal expansion. Such a model would undoubtedly be valuable in the previously mentioned model for axial fuel movement. Where applicable, the fuel mechanics model in SAS1A will be used.

3.3.2. Transient Analysis to Fuel Failure

The course of a transient arising from any of the initiating conditions defined in activity 211 will be analyzed to determine the consequences for the core, primary loop, and engineered safety features. In particular, the conditions of the coolant and fuel will be closely monitored during the course of the transient. The power history, the reactivity history, and the transient temperature distributions in the various core components will be recorded; incipient failure states will be determined and identified. In some cases, it will have to be decided at the failure point whether to switch to a compaction code, disassembly code, or hydrodynamic code. This decision will be based on the rate of reactivity insertion, condition of coolant, fraction of molten and/or vaporized fuel, and other parameters. Sensitivity studies will be performed for the more important parameters.

3.3.2.1. Methods

As long as the fuel remains intact, a number of methods may be used to calculate the course of the transient; most of these methods are standard and include FORE-II, AIROS-IIA,[19] and TART. The SAS1A program includes this segment of the analysis as part of the complete calculation. The multichannel capability and one-dimensional option in TART make it more desirable than FORE-II or AIROS-IIA in a large majority of cases, although the latter has good multichannel representation. SAS1A, however, is capable of extending the calculation into the disassembly phase when appropriate. For these reasons, TART and SAS1A will probably form the nucleus for analysis of accidents of this nature; however, FORE-II may be used as a benchmark early in the study since it can be operated with a high degree of confidence.

3.3.2.2. Application to Analyses

As in the analyses for initiating conditions, an attempt will be made to operate TART and SAS1A in a complementary manner. In this particular instance, SAS1A becomes very important to

the analysis since it is probably the most reliable method available for defining fuel failure states. The SAS program will monitor the fuel conditions and indicate the time and mode of fuel failure; it will also be used to determine coolant behavior and the inception of coolant boiling. Accurate definition of fuel failure and coolant boiling phenomona is central to these analyses since the best way to continue the calculations (coolant-fuel interaction, fuel slumping, disassembly, etc.) must be decided at fuel failure. This decision will depend largely on the conditions of the fuel and coolant at the time of failure. TART will be used to investigate the multichannel effects and the influence of noncoherence in the accident sequence. In some cases the one-dimensional option in TART may play a crucial role in describing spatial effects.

3.3.3. Fuel Failure Through Core Compaction

Once the integrity of the fuel has been lost, a number of events become possible; for example, core compaction or slumping of molten fuel. Major unknowns in this area are the amount of fuel that fails and the manner in which local failures become general. It is generally felt that rapid propagation of melting or failure is necessary to cause core compaction. Unfortunately, the phenomenon of fuel motion is poorly understood, especially in the case of oxide fuels. In any event, under certain circumstances we cannot absolutely preclude the possibility of compaction of the core into a more reactive configuration. Therefore, the following must be determined:

1. Direction and rate of fuel motion.
2. Reactivity history as a consequence of item 1.
3. Extent to which fuel collapse aggravates the transient that initiated collapse.
4. Degree of coherence in the slump or dispersal.

None of these problems can be treated in a completely deterministic manner at this time. However, it is generally believed that only in the case of relatively slow reactivity insertions, $\partial \rho / \partial t < \approx 10$ \$/s, will the time span of the accident be slow enough to allow appreciable contribution from fuel slumping.[20]

3.3.3.1. Methods

Owing to the rudimentary understanding of the fuel motion phenomenon, there are essentially no good methods of describing the events. However, there are at least two computer programs that address themselves to the problem of core compaction: MELT-1 and PREAX. MELT-1 has several rather severe limitations:

1. The motion is assumed to be gravity controlled.

2. There are no fuel mechanics considerations, so that available void volume and stress-strain relationships are essentially ignored.

3. The heat transfer treatment is inadequate.

An advanced version of this program, MELT-2, is in the programming stage and is expected to correct many of the definciencies of MELT-1.

PREAX is an ANL code written as a segment of the AX program. The documentation is sparse, and the program has not been available to B&W.

3.3.3.2. Application to Analyses

In cases where core compaction is a possible consequence of fuel failure, MELT-1 will be used to determine the influence of the collapse on the further course of the accident. Some care must be exercised to ensure that a degree of realism is preserved. In the absence of better methods, the studies performed with MELT-1 will require extensive parametric evaluation. The MELT program will be used to determine rates of reactivity insertion at the disassembly threshold for use in weak explosion programs. It is hoped that an advanced method of treating compaction will be available soon for use in the Accident Analysis and Safety System Design Study.

3.3.4. Nuclear Disassembly

For accidents involving gross melting, the resultant compaction of the core into a denser configuration can produce large, rapid increases in reactivity. This effect may be compounded by gross, rapid expulsion of the sodium coolant; however, coolant expulsion does not require compaction as an initiating condition but may produce large reactivity insertions independently. These reactivity increases can result

in a prompt critical excursion which is terminated by motion of the core components. In general, such displacements of core materials are produced by high pressures generated in the fuel during the power burst. Since accidents such as these have potentially high efficiencies for conversion of thermal energy to work, some account of them must be taken in the safety analyses. It is unusually difficult to define a credible accident path that leads to nuclear disassembly, but the potential consequences of such an accident cannot be dismissed. Therefore extreme caution must be exercised in analyses of this type to ensure that the calculations are pertinent. It is perhaps easier to go astray in this type of analysis than in any other.

Ideally, with a knowledge of the temperature-pressure-energy-density relationship and the history of the power burst, a coupled neutronic hydrodynamic calculation could be performed to determine the behavior of the core in the disassembly phase. In reality, the problem is so complex that one is forced to rely on certain semianalytic techniques of analysis such as that developed by Bethe and Tait.[22-24] The usual result of such a calculation is the energy yield of the power burst; further assumptions are necessary to determine the fraction available for work on the environment.

3.3.4.1. Methods

Since the problem of nuclear disassembly is of historic interest in the analysis of fast breeder reactors, there is a wide variety of methods from which to choose. These methods have various degrees of sophistication, but in general the majority in use now belong to the Bethe-Tait or the modified Bethe-Tait classification. Included among these programs are WEAK EXPLOSIONS,[25] MARS,[26] MAX,[27] and the weak explosions module of SAS1A, which is basically a modification of MARS. A more sophisticated program, VENUS, is being developed at ANL and includes a complete hydrodynamics treatment in La Grangian space.

It is anticipated that MARS, SAS1A, and perhaps VENUS will form the nucleus of these calculations. WEAK EXPLOSIONS and MAX have a major limitation in being one dimensional, although they are well suited to survey calculations. The MARS program

and the disassembly module of SAS1A are two dimensional with a perturbation treatment of the neutronics. The SAS module is capable of accounting for the effect of density changes near zone interfaces during a power burst; this is potentially important in certain circumstances. Both programs are fairly rapid and convenient to use.

3.3.4.2. Application to Analyses

In the event that a combination of failures or malfunctions that lead to nuclear disassembly can be identified, the MARS or SAS1A programs will be used to determine the energy yield of the destructive burst. The rate of reactivity insertion at the threshold of disassembly will be determined from TART, SAS1A, MELT-1 or MELT-2 as appropriate. SAS1A has a distinct advantage in accidents involving large reactivity insertion rates (accidents in which fuel slump is relatively unimportant) because it is capable of integrally treating an accident from its inception to final termination by disassembly. Because large uncertainties exist in many of the parameters, such as equations of state and nuclear properties, these studies will probably be subject to extensive sensitivity studies. Various core conditions at the onset of disassembly will be considered. If VENUS were to become available, it would be valuable in extending the analysis to include hydrodynamic response of the various core segments.

3.3.5. Sodium-Fuel Interaction

Once an accident reaches the point where the cladding is breached, a number of phenomena become possible. One of these is the core compaction-nuclear disassembly process, which has been discussed earlier. Another process that may occur if quantities of hot molten fuel are ejected into the coolant channel is the sodium-fuel interaction. This interaction is not well understood, but it can lead to rather violent "vapor explosions" with consequent high pressure pulses. Usually the pressure generated depends on the manner and rate that fuel is dispersed in the coolant. The accident sequence is also important in that some sequences of coolant boiling and fuel failure may always lead to a vapor explosion while others may never do so.

Hence, two questions are of extreme importance in treating a vapor explosion:

1. Under what conditions of temperature, interfacial area, and energy generation rate is a vapor explosion possible?

2. What is the magnitude of the pressure generated in the event an explosion takes place?

Before one could hope to answer these questions, a method of accurately defining the condition of the fuel and coolant at the time of cladding failure must be available. In addition, it would be very helpful to calculate the gas volume and internal pressures in pins at the inception of failure.

3.3.5.1. Methods

Currently, the only way of estimating the magnitude of the pressure pulse resulting from a vapor explosion is to perform a calculation similar to that of Hicks and Menzies.[28] Such a calculation postulates instantaneous mixing and heat transfer in the fuel-sodium system. The pressure is then calculated by permitting the mixture to reach thermodynamic equilibrium at constant volume. The BANGO program developed at B&W carries out an analysis that is essentially similar to Hicks and Menzies' method. BANGO assumes instantaneous mixing and thermodynamic equilibrium in the fuel-sodium system. It then allows relief of the resultant pressure by accelerating the core of sodium above the core. Heat transfer between the bubble and the surrounding sodium is assumed to be governed by the equation

$$h(Btu/h\text{-}ft^2\text{-}°F) = 22,000 - \frac{36,000}{\Delta T}.$$

The work that ANL is performing in this area, especially for acoustically restrained nonequilibrium systems, should improve our ability to reliably calculate the dynamics of sodium-fuel interaction.

3.3.5.2. Application to Analyses

For accidents involving failure of the cladding, the fraction of fuel that is molten at that point (if any) will be determined, as will the average temperature of this fraction. This calculation can be performed for a melt-through of any extent, from a single pin to the whole core. These parameters will serve as input to the BANGO code, which will then determine the time dependence of pressure generation

3-16

and relief. As a result, the pressures in the primary loop and the cover gas are determined. At present BANGO has no provision for determining the implusive loading of the cover structure due to sodium "hammer."

3.3.6. Hydrodynamic Response of Primary System

For accidents that lead to large pressure pulses, such as nuclear disassembly or sodium fuel interaction, it is necessary to investigate the response of the reactor system, including the reactor cover structures. To predict the response with any degree of confidence, one must know in detail the propagation history of shock waves, the loading imposed on the various system components, and the damage produced by these loads. The failure sequence of the various components is of extreme importance, since early failure of a component may drastically alter the loading of the remainder of the system. This problem is complex in the extreme but is basic to the design of engineered safety features.

One must determine at all times the displacement, velocity, pressure, internal energy, density, and strain of the system components at each point. From these parameters the dynamic loadings on the structures can be estimated.

3.3.6.1. Methods

There is one hydrodynamics code that represents the state of the art. This code, developed at ANL by Chang and Gvildys, is operational at B&W under the common file name BANG. The BANG program represents the reactor primary system in two-dimensional La Grangian coordinates; for a seven-composition system, it is capable of calculating the following variables at each time and each space point: radial and axial displacements, axial and radial velocities, total zonal pressures, zonal viscous pressure, zonal specific internal energy, zonal densities, radial and axial strains, and angular strains. It is assumed that the neutronic behavior of the system has ceased to be important. In view of the availability of this code, the choice of another, less sophiscated method of analysis is not justified.

3.3.6.2. Application to Analyses

This code will be used to calculate the stresses and impulsive loadings on the primary system components, the reactor vessel, and the cover structure due to expansion of the large volumes of vapor that may be generated during a disassembly accident or a vapor explosion accident. The BANG program was primarily designed for use in the terminal phase of a disassembly accident, but very little modification will be required to permit calculation of the outcome of a vapor explosion. Some care must be taken, however, to ensure that the results of a vapor explosion calculation are conservative.

The problem here arises from the fact that BANG assumes no neutronic influences, such as fission heating in the dispersed fuel. It is believed that the time scale of a typical vapor explosion is such that the neglect of fission heating will not lead to a large error. The code will require initial conditions which may be taken from MARS and BANGO calculations. The result of these calculations will be an estimate of the dynamic loadings on the cover structures. A significant parametric effort will be required to identify uncertain or sensitive areas in the analysis.

3.4. Factors Influencing Functional Requirements

The work plan for the Accident Analysis and Safety System Design Study (BAW-1339) indicates that four areas of effort are required in establishing functional requirements:

1. Core protective systems and devices.
2. Emergency decay heat removal systems.
3. Primary containment.
4. Secondary containment safety features.

Establishing the functional requirements for the core protective systems and devices requires knowledge of the transient behavior of the reactor under a wide variety of conditions. Virtually all of the safety analyses will influence these functioanl requirements.

In order to establish the functional requirements for the decay heat removal systems, knowledge of the time-dependent fission product concentrations and the time-dependent system thermal transients is required.

Likewise, to set functional requirements for the primary containment one must determine the concentrations of fission products and plutonium, as well as the hydrodynamic response of the primary system to large pressure pulses.

The establishment of functional requirements for the secondary containment and its safety features will include the investigation of sodium fires, disposition of fission products, determination of the plutonium burden, and determination of direct dose rates and leakage. In summary, one needs methods for determining the following:

1. The time-dependent concentrations of fission products.

2. The effect of the release of fission products to the environment.

3. The pressure-temperature history of the containment as a result of sodium fires.

4. The system hydrodynamic response.

5. The thermal transients in the system.

Item 4 is discussed in section 3.3.5, so it is not discussed further here.

3.4.1. Fission Product Concentrations and Distributions

In a reactor with vented fuel pins, the distribution of fission products among the system components and their concentration in each component become important in analyzing the consequence of an accident that tends to alter or disrupt any of these components. One of the potential consequences of disrupting a component is the release of the fission products that it contains. The problem of describing the time-dependent behavior of released fission products is twofold:

1. What fission products exist in each system component (fuel, coolant, cover gas) and what are their concentrations at the time of release?

2. How many of these fission products are released and how do their concentrations vary with time after release?

3.4.1.1. Methods

A number of methods can be used to describe the distribution and concentration of fission products in a reactor system.

Babcock & Wilcox has two computer programs, BURP and RIBG, available for use in fast reactor analysis; in combination, they may be used to determine most of the significant parameters. The BURP program, written at B&W, has a multicompartment model that computes the activity levels of a maximum of 209 nuclides in each compartment at every time step. The activity level of each nuclide is multipied by its gamma yield in each of six energy groups, and the total gamma source strength in each compartment is given.

The RIBD program was written at DUN for use in calculating the fission product content of irradiated reactor fuels. RIBD is a grid processor which calculates isotopic concentrations resulting from dual fission sources with normal down chain decay by beta emission and isomeric transfer and interchain coupling resulting from n-gamma reactions. The buildup portion of RIBD differs from that of BURP in that it does not use the Bateman equations for its solution form and is therefore not limited to simple nonbranching chains. The RIBD code has a one-compartment model.

3.4.1.2. Application to Analyses

The RIBD and BURP codes will be used in conjunction to determine the time-dependent distributions and concentrations in the fuel, coolant, and cover gas filters. BURP, although having the advantage of a three-compartment model, has several limitations: (1) it does not provide for transmutation, (2) it cannot properly treat short-lived isotopes, and (3) it handles a limited number of nuclides. Therefore, RIBD will be used to normalize the multicompartment results of BURP to initial concentration calculations.

3.4.2. Environmental Analysis

In any comprehensive evaluation of the potential radiological hazards presented to the local environment by the presence of a nuclear power plant, the possible release of airborne radioactive materials to the atmosphere must be considered. Such a cloud of radioactivity presents a radiological hazard to the general public owing to inhalation and external gamma and beta exposure from the cloud itself, external gamma and beta exposure from deposited radioactive materials, and ingestion of contaminated food and water. The first two sources are

limiting for short-term postaccident dosage calculations. The radiological hazard from inhalation is generally more severe than that from external exposure, particularly when considering the release of gross fission product inventories. An estimate of dose rates is needed for the analysis of the environmental effects resulting from a large release.

3.4.2.1. Methods

The only analytical tool available for use in these analyses, aside from the traditional, conservative hand calculations, is the digital program CLOUD. CLOUD calculates the external gamma-ray dose rate and the total integrated dose due to a release of radioactive materials to the atmosphere. The basis of the dispersion model lies in the work of O. G. Sutton.[30] Items to be considered are meteorological parameters such as wind velocity and lateral and vertical diffusion coefficients, stability parameters, and physical boundaries such as temperature inversion layers. An option to include depletion due to washout and fallout is available. Either a one- or two-compartment source-release model may be selected. The source decays by a simple parent-daughter decay scheme or by a Way-Wigner relationship. In addition a modification has been made to determine the space-time atmospheric concentrations of radioactive materials due to the continuous release of material from a ground or elevated source. This modification will aid in evaluating the biological hazard due to inhalation.

3.4.2.2. Application to Analyses

The CLOUD program will be used to calculate the external gamma ray dose and the total integrated dose due to the release of radioactive material for selected accident conditions. The program will also be used to aid in calculating inhalation doses for these accidents. The effects of various initial concentrations and various atmospheric conditions will be investigated. These studies are expected to help set the functional requirements for the secondary containment support systems.

3.4.3. Analysis of Sodium Fires

The sodium coolant used in a typical LMFBR is capable of reacting exothermically with a wide variety of common substances.

Since a large sodium fire could overpressurize the containment building or jeopardize its integrity by overheating, the dynamics of sodium fires is an important part of a safety analysis. The most important variables to be determined are as follows:

1. Quantity of sodium available for burning.
2. Condition of sodium initially (spray, jet, pool, etc.).
3. Location of the sodium.
4. Temperature history of the various components.
5. Pressure history of the containment structures.

3.4.3.1. Methods

Although several sodium fire codes are in use at Atomics International on a developmental basis, only one is now available at B&W. This is the FIRE code, which is discussed in some detail in the appendix. Basically it is a modification of the AI SOFIRE[31] program with a routine included to calculate the effects of an initial spray fire. The geometry in FIRE consists of a two-cell model with a variable opening between cells; heat transfer by conduction, convection, and radiation is accounted for in this treatment. The initial location of the fire and the type of fire (pool or spray) is specified in the input; oxygen depletion in the compartments is taken into account. The temperature distributions are calculated as a function of time, and pressure histories in the various compartments are determined.

3.4.3.2. Application to Analyses

The FIRE code will be used to determine the effects of sodium fires on the containment building and associated structures. The location of the sodium and the amount available for burning will vary with the type of accident being considered. In each case the temperature of the components and the containment building atmosphere will be calculated along with the containment building pressure. The FIRE program may be used to evaluate the consequence of spraying sodium into the containment building during accidents of the "sodium hammer" type. These analyses will aid in fixing the functional requirements for the cover structure seals and restraining devices.

3.4.4. Thermal Transient Analysis

Transient thermal analysis of system components is important from the standpoint of functional requirements because it may influence the design of a number of consequence-limiting features. In particular, the design of the emergency decay heat removal system is dependent upon time-dependent thermal conditions that may develop after an accident. The design of devices intended to maintain the integrity of the liner on the biological shield is particularly sensitive to the thermal transients.

3.4.4.1. Methods

A number of excellent transient thermal analysis codes are available for use in this area. Among these are TIGER V, TIGER VI, and ARGUS. These codes are widely known throughout the industry and form part of the standard engineering methods used for such problems. It is likely that any one of these codes will be adequate for these analyses.

3.4.4.2. Application to Analyses

The transient heat transfer codes will be used to evaluate the cooling requirements for damaged and relocated cores. Several potential configurations will be identified and incorporated into these analyses. The heat removal requirements will be based on the maximum fission product energy sources and on the maximum levels of energy stored during the transient.

3.5. Standard Engineering and Design Methods

A number of activities will be carried out in support of both the accident analyses and of the safety systems design; both efforts will require considerable analytical work. The analytical tools to be used in this area are largely standard engineering or design methods which represent no significant departure from the methods used in the 1000-MWe follow-on study. The design effort will be limited largely to four areas:

1. Design of protective systems and devices.
2. Design of emergency decay heat removal systems.

3. Design of primary containment safety features.

4. Design of secondary containment support systems.

Many of the calculations that will be performed in support of these design activities are amenable to hand calculation, and no extensive modeling is required. The analytical methods for such calculations are relatively standard not only in the nuclear industry but also in industry in general. However, some areas may require more extensive or specialized calculations. The principal areas in this category include thermal analysis and hydraulic analysis. Several programs are available in each of these areas:

1. TIGER V — a three-dimensional transient thermal analysis code in x-y-z geometry.

2. ARGUS — a two-dimensional transient thermal analysis code in r-z geometry.

3. TAMPA — a steady state thermal analysis code with fuel mechanics.[32]

4. CHESS — a single-phase, thermal-hydraulic analysis code.

These and other methods will be applied in the design activities as required. Since these methods are standard, they are not discussed further.

3.6. Assessment of New Methods

The Accident Analysis and Safety System Design Study will be performed over a span of three years, during which time many of the methods available today are likely to be replaced by better, more sophisticated methods. Therefore, although it is desirable to plan the analyses to the best of one's ability based on current knowledge, a rigid plan based on the present state of methods development must be avoided. Since new and important methods are expected to become available during the next few years, appropriate sources in the literature will be constantly surveyed. Three documents will be followed in particular: ANL quarterly progress reports, FFTF progress reports and analysis reports, and General Electric progress reports.

If a preliminary survey discloses a method of interest to these safety analyses, more information will be sought. ANL may have to be called upon occasionally to provide aid in assessing methods development. Close contact will be maintained between B&W's analysis groups and ANL's experimental or methods development groups. When a method of definite interest or applicability has been identified, it will be obtained, if possible, and incorporated into the analyses. In this fashion the most current methods will be identified and implemented in the study. In the absence of an acceptable method, experimental data, if available, may be used to obtain an approximate solution. If the absence of a method poses a significant obstacle to the execution of the safety analyses, ANL will be consulted, and additional work will be proposed if necessary. Several problem areas in safety analysis methods are outlined in the following section.

4. PROBLEM AREAS

4. 1. General

It should be evident from the foregoing discussions that there are several areas in which knowledge of basic phenomena and analytical methods is currently inadequate. Most of the problems in fast reactor safety analysis arise in attempting to describe the course of an accident once the movement of components begins. The difficulties stem largely from a lack of understanding of the important parameters that determine how an accident proceeds beyond fuel motion or coolant boiling. The experimental data to date have been limited and rather inconclusive. As a result, in fast reactor safety analyses it has been traditional to make some very conservative assumptions in these phases of the calculation. As breeder technology advances, however, it is both necessary and desirable to remove as much conservatism as possible in these calculations since the cost penalty for undue conservatism is likely to be prohibitive. Economic considerations aside, it is always desirable to be able to predict with maximum accuracy all aspects of reactor behavior.

This section presents three of the most urgent problems in fast reactor safety analyses; indeed, no comprehensive analysis can be performed without treating these problems in some fashion. The three areas of interest are fuel failure propagation, sodium-fuel interaction, and sodium boiling phenomena. The relation of these problems to safety is discussed in the following sections, along with a description of the major analytical problems. Prospective approaches to the solution of these problems are considered where appropriate.

4. 2. Fuel Failure Propagation

The propagation of fuel failure is a matter of central importance in fast reactor design and safety analysis. The importance of this problem stems from the fact that single failures may occur with some

frequency. The consequent possibility of a single failure precipitating failures in surrounding fuel presents a significant safety risk. We ask, then, the general questions of how the fuel behaves at failure, what causes it to fail, and what modes of failure can lead to propagation of failure. Implicit in all these questions is the problem of time: the rates of propagation for the various failure modes, and the time available for the protection systems to act. In the following discussions a distinction is made between pin-to-pin and assembly-to-assembly propagation of failure.

4.2.1. Pin-to-Pin Propagation

Local failure of a single pin is among the more likely malfunctions that could occur in a reactor core. Such failures are by nature difficult to detect reliably; however, it most cases, there is no pressing need to detect the failure of a single pin if we can be assured that such a failure will not lead to other failures. Then the task becomes a matter of determining (1) the modes of failure that could conceivably lead to propagation of damage and (2) the time available for the protection system to act to limit failure.

4.2.1.1. Relation to Safety

The central issue in pin-to-pin propagation studies is whether a pin can fail in such a manner as to cause the failure of adjacent pins. If such were indeed possible, then the event could develop from an acceptable malfunction into a serious accident ultimately involving an entire subassembly. If pin failure propagated rapidly enough and extensively enough, a number of very undesirable conditions could develop, including (1) local reactivity effects, (2) damage or burn-through of subassembly walls, (3) generation of large pressure pulses and (4) sodium-fuel interaction on an assembly scale. If the propagation of damage from one pin to another were possible, one would then be faced with the task of detecting such a failure before extensive propagation occurred. This is extremely difficult to do with any acceptable degree of reliability, since the failure of only a few pins is unlikely to generate an unambiguous signal. We have, then, to define the modes of pin failure and failed pin behavior.

4.2.1.2. Analytical Problems and Methods Status

To simplify the discussion somewhat, it will be assumed that we are not concerned with pin failures due to power transients or general loss of flow, since both of these classes of accidents produce signals that can be reliably detected. The action of the protection system on detection of a signal would be to limit the extent of propagation. We are concerned here with failures that occur so as to be practically undetectable in the initial phase. In the absence of a power excursion or general loss of flow, the three most likely initiating events for pin failure are:

1. Undercooling due to externally caused flow reductions such as that caused by a blockage accident.

2. Undercooling due to local changes in geometry such as pin swelling, bowing, or deformation.

3. Vent blockage.

Although these modes of failure are relatively easy to identify, defining the point of fuel failure or the fuel failure states is far from simple. Factors such as irradiation history and material properties enter here, for some pins may require more cooling than others because of internal pressurization, radiation damage to cladding, and so forth. Nonetheless, given the fuel failure states and the flow redistribution histories, the point in time at which the fuel pin fails could probably be calculated with good results. It is considerably more difficult, however, to predict the behavior of the pin after failure has occurred. Unfortunately, the behavior of the fuel after failure is likely to have the greatest single influence on the propagation of damage to adjacent pins.

In this discussion we will make a distinction between two types of behavior following failure: explosive and nonexplosive. Explosive failures produce significant pressure pulses, either from a sodium-molten fuel interaction or from a sudden release of internal pressure. In addition to pressure pulses there are likely to be large quantities of debris from such a failure. It is rather difficult to see how a single pin could fail explosively from the initiating events defined at the

beginning of this section, but no calculations or experimental data exist to bolster this opinion. Explosive failure is discussed further later on.

In the event that a nonexplosive failure occurs, several mechanisms that could potentially propagate damage can be identified:

1. Deposition of debris in adjoining channels.
2. Deformation of failed pins so that adjacent channels are restricted.
3. Fission or bond gas blanketing of adjacent pins for a time long enough to produce over-heating of cladding.
4. Formation of pockets of stagnant sodium.

In order to treat these problems in a deterministic manner, many things must be known about the time-dependent behavior of the failed pin, the rate of flow reduction, the final reduced flows, and the thermal and mechanical conditions in adjacent pins. However, it should be possible to construct a model that will provide rates for the propagation of failure due to nonexplosive accidents. For pin deformation or blockage by debris, the model should consider four items:

1. Rate of distribution of debris or of pin deformation.
2. Degree of flow blockage.
3. Flow redistribution in unblocked channels.
4. Thermal conditions in adjacent pins.

Once these parameters are determined a transient thermal hydraulic calculation could be performed to determine the temperature transients in the adjacent pins, which would then be monitored for the inception of failure. In this manner a propagation rate for a specific type of failure could be determined to provide an estimate of the time required for failure to propagate through the assembly.

The problem of vapor blanketing is somewhat different. The major question is whether a vapor jet or stagnant bubble can blanket adjacent pins long enough to cause them to fail. Presumably, a release rate of gas into the coolant channel could be determined. The conditions in the adjacent pins could then be monitored to determine the length of time required to fail them. One could then decide whether

sufficient volume were available to blanket the pin for the length of time required to cause failure.

The question of the formation of stagnant sodium volumes is directly related to another problem area—the sodium boiling phenomenon—which will be discussed later. There are two effects associated with the stagnation of coolant that tend to lead to failure of the pins contacting stagnant areas:

1. Reduction of heat removal capacity, conduction being the only operative mechanism.

2. Possibility of sodium boiling, which could then lead to vapor blanketing.

The first thing to be determined is whether this mechanism can contribute to the propagation of failure. With respect to the first effect, unless a pin is completely surrounded by stagnant sodium, it may not fail at all, for heat transfer on the unaffected surfaces may cool the pin enough to prevent damage. The problem is then to determine what fraction of the pin's surface must be contacting flowing sodium to prevent failure. As to the second effect, it is difficult to see how vapor growth in a few channels could be of sufficient extent or duration to cause rapid failure of adjacent pins. However, this matter has not received enough analysis to warrant a firm judgment. The four propagation mechanisms have been discussed as if they were independent, mutually exclusive phenomena, but in reality they may occur simultaneously. Therefore, care must be taken in performing propagation analyses to make certain that the limiting case is being considered.

In the case of explosive failure of a fuel pin, we must determine whether such failure can cause a similar explosive failure in other pins. In the absence of a power excursion or general flow reduction, the most probable sequence of events is that an explosive failure in one pin will lead to nonexplosive failures in adjacent pins. It is assumed that a significant volume of molten fuel is required to produce explosive failure. If only one or a few pins are molten because of a local event, such as partial blocking, only the initial failures will be explosive, and propagation beyond that point may be treated as nonexplosive. If a large number of fuel pins are melted because of complete assembly blockage, for example, then the propagation will be so rapid

that we may conservatively assume that failure is coherent within that assembly. This, then, will be considered as part of the problem of assembly-to-assembly propagation.

The most important aspect of these analyses is the determination of the maximum realistic propagation rate, for this parameter determines how early failure must be detected and how rapidly and in what manner the protection systems must operate.

4. 2. 2. Assembly-to-Assembly Propagation

The problem of assembly-to-assembly failure essentially reduces to the question of whether local damage can become general. This question has serious ramifications not only for the protection systems' design requirements but also for the design basis of the engineered safety features and the primary system in general.

4. 2. 2. 1. Relation to Safety

It is reasonable to assume that fast breeder reactors may be designed so as to preclude very large reactivity insertions or flow stoppages as initiating events for accidents. In the absence of these "whole core" accidents, the only path to general core damage is through assembly-to-assembly propagation of damage. However, should certain modes of propagation prove to be exceedingly rapid, they may approach the whole core accident in severity. We have, then, to analyze the potential modes of assembly-to-assembly propagation and assure ourselves that the reactor can be designed so that very rapid propagation of damage is impossible. Thus, it would seem that if the propagation of damage from assembly to assembly could be limited, then general core damage could be obviated.

4. 2. 2. 2. Analytical Problems and Methods Status

For this discussion, it will be assumed that the possibility of "whole core" accidents has been eliminated through excellence of design. This means that gross core damage (more than a few assemblies) can occur only as a result of the uncontrolled propagation of damage from one assembly to another. It would seem that the designer is confronted with two problems:

1. To convince himself that the reactor is designed so that very rapid propagation (whole core damage in a few seconds) is not credible.

2. To determine the rate of propagation for credible modes so that the impact on the design requirements for the protection systems may be determined.

The first problem may be treated rather directly. It would seem that the only mechanism available for inducing rapidly expanding damage is the generation of highly energetic shock waves. A large pressure pulse in the core is required to initiate such shock waves. More analyses need to be performed to ensure that this is the only mode of propagating damage rapidly. Assuming for the moment that no other modes of rapid propagation can be identified, the following steps are suggested for analysis of the accident:

1. Determine which event, occurring in a single assembly, leads to the largest pressure pulse.

2. Calculate the attenuation of the shock wave through the array of assemblies.

3. Determine the dynamic load on each assembly as a result of the passing shock wave.

4. Calculate, where possible, the stress-strain rates in each assembly.

5. Determine whether failure thresholds have been exceeded in any assembly.

6. Construct a map showing the location of failed assemblies as a function of time.

7. Determine whether sufficient control is available to ensure eventual shutdown.

Alternatively one might calculate the pressures required to damage a given fraction of assemblies, construct a relationship between pressure and fractional damage, and then estimate the maximum extent of damage from the maximum credible pressure pulse. This sounds deceptively simple, but the problems involved in performing such calculations are many and great, and several steps cannot be accurately executed at this time. However, this method of investigating rapid failure propagation should be sound, at least in concept. Implicit in the foregoing model is the assumption that the damaged assemblies

contribute little to the destructive pulse. If they fail in a violent manner, which is unlikely in the absence of a "whole core" accident, then the analysis becomes much more complicated.

In the area of more slowly propagating phenomena a number of mechanisms that could lead to assembly-to-assembly propagation of damage can be identified:

1. Burn-through of an assembly wall by molten fuel.

2. Deformation of an assembly wall so that the peripheral pins are undercooled.

3. Passage of sodium vapor out of the entrance nozzle of one assembly into the entrance of another.

4. Thermal stress failures in the can wall.

There are two salient aspects common to each of these failure modes: they are relatively slow, requiring much longer than the passage of a shock wave, and they do not lead directly to failure of adjacent assemblies but rather to the failure of a few pins in the adjacent assembly, so that one is faced with a pin-to-pin failure problem. There are other standard techniques for treating the first and fourth mechanisms[33] although recent experimental data indicate that the models are not always conservative. The course of events initiated by the third mechanism can be calculated in an approximate manner if reliable data on sodium vapor growth and coolant expulsion can be obtained. The second mechanism perhaps deserves a few words of explanation.

If a pressure pulse of sufficient magnitude to deform the can wall arises in an assembly, it may also deform the walls of adjacent cans, leading to reduction of flow in the peripheral channels or crushing of the pin array in large segments of the assembly. The problem then is to determine the rate at which failure propagates from pin to pin, which is obviously a function of the degree of initial crushing. Therefore, it is important that the resistance to crushing of an entire assembly be calculated as accurately as possible. Unfortunately, this is rather difficult at the present time because of the lack of adequate methods.

In any event, if rapidly propagating shock damage can be eliminated, it appears that the other modes of propagation

quickly reduce to pin-to-pin failure, which is relatively slow and can very probably be limited to an acceptable level by protective action. However, in various portions of the analyses discussed above, improved methods are needed to ensure maximum accuracy. This is especially true in calculating dynamic loading and component crushing.

4.3. Sodium-Fuel Interaction

One of the most urgent problems in fast reactor safety analysis is the possibility of an explosive interaction between the sodium coolant and the hot reactor fuel. The concern over this phenomena stems from the fact that sodium is a good working fluid and that a large temperature difference exists between the sodium and the hot fuel. In addition, experimental evidence tends to indicate that some fuel failure modes may be violent enough to lead to rapid fragmentation and dispersal of the fuel, a condition that could lead to a very rapid interchange of energy between the two media. The sodium could undergo a phase change and, if restrained, develop exceedingly high pressures.

4.3.1. Relation to Safety

There is reason to believe that the thermodynamic interaction of sodium and hot or molten fuel can lead to a "vapor explosion" with resultant high pressures.[34] These large pressures can lead to violent expulsion of the sodium coolant in the affected channels or to damage to the core structure. Indeed, the vapor explosion is probably the most likely source of the high pressures discussed in the previous section in connection with rapidly propagating fuel failure. The situation is further complicated by the fact that the process may potentially occur in any accident involving molten fuel however small the molten fraction. Therefore, it must be considered as an adjunct to any transient that melts fuel. Although the large pressure pulse associated with a vapor explosion can be easily and unambiguously detected, the reaction is likely to be so rapid that the protection system may be unable to prevent significant damage. Therefore, the problem facing the designer is to determine what limits may be placed on the interaction, what its dynamics are, and what impact it has on the design of the engineered safety features.

4.3.2. Analytical Problems

The interaction between sodium and molten fuel is basically thermodynamic, but the mechanisms controlling it are so poorly understood that realistic calculations are extremely difficult. The course of an interaction depends on a number of things:

1. The relative quantities of each component.

2. The fragmentation rate of the fuel and the interfacial area between fuel and sodium.

3. The temperature differences between the media.

4. The degree to which the sodium is constrained.

Depending on the nature of these variables the interaction may produce only mild pressures or a true explosion. A vapor explosion might or might not occur upon the injection of hot fuel into the sodium; however, significant pressures (pressurization by simple vapor growth) can be developed even though a true explosion never occurs.

Perhaps the most influential of the foregoing parameters is the rate of fragmentation, which controls the heat transfer area available to the interaction.[35] The fragmentation and mixing of molten UO_2 in sodium are poorly understood in the analytical sense. The work being performed at ANL indicates that two effects may control fuel fragmentation: the velocity effects and the acceleration effects. The velocity effects are closely related to the Weber number, and this may allow some calculation of particle sizes. The acceleration effects tend to cause the two fluids in contact to jet into each other. The acceleration effects have been linked to the Taylor instability phenomena. In addition, experimental work being performed at ANL should contribute to a better understanding of the entire process.

Currently the only method available from which to estimate the pressures resulting from a vapor explosion is the method of Hicks and Menzies. This method assumes instantaneous thermal equilibrium in the sodium fuel system. The pressure is calculated from the equilubrium temperature of the mixture assuming constant volume. As discussed earlier, the BANGO program performs a calculation that is essentially similar to the method of Hicks and Menzies.

The work reported by R. O. Ivins in ANL-7561 and in the preliminary draft of the Safety Test Facility Project Report potentially provides a much better method of estimating pressures resulting from a sodium-fuel interaction. A detailed exchange of information between B&W and ANL is desirable in this area.

It is important to be able to define the conditions under which a vapor explosion will occur and the magnitude of the resultant pressure pulse. To do this, the rate of energy transfer must be determined. It is at this point that current analytical models fail. Until a satisfactory treatment of energy transfer rates is devised the only alternative is the Hicks-Menzies type calculation, which may be prohibitively conservative.

4.4. Sodium Boiling and Superheat Phenomena

One of the primary concerns of the reactor analyst is the behavior of the sodium coolant during abnormal reactor operation. There are a number of reasons for this concern, such as:

1. The possibility that large degrees of superheat are required to initiate boiling, which could lead to the production of significant pressures and rapid expulsion.
2. The rather large reactivity effects associated with sodium density changes.
3. The uncertainty in sodium behavior beyond boiling inception.

In the safety analysis, one must be able to predict accurately the dynamics of coolant behavior in accidents that approach incipient boiling.

4.4.1. Relation to Safety

The reactor designer is concerned with any type of behavior that could conceivably lead to a severe transient or act in such a way as to worsen an initiating transient. Because the large fast breeder reactors being designed today typically have rather large positive sodium density reactivity coefficients, the possibility of sodium boiling is naturally a concern. Additionally, if the sodium boiling is rapid the violent expansion of the vapor bubble and its recondensation may produce pressure pulses of destructive magnitude. The safety analyst is interested, then, in three aspects of the problem:

1. The conditions that lead to sodium boiling and the parameters that influence its inception most strongly.

2. The rates of sodium voiding and expulsion. This is important for assessing the reactivity effects accurately.

3. The magnitude of the pressure pulses accompanying expulsion and recondensation.

These problems must be treated in some acceptable fashion in a comprehensive safety analysis since the removal of sodium is potentially one of the most serious sources of reactivity addition.

4.4.2. Analytical Problems and Method Status

The experimental data to date have been incomplete and very inconclusive.[36,37] However, as more data are reported, a clearer pattern of behavior begins to emerge. Most of the uncertainties in behavior stem from three areas: superheat phenomena, expulsion dynamics, and recondensation and re-entry dynamics.

The large degrees of superheat that are apparently required to initiate boiling in liquid metals are a source of considerable concern primarily because this stored energy could be released very quickly at the inception of boiling. The potential consequences of such a release include rapid voiding and large pressure pulses. The data on superheat to date have indicated that the degree of superheat required to initiate boiling is a very complex function of many parameters, among which are the pressure-temperature history of the system, heat flux, fluid velocity, initial quantity of dissolved gas, and fluid purity.[38] Obviously, defining the degree of superheat required to initiate boiling in a particular circumstance is a complex, virtually impossible task at present. More experimental data are needed before this process can be adequately treated.

The rate of vapor growth has traditionally been determined using a model that assumes an isolated bubble in an infinite, uniformly superheated fluid. This work, unfortunately, has limited application in reactor situations because the nonuniform superheat in the channel and the presence of the fuel pin array can be expected to significantly alter the pressure transient in the bubble.

Two approaches may be taken to the problem of describing void formation in the reactor channel. An equilibrium or a non-equilibrium thermodynamic model may be assumed. The first approach leads to the development of models similar to those of MacFlane[39] and Noyes,[40] and the second leads to models such as BLOW,[41] VOID,[42] and that of Fauske and others.[43] The equilibrium assumption may be good for saturated boiling or for systems in forced convection. In these circumstances the annular or separated flow regimes may dominate. In stagnant sodium or in circumstances where there is significant superheating, the nonequilibrium assumption is probably better since it usually employs a slug flow regime.

The Fauske model and the BLOW model seem to be the best of the nonequilibrium models. Both of these assume slug flow with a liquid film on the heating surface. The Cronenberg, Fauske, and Bankoff model further assumes vaporization of sodium from the upper and lower interfaces. In short, it seems that the expulsion models are adequate, at least for single channels, if the required degree of superheat can be defined.

It has recently become clear that quite high pressures can arise as a result of recondensation of sodium vapor in subcooled sodium. It is not clear, however, what the duration of these pressures is likely to be. Further, the magnitude of these pulses increases sharply with increasing subcooling. Attempts to correlate experimantal data with theoretical descriptions of sudden vapor collapse have had only limited success. In order to determine the extent of possible mechanical damage from these pulses, a better understanding of the dominant processes is needed. This will probably be possible after extensive experimentation.

Virtually no attention has been given to the related process of sodium re-entry into hot, voided channels. For sufficiently rapid re-entry, a sodium hammer may result with consequent mechanical damage to the channel. If there are significant quantities of molten fuel in the channel at re-entry, a true vapor explosion may be produced. It is evident that much work needs to be done in this area before reliable analyses can be made.

In summary, it appears that one can adequately handle analyses involving sodium expulsion. However, the current understanding of superheat, recondensation, and re-entry is woefully inadequate for our analytical needs.

REFERENCES

[1] 1000-MWe LMFBR Follow-On Study, Babcock & Wilcox, BAW-1328, Vol 1, Lynchburg, Virginia, March 1969.

[2] Stevenson, M. G. and Bingham, B. E., "TART — An LMFBR Transient Analysis Project," Conference on the Effective Use of Computers in the Nuclear Industry, University of Tennessee, April 21-23, 1969.

[3] Duncan, D. S., CLOUD — An IBM-709 Program for Computing Gamma-Ray Dose Rate From a Radioactive Cloud, Atomics International, NAA-SR-MEMO-4822.

[4] Roy, D. H., et al., FARED: A One-Dimensional Fast Reactor Physics Design and Analysis Code, Babcock & Wilcox, BAW-3867-9, Vol 1, Lynchburg, Virginia, October 1969.

[5] Katz, R., Gerber, M. J., and Hamrick, J. R., ELBOW, Fuel Element Bowing Code, GAMD-6334 (to be released).

[6] Fischer, G. J., et al., "Fast Reactor Study Code SAS1A," Conference on the Effective Use of Computers in the Nuclear Industry, University of Tennessee, April 21-23, 1969.

[7] Burris, J. R. and Trost, R. J., 1000-MWe LMFBR Follow-On Study — Control Study, Babcock & Wilcox, BAW-1330, Lynchburg, Virginia, October 1968.

[8] Hassitt, A., A Computer Program to Solve the Multigroup Diffusion Equations, TRG Report 229(R) (1962).

[9] Little, W. W., Jr. and Hardie, R. W., 2DB Users Manual — Revision I, BNWL-831-REV1, February 1, 1969.

[10] Hardie, R. W. and Little, W. W., Jr., PERT-IV, A Two-Dimensional Perturbation Code in Fortran IV, BNWL-409, April 1967.

11 Waltar, A. E., MELT 1 — A Simplified Meltdown Code for Fast Reactor Safety Analyses, BNWL-944, December 1968.

12 Sha, W. T. and Hughes, T. H., VENUS, A Two-Dimensional Severe Disassembly Code Employing Two-Dimensional Hydrodynamics, ANL (to be published).

13 Chang, Y. and Gvildys, J., A Computer Code for the Numerical Calculation of Hydrodynamic Response of Primary Containment to High Excursions (to be published).

14 Gumprect, R. O., Mathematical Basis of Computer Code RIBD, Douglas United Nuclear, DUN-4163, June 17, 1968.

15 Perry, J. B. and Alcorn, J. M., BURP — A Computer Program for Calculating Buildup and Decay of Radioactive Fission Products, Babcock & Wilcox, BAW-TM-444, Lynchburg, Virginia, November 1966.

16 Briggs, D. L., TIGER, KAPL-M-EC-29, February 1, 1963.

17 Schoberle, D. F., Heestrand, J., and Miller, L. B., A Method of Calculating Transient Temperatures in a Multi-Region, Axisymmetric, Cylindrical Configuration, ANL-6654, November 1963.

18 Fox, J. N., Lawler, B. E., and Butz, H. R., FORE II, A Computational Program for the Analysis of Steady-State and Transient Reactor Performance, General Electric, GEAP-5273, September 1966.

19 Blaine, R. A. and Berland, R. R., Simulation of Reactor Dynamics, A Description of AIROS-IIA, NAA-SR-12452, Vol 1, September 1967.

20 Waltar, A. E., Little, W. W., and Harris, R. A., "Preliminary Analysis of Core Meltdown Transients in a Fast Test Reactor," Proc. ANS Conf., Volume 11, No. 1 p 333, June 1968.

21 Private communication, A. E. Waltar to M. G. Stevenson.

22 Bethe, H. A. and Tait, J. H., An Estimate of the Order of Magnitude of the Explosion When the Core of a Fast Reactor Collapses, British Report UKAEA-RHM (56)/113 (1956).

23 Nicholson, R. B., Methods for Determining the Energy Release in Hypothetical Reactor Meltdown Accidents, APDA-150 (1962).

[24] Meyer, R. A., et al., Fast Reactor Meltdown Accidents Using Bethe-Tait Analysis, GEAP-4809, January 1967.

[25] Stephenson, J. W., Jr. and Nicholson, R. B., Weak Explosion Program, ASTRA 417-GO (1961).

[26] Hirakawa, N., MARS, A Two-Dimensional Excursion Code, APDA-198 (1967).

[27] Little, W. W., Jr., MAX — A One Dimensional Maximum Hypothetical Accident Code in FORTRAN-IV, BNWL-612, March 1968.

[28] Hicks, E. P. and Menzies, D. C., Theoretical Study on the Fast Reactor Maximum Accident, ANL-7120, p 654, October 1965.

[29] Ivins, R. O., Pressure Generation Due to Violent Meltdown, ANL-7577, p 192, April 1969.

[30] Sutton, O. G., "The Problem of Diffusion in the Lower Atmosphere," Roy. Meteorological Soc., 73, p 257, July 1947.

[31] SOFIRE-B, private communication, Atomics International to B. E. Bingham, Babcock & Wilcox.

[32] Trost, R. J., TAMPA — A Computer Program for the Analysis of Reactor Fuel and Clad, BAW-TP-349, April 1968.

[33] 1000-MWe Follow-On Study, Task I, GEAP-5618, Appendix F, p 331, February 1969.

[34] Ivins, R. O., Pressure Generation Due to Violent Meltdown, ANL-7561, p 99, March 1969.

[35] Ibid.

[36] Le Gonidec, et al., "Experimental Studies on Sodium Boiling," Proc. International Conf. on the Safety of Fast Reactors, Aix-en-Provence, France, September 1967.

[37] Grass, G., et al., "Measurements of the Superheating and Studies About Boiling Phenomena in Liquid Metals," Proc. International Conf. on Safety of Fast Reactors, Aix-en-Provence, France, September 1967.

38 Peppler, W., et al., Sodium Boiling and Fast Reactor Safety, KFK-612, June 1967.

39 MacFarlane, D. R., "Transient Sodium Boiling Calculations-II," Nuclear Eng. and Design, 6, p 103 (1967).

40 Noyes, R. C., et al., Transfugue-I, A Digital Code for Transient Two-Phase Flow and Heat Transfer, Atomics International Report, NAA-AR-11008, July 1965.

41 Peppler, W., et al., Sodium Boiling and Fast Reactor Safety, KFK-612, June 1967.

42 Meinhardt, W. G., "Calculating Vapor Growth in a Superheated Liquid Metal Within a Heated Channel," ANS Conference, Pittsburg, Pennsylvania, October 1966.

43 Cronenberg, A. W., Fauske, H. K., and Bankoff, S. G., "Simplified Model for Sodium Coolant Expulsion and Re-entry," ANS Conference, Seattle, Washington, June 1969.

APPENDIX
Computer Programs and Models

FOREWORD

This appendix presents a rather detailed discussion of the less widely known computer programs and models that will be used in the Accident Analysis and Safety System Design Study. For the most part these codes have been developed or extensively modified at Babcock & Wilcox.

1. TART LMFBR Transient Analysis Code

1.1. Introduction

The design and safety analysis of a large LMFBR require detailed computational models and programs to describe the transient response of the reactor core and plant to a variety of conditions. The Babcock & Wilcox TART (Thermal Analysis - Reactor Transients) code will be used to provide a means to analyze the dynamic characteristics of large LMFBRs as accurately as necessary at a minimum computational cost.

Both point kinetics and one-dimensional, multigroup diffusion neutronics models are available as separate versions of the TART program. Both the point and diffusion neutronics models can be coupled with either a region-averaged (fuel, cladding, and coolant nodes) or a detailed (two-dimensional multinode) thermal-hydraulics solution for an average fuel pin in each thermal-hydraulics region. A primary coolant model corresponding to the pool primary system used in B&W's 1000-MWe LMFBR reference design[1] may be included with either thermal-hydraulics solution, and the actions of the reactor control and safety system can be simulated at the user's option. The time steps used in the thermal-hydraulics solution may be an integral number of neutronics solution time steps with each being selected according to preset error criteria. A flow diagram of the TART program is shown in Figure A-1.

1.2. Neutronics Solutions

The neutronics solutions in TART are based on the exponential extrapolation methods developed under the supervision of K. Hansen. Either the point[2] or the diffusion[3] method yields a comparatively fast solution and is numerically stable for any size of time step. Up to six neutron energy groups are allowed in the diffusion version of TART, and six delayed neutron groups may be used in either version.

Both methods are based on approximating the time-dependent behavior of the neutron density (or group fluxes) and the precursor concentrations by an exponential over each time step. The set of ordinary differential equations corresponding to the point model or to the spatial-differenced diffusion equations is then integrated over the time step using

Figure A-1.   TART Flow Chart
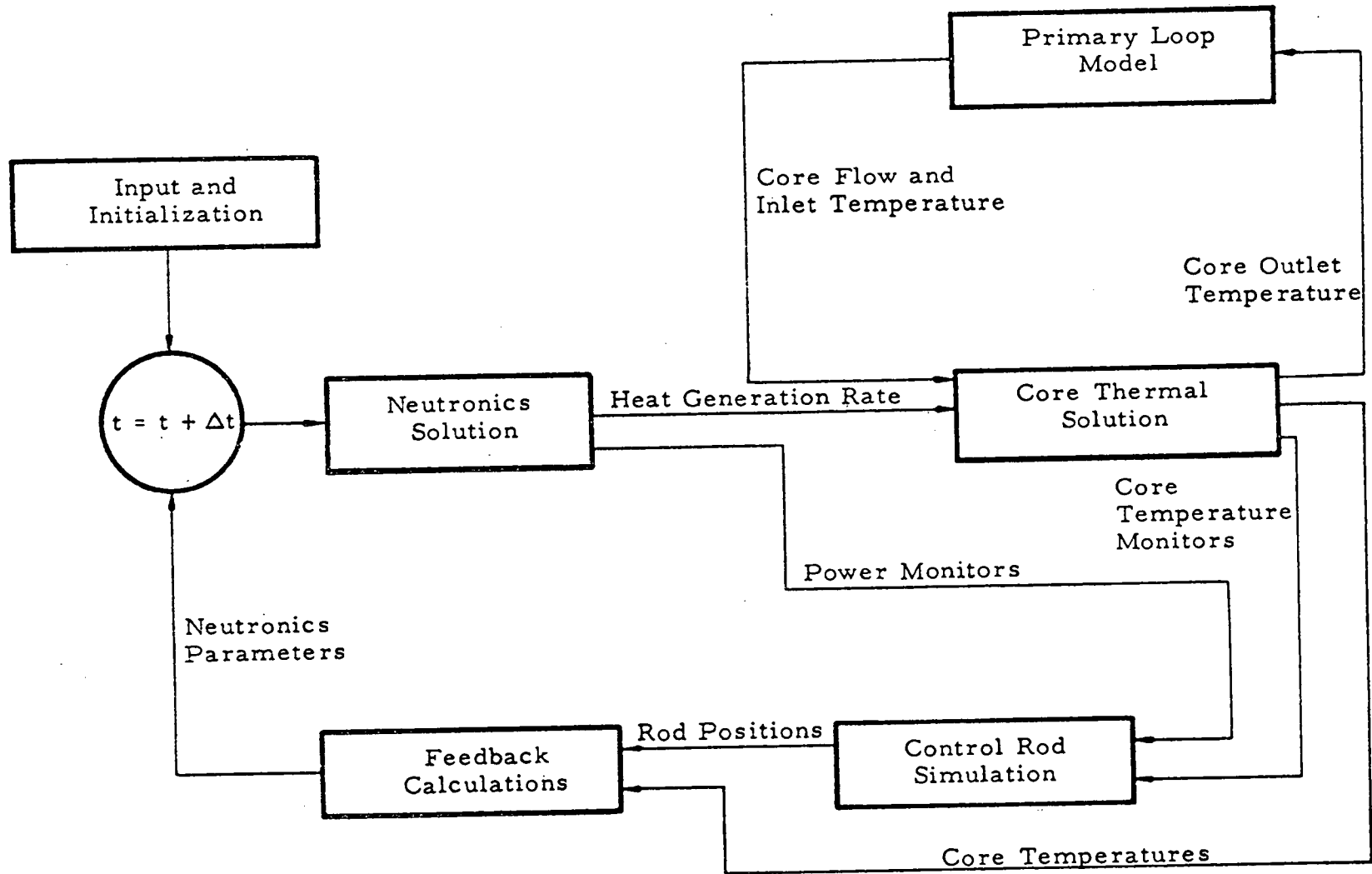
this approximation. The resultant set of algebraic difference equations can be solved explicitly in the point kinetics case and can be solved using Gaussian elimination in the one-dimensional case.

1.2.1. Point Kinetics Solution

The point kinetics equations are written in conventional form as

$$\frac{dn}{dt} = \frac{\rho - \bar{\beta}}{\Lambda} n + \sum_i \lambda_i c^i$$

$$\frac{dc^i}{dt} = \frac{\bar{\beta}_i}{\Lambda} n - \lambda_i c^i$$

where $n = n(t)$ is the neutron density amplitude factor, $\rho = \rho(t)$ is the net reactivity, Λ is the prompt neutron generation time, c^i is the normalized weighted average delayed neutron precursor concentration for delayed group i, λ_i is the decay constant for group i, $\bar{\beta}_i$ is the effective delayed fraction for group i, and $\bar{\beta} = \sum_i \bar{\beta}_i$.

These equations can be rearranged in the form

$$\frac{dn}{dt} + \gamma n = \sum_i \lambda_i c^i$$

$$\frac{dc^i}{dt} + \lambda_i c^i = \frac{\bar{\beta}_i}{\Lambda} n$$

where

$$\gamma = -\left[\frac{\rho - \bar{\beta}}{\Lambda} \right].$$

Each equation is multiplied by the appropriate weighting factor to result in

$$\frac{d[e^{\gamma t} n]}{dt} = e^{\gamma t} \sum_i \lambda_i c^i ,$$

$$\frac{d\left[e^{\lambda_i t} c^i\right]}{dt} = e^{\lambda_i t} \frac{\bar{\beta}_i}{\Lambda} n.$$

Assuming constant reactivity, these can be integrated over the time step $h_j = t_{j+1} - t_j$ to give

$$e^{\gamma h} n_{j+1} - n_j = \sum_i \lambda_i \int_0^{h_j} e^{\gamma \xi} c^i(\zeta) d\xi,$$

$$e^{\lambda_i h} c_{j+1}^i = \frac{\bar{\beta}_i}{\Lambda} \int_0^{h_j} e^{\lambda_i \xi} n(\zeta) d\xi.$$

The assumption is then made that for $t_j \leq t_j + \xi < t_j + h_j$

$$n(\xi) = e^{\omega_0^j \xi} n_j$$

$$c^i(\xi) = e^{\omega_i^j \xi} c_j^i$$

and the integrals on the right-hand side can be evaluated to give

$$e^{\gamma h_j} n_{j+1} - n_j = \sum_i \lambda_i \left[\frac{e^{(\omega_i^j + \gamma)h_j} - 1}{\omega_i^j + \gamma} \right] c_j^i,$$

$$e^{\lambda_i h_j} c_{j+1}^i - c_j^i = \frac{\bar{\beta}_i}{\Lambda} \left[\frac{e^{(\omega_0^j + \lambda_i)h_j} - 1}{\omega_0^j + \lambda_i} \right] n_j,$$

or

$$n_{j+1} = e^{-\gamma h_j} n_j + \sum_i \lambda_i \left[\frac{e^{\omega_i^j h_j} - e^{-\gamma h}}{\omega_i^j + \gamma} \right] c_j^i ,$$

$$c_{j+1}^i = e^{-\lambda_i h_j} c_j^i + \frac{\bar{\beta}_i}{\Lambda} \left[\frac{e^{\omega_o^j h_j} - e^{-\lambda_i h}}{\omega_o^j + \lambda_i} \right] n_j .$$

The ω extrapolation parameters are determined by

$$\omega_o^j = \frac{1}{h_{j-1}} \ln(n_j/n_{j-1}) ,$$

$$\omega_i^j = \frac{1}{h_{j-1}} \ln(c_j^i/c_{j-1}^i) .$$

1.2.2.   One-Dimensional Multigroup Solution

To summarize the basis of the neutronics method for the one-dimensional diffusion case as given by Andrews and Hansen,[3] the set of ordinary differential equations resulting from a conventional spatial-differencing is written as

$$\frac{d\psi}{dt} = A\psi \tag{1}$$

where the vector ψ contains the multigroup flux and precursor concentrations at each mesh point. The matrix A is factored as

$$A = \Gamma + L + U + H \tag{2}$$

A-7

where L and U are strictly block lower and upper triangular, respectively, and Γ and H are block tridiagonal. For the flux variables the submatrices H_g and Γ_g are defined by

$$H_g = v_g \frac{\delta D \delta}{h_x^2}$$

(3)

and

$$\Gamma_g = v_g (\chi_g \nu \Sigma_g^f - \Sigma_g^t)$$

(4)

where $\delta D \delta / h_x^2$ represents the difference form of the diffusion term. It should be noted that all submatrices are diagonal except H_g, which are tridiagonal.

If equation 1 is then written as

$$\frac{d\psi}{dt} - \Gamma\psi = (L+U+H)\psi$$

(5)

and integrated over the time interval $h = t_{j+1} - t_j$, assuming that the matrix elements are constant over h, then the result can be written as

$$\psi_{j+1} = \exp(\Gamma h)\psi_j + \int_0^h d\xi \, \exp\left[\Gamma(h-\xi)\right](L+U) \, \psi(t_j+\xi)$$

$$+ \int_0^h d\xi \, \exp\left[\Gamma(h-\xi)\right]H \, \psi(t_j+\xi).$$

(6)

If $\psi(t_j + \xi)$ in the first integral is replaced by

$$\psi(t_j+\xi) = \exp(\omega\xi)\psi_j$$

(7)

and in the second integral by

$$\psi(t_j+\xi) = \exp\left[-\omega(h-\xi)\right]\psi_{j+1}$$

(8)

where ω is an extrapolation parameter, then the integrals can be evaluated. The flux vector at time t_{j+1} is then given by the solution to

$$\left[I - (\omega I - \Gamma)^{-1} \left\{ I - \exp[(\Gamma - \omega I)h] \right\} H \right] \psi_{j+1} = \left[\exp(\Gamma h) \right.$$
$$\left. + (\omega I - \Gamma)^{-1} \left\{ \exp(\omega h I) + \exp(\Gamma h) \right\} (L + U) \right] \psi_j. \tag{9}$$

It should be noted that since the matrix on the left side of 9 is block tridiagonal, this set of equations can be solved directly by Gaussian elimination. The resultant solution method can be shown to be numerically stable and to yield the asymptotic solution for the case of a step change in the properties of the system.

The initial version of the one-dimensional, time-dependent multigroup diffusion solution in TART used an ω extrapolation factor based on a single energy group. In order to improve truncation error and stability properties, this model has been modified to use group-dependent ωs and to iterate these ωs. That is, after each time step, an ω is calculated for each energy group g and spatial region n by

$$\omega_{gn}^j = \frac{1}{h_{j-1}} \ln (\psi_{gn}^j / \psi_{gn}^{j-1}) \tag{10}$$

where ψ_{gn}^j is the group g flux in the center of region n and h_{j-1} is the time step from t_{j-1} to t_j. If ω_{gn}^j does not agree within a specified error with the predicted ω_{gn}^j (actually ω_{gn}^{j-1}), then the time step is repeated. This process is repeated until the error criterion is satisfied. Since a separate ω is used for each group and each region, then the ω used in the foregoing derivation of the method is actually a diagonal matrix; however, the general outline remains much the same.

1.3. Core Thermal Models

1.3.1. Region-Averaged Model

Each of the two thermal-hydraulics models used in TART is based on a thermal analysis of an average fuel pin in each

thermal-hydraulics region. The first of these models, the "region-averaged" model, considers a single fuel node, cladding node, and coolant node in each region. The equations describing the average temperatures corresponding to these nodes are for each region:

$$(\overline{\rho c V})_f \frac{d\overline{T}_f}{dt} = -(\overline{UA})_f (\overline{T}_f - \overline{T}_{cl}) + r_f q, \tag{11}$$

$$(\overline{\rho c V})_{cl} \frac{d\overline{T}_c}{dt} = (\overline{UA})_f (\overline{T}_f - \overline{T}_{cl}) - (\overline{UA})_c (\overline{T}_{cl} - \overline{T}_c) + r_{cl} q, \tag{12}$$

$$(\overline{\rho c V})_c \frac{d\overline{T}_c}{dt} = (\overline{UA})_c (\overline{T}_{cl} - \overline{T}_c) + W[(c_c^{in} + c_c^{out})T_{in}$$

$$- 2 c_c^{out} \overline{T}_c] + r_c q, \tag{13}$$

where

T_{in} = core inlet temperature,

$\overline{T}_f$ = average fuel temperature,

$\overline{T}_{cl}$ = average cladding temperature,

$\overline{T}_c$ = average coolant temperature,

$(\overline{UA})_f$ = overall fuel-to-cladding conductance times heat transfer area,

$(\overline{UA})_c$ = overall cladding-to-coolant conductance times heat transfer area,

ρ = density,

c = specific heat,

V = volume,

W = coolant flow rate,

q = total heat generation rate,

r_f = fraction of heat generated directly in fuel,

r_{cl} = fraction of heat generated directly in cladding,

r_c = fraction of heat generated directly in coolant.

The set of ordinary differential equations for the temperatures in each region is central differenced in time (trapezoidal rule integration), and the resultant set of simultaneous equations is solved at each time step by Gaussian elimination. To simplify the input description

for this model, the initial average fuel, cladding, and coolant temperatures are input for each thermal-hydraulics region, and the overall conductances and initial flow in each region are then calculated using these temperatures. These initial temperatures can be obtained from detailed steady state calculations. Coolant properties are expressed in polynomial form and evaluated in each region during a transient, but input fuel and cladding properties are assumed to remain constant throughout a transient.

1.3.2. Detailed Thermal Model

The detailed thermal model used in TART is based on the heat conduction equation in the fuel and cladding:

$$\rho c \, \frac{\partial T}{\partial t} = \nabla \cdot k \nabla T + q_1 \tag{14}$$

where k is the thermal conductivity and q_1 is the volumetric heat generation rate. If axial heat conduction is neglected and azimuthal symmetry is assumed, then this equation in cylindrical geometry becomes

$$\rho c \, \frac{\partial T}{\partial t} = \frac{1}{r} \left[\frac{\partial}{\partial r} \left(rk \, \frac{\partial T}{\partial r} \right) \right] + q_1 (r, z, t).$$

Spatial difference equations are obtained from the conduction equation by using Simpson's rule integration over a radial mesh interval from $r_{j-1/2}$ to $r_{j+1/2}$; that is

$$\int_{r_{j-\frac{1}{2}}}^{r_{j+\frac{1}{2}}} r\rho c \, \frac{\partial T}{\partial r} \, dr = \int_{r_{j-\frac{1}{2}}}^{r_{j+\frac{1}{2}}} \frac{\partial \left[rk \, \frac{\partial T}{\partial r} \right]}{\partial r} \, dr + \int_{r_{j-\frac{1}{2}}}^{r_{j+\frac{1}{2}}} r \, q_1(t) \, dr$$

and

$$\frac{\Delta r}{6} \left\{ r_{j-\frac{1}{2}} \left(\rho c \, \frac{\partial T}{\partial t} \right)_{j-\frac{1}{2}} + 4r_j \left(\rho c \, \frac{\partial T}{\partial t} \right)_j + r_{j+\frac{1}{2}} \left(\rho c \, \frac{\partial T}{\partial t} \right)_{j+\frac{1}{2}} \right\}$$

$$\tag{15}$$

$$= -r_{j-\frac{1}{2}} k_{j-\frac{1}{2}} \left. \frac{\partial T}{\partial r} \right|_{j-\frac{1}{2}} + r_{j+\frac{1}{2}} k_{j+\frac{1}{2}} \left. \frac{\partial T}{\partial r} \right|_{j+\frac{1}{2}} + \frac{1}{2} q_1 \left[(r_{j+\frac{1}{2}})^2 - (r_{j-\frac{1}{2}})^2 \right].$$

To evaluate the temperatures at half-intervals the averages are used:

$$T_{j-\frac{1}{2}} = \frac{1}{2} (T_{j-1} + T_j),$$

$$T_{j+\frac{1}{2}} = \frac{1}{2} (T_j + T_{j-1}),$$

and the derivatives are evaluated by

$$\left. \frac{\partial T}{\partial r} \right|_{j-\frac{1}{2}} = \frac{T_j - T_{j-1}}{\Delta r},$$

$$\left. \frac{\partial T}{\partial r} \right|_{j+\frac{1}{2}} = \frac{T_{j+1} - T_j}{\Delta r}.$$

This results in the final form of the spatial differenced equations:[4]

$$\frac{1}{12}\left\{ (1 - \frac{\Delta r}{2r_j})\rho c_{j-\frac{1}{2}} \frac{dT_{j-1}}{dt} + [(1 - \frac{\Delta r}{2r_j})\rho c_{j-\frac{1}{2}} + 8\rho c_j + (1 + \frac{\Delta r}{2r_j})\rho c_{j+\frac{1}{2}}] \frac{dT_j}{dt} \right.$$

$$\left. + (1 + \frac{\Delta r}{2r_j})\rho c_{j+\frac{1}{2}} \frac{dT_{j+1}}{dt} \right\} = -\frac{k_{j-\frac{1}{2}}}{(\Delta r)^2} (1 - \frac{\Delta r}{2r_j})(T_j - T_{j-1})$$

$$+ \frac{k_{j+\frac{1}{2}}}{(\Delta r)^2} (1 + \frac{\Delta r}{2r_j})(T_{j+1} - T_j) + q_1. \tag{16}$$

The conductivities $k_{j\pm i/2}$ are evaluated by

$$k_{j\pm\frac{1}{2}} = k(T_{j\pm\frac{1}{2}})$$

and the density and specific heat are taken as averages; i.e.,

$$\rho c_{j\pm\frac{1}{2}} = \frac{1}{2} (\rho c_j + \rho c_{j\pm1})$$

where $\rho c_j = \rho c(T_j)$.

The heat convection equation describing the temperature of the coolant is approximated by

$$\rho c \frac{\partial T_c(z,t)}{\partial t} = - W \frac{\partial [c T_c(z,t)]}{\partial z} + q_2 + q_3 \tag{17}$$

where q_2 represents the heat source input to the axial segment from the cladding and q_3 represents the heat generated directly in the coolant. The coolant temperature is assumed to vary linearly within each axial segment, and the resultant spatial difference equation for axial segment m is

$$(\rho c)_m \frac{dT_m}{dt} = - W[2c_{m+1/2} T_m - (c_{m+1/2} + c_{m-1/2}) T_{m-1/2}] + q_2^m + q_3^m . \tag{18}$$

The set of ordinary differential equations describing the fuel, cladding, and coolant temperatures in a given axial segment m is integrated over a time step using trapezoidal rule integration (central differencing) but assuming constant properties over that time step. That is, the equations for a given segment m can be written in the form

$$A \frac{dT}{dt} = BT + Q$$

where both A and B are tridiagonal matrices and where the Q vector contains the heat generation rates and the term containing the temperature of the coolant inlet to segment m. With trapezoidal integration this becomes

$$A(T^{j+1} - T^j) = \frac{h_j}{2} B(T^{j+1} + T^j) + \bar{Q}^{j+1}$$

where the integral of the Q vector is represented by $\bar{Q}_{j+1}$:

$$\bar{Q}^{j+1} = \int_{t_j}^{t_j+h_j} Q(\xi)d\xi.$$

This then results in

$$\left(A - \frac{h_j}{2}B\right) T^{j+1} = \left(A + \frac{h_j}{2}B\right) T^j + \bar{Q}^{j+1}.$$

This set of simultaneous equations is solved by Gaussian elimination, and the solution can be written as

$$T^{j+1} = \left(A - \frac{h_j}{2}B\right)^{-1} \left[\left(A + \frac{h_j}{2}B\right) T^j + \bar{Q}^{j+1}\right].$$

Calculation of temperatures in structural (subassembly cans) and additional materials (spacers, control assemblies) is also included in the detailed thermal model to ensure proper heat balance and to provide the thermal information necessary for expansion feedback models. An equation for the time-dependent average structural temperature in each axial segment m and radial region or channel n can be written as

$$(\rho cV)_{m,n}^s \frac{dT_{m,n}^s}{dt} = (UA)_{m,n}^s (T_{m,n}^c - T_{m,n}^s) + r_{m,n}^s q_{m,n} \tag{19}$$

where $(\rho cV)_{m,n}^s$ is the total heat capacity of the segment, $(UA)_{m,n}^s$ is the overall conductance times area, and $r_{m,n}^s q_{m,n}$ is the internal heat generation rate. A similar equation can be written for the additional material.

To ensure a numerically stable solution, trapezoidal integration over a time step (central differencing) is used; i.e., assuming constant properties and dropping the subscripts for convenience,

$$(\rho cV)^s[T^{s,j+1} - T^{s,j}] = \frac{\Delta t}{2}\left\{(UA)^s[(T^{c,j+1} + T^{c,j})\right.$$

$$\left. - (T^{s,j+1} + T^{s,j})] + r^s(q^{j+1} + q^j)\right\}. \qquad (20)$$

Although this difference scheme is implicit, equation 20 can be solved directly for $T^{s,j+1}$. This solution and a similar solution for the additional material can be substituted back into the central-differenced equation for the coolant. In this way, the implicit solution for the fuel pin thermal model can be retained without losing the tridiagonality of the solution matrix while still adding these additional nodes in the coolant channel.

A variable fuel-cladding gap size and conductance model[5] may be used with the detailed thermal model. The gap radius, Δr_g, is calculated at each axial segment in each radial channel assuming linear expansion in the fuel and cladding; i.e.,

$$\Delta r_g(t) = \Delta r_g(o) + \gamma_{cl}\bar{T}_{cl}[r^i_{cl}(o)] - \gamma_f\bar{T}_f[r^o_f(o)] \qquad (21)$$

where γ_{cl} and γ_f are the constant expansion coefficients of the cladding and fuel, $\bar{T}_{cl}$ and $\bar{T}_f$ are the average temperatures of the cladding and fuel, $r^i_{cl}(o)$ is the initial inner radius of the cladding, and $r^o_f(o)$ is the initial outer radius of the fuel.

If the gap is calculated to be open, that is, if Δr_g is positive, then the heat transfer coefficient is given approximately by

$$h_g = K_g/\Delta r_g \qquad (22)$$

where K_g is the thermal conductivity of the gas in the gap. If the gap is closed, that is, if Δr_g is negative or zero, then the gap coefficient is considered to be the sum of three coefficients corresponding to conduction through the gas, conduction through the solid-solid contact, and radiation across the gap; i.e.,

$$h_g = h_K + h_s + h_R. \qquad (23)$$

The gas conduction coefficient is given by

$$h_K = \frac{K_g}{c_g(R_f + R_c)} \tag{24}$$

where R_f and R_c are the arithmetic mean roughness of the fuel and cladding surface, respectively, and c_g is the pressure effect coefficient given by[4]

$$C_g = 2.75 - 1.7 \times 10^{-4} \, P_{con}. \tag{25}$$

The contact pressure P_{con} is given by

$$P_{con} = \frac{-E_{cl}[\Delta r_{cl}]\Delta r_g}{(r_{cl}^1)^2} \tag{26}$$

where E_{cl} is the modulus of elasticity of the cladding and Δr_{cl} is the thickness of the cladding.

The solid-solid coefficient h_s is given by

$$h_s = \frac{K_m P_{con}}{Y^{\frac{1}{2}}H} \tag{27}$$

where K_m is the mean cladding-fuel conductivity, Y is the root-mean-square separation distance of the fuel-cladding interface during contact, and H is the Meyer hardness of the cladding.

The radiation coefficient h_R is given by

$$h_R = \frac{\sigma}{\left[\frac{1}{\epsilon_f} + \frac{1}{\epsilon_c} - 1\right]} \left[T_f^3 + T_f^2 T_c + T_f T_c^2 + T_c^3\right] \tag{28}$$

where σ is the Stefan-Boltzmann constant, ϵ_f and ϵ_c are emissivities of fuel and cladding, and T_f and T_c are outer fuel and inner cladding temperatures, respectively, in degrees Rankine.

Functional expressions are built into the program for the fuel density, specific heat, and thermal conductivity, and for the coolant density and specific heat. Input information is used for the central void radius and for the fuel-cladding gap size and conductance. Different pin sizes may be used to correspond to actual pin dimensions in the core and radial blanket. The initial steady state solution is obtained by first putting in the initial coolant temperature rise in each thermal-hydraulics region and then calculating the temperatures in each region by a linear iteration technique.

The thermal model will account for the heat of fusion when the fuel melts. The method used is approximate since it allows the fuel temperature at a melting node to rise one degree and replaces the heat capacity of the node in that one degree range by the heat of fusion. A check on old and new values of the temperature of each node that is close to melting prevents the possibility of the temperature going past the melting point without being corrected. Through the use of this scheme no additional storage is required, and the errors involved are negligible. The model also accounts for the heat of fusion during solidification of a liquid node.

An approximate model simulating sodium voiding may also be used with the detailed thermal model. Voiding begins whenever the coolant temperature in any axial segment and any thermal region exceeds an input trip temperature. The void is assumed to extend radially throughout that region and to propagate axially according to input time tables corresponding to upward and downward movement. The cladding-coolant heat transfer coefficient for a voided segment is also given by an input time table. The void feedback at any time is determined from the voided fraction of each segment and the void reactivity coefficient for that segment and region. This model does not satisfy the conservation equations for the problem; however, it does provide a flexible means of using new information as it becomes available from experiments and detailed numerical solutions.

1.4. Feedback Models

1.4.1. Point Kinetics Feedback

The net reactivity for the point kinetics model is given by

$$\delta\rho(t) = \delta\rho_P(t) + \delta\rho_D(t) + \delta\rho_V(t) + \delta\rho_R(t) + \delta\rho_X(t)$$

where $\delta\rho_P(t)$ is the input or programmed reactivity, $\delta\rho_D(t)$ is the fuel temperature or Doppler reactivity, $\delta\rho_V(t)$ is the sodium density or void reactivity, $\delta\rho_R(t)$ is the control rod reactivity, and $\delta\rho_X(t)$ is the axial expansion feedback. In general, the Doppler reactivity effect is given by

$$\frac{\partial\rho}{\partial T} = AT^k$$

where T is some average fuel temperature (absolute). If $k = -1$, then

$$\rho(t) = A\ln[T(t)/T(0)]$$

and, if $k \neq -1$, then

$$\rho(t) = \frac{A}{k+1}[T(t)^{k+1} - T(0)^{k+1}].$$

The local Doppler effect is assumed to depend linearly on the local sodium density; thus, for axial segment m in region n, it is given by

$$\delta\rho_{mn}(t) = \left[A_i \frac{P_{mn}(t)}{P_{mn}(0)} + A_o\left(1 - \frac{P_{mn}(t)}{P_{mn}(0)}\right)\right] \ln[\bar{T}_{mn}(t)/\bar{T}_{mn}(0)].$$

Or, if $k \neq -1$, then

$$\delta\rho_{mn}(t) = \frac{1}{k+1}\left[A_i \frac{P_{mn}(t)}{P_{mn}(0)} + A_o\left(1 - \frac{P_{mn}(t)}{P_{mn}(0)}\right)\right]\left[\bar{T}_{mn}(t)^{k+1} - \bar{T}_{mn}(0)^{k+1}\right]$$

where A_i is the total core Doppler coefficient with full dense sodium, A_o is the Doppler coefficient with the core completely voided, $P_{mn}(t)$ is the sodium density, and $\overline{T}_{mn}(t)$ is the volume-averaged fuel temperature in segment m in region n.

Three options are available for spatial weighting of the Doppler reactivity. The first uses the square of the local power fraction q_{mn} as the weighting; i.e., for this option

$$\delta\rho_D(t) = \frac{\sum\limits_{m,n} q_{mn}^2\, \delta\rho_{mn}(t)}{\sum\limits_{m,n} q_{mn}^2}.$$

The second optional weighting uses separable weighting functions such as might be obtained using one-dimensional flux distributions; i.e.,

$$\delta\rho_D(t) = \frac{\sum\limits_{m,n} W_m\, W_n\, \delta\rho_{mn}(t)}{\sum\limits_{m,n} W_m\, W_n}.$$

The third form uses two-dimensional Doppler distributions; i.e.,

$$\delta\rho_D(t) = \frac{\sum\limits_{m,n} W_{mn}\, \delta\rho_{mn}(t)}{\sum\limits_{m,n} W_{mn}}.$$

Two options are available for weighting the sodium density feedback. The first uses separable weighting functions; i.e.,

$$\delta\rho_V(t) = \frac{\sum\limits_{n} W_n \sum\limits_{m} \alpha_m^V \left\{ [P_{nm}(t) - P_{nm}(0)]/P_{nm}(0) \right\}}{\sum\limits_{n} W_n}$$

where in this case a_m^v is the reactivity effect due to voiding segment m in all radial regions. Two-dimensional void reactivities may be used with the second option; i.e.,

$$\delta\rho_V(t) = \sum_n \sum_m \alpha_{nm}\left\{[P_{nm}(t) - P_{nm}(0)]/P_{nm}(0)\right\}.$$

The reactivity due to control rod action is given by

$$\delta\rho_R(t) = \sum_n \alpha_n^R f(R_n)[R_n(t) - R_n(0)]$$

where a_n^R is the reactivity worth of the control rods in region n, f(R) is an optional function which allows a rod reactivity axial distribution, and $R_n(t)$ is the rod position from 0 at full out to 1 at full in.

The axial expansion feedback is given by

$$\delta\rho_X(t) = \alpha_X \frac{\sum_n q_n^2 \Delta L_n(t)/L_o}{\sum_n q_n^2}$$

where a_X is the total core axial expansion reactivity coefficient, q_n is the power fraction in region n, ΔL_n is the change in core height (optionally given by expansion of fuel, cladding, or structural materials), and L_o is the initial core height.

1.4.2.   One-Dimensional Multigroup Feedback

The feedback model for the one-dimensional multigroup model takes the form

$$\delta\Sigma_n(t) = \frac{\partial\Sigma_n}{\partial\bar{T}_n^f}[\bar{T}_n^f(t) - \bar{T}_n^f(0)] + \frac{\partial\Sigma_n}{\partial\bar{P}_n^c}[\bar{P}_n(t) - \bar{P}_n(0)]$$

$$+ \Delta\Sigma_n f(R_n)[R_n(t) - R_n(0)]$$

for each of the group cross-sections, and

$$\delta(1/D_n(t)) = \frac{\partial}{\partial P_n} [1/D_n][\bar{P}_n(t) - \bar{P}_n(0)]$$

$$+ \Delta(1/D_n) f(R_n)[R_n(t) - R_n(0)]$$

for the group diffusion coefficients. In this case, $\bar{T}_f^n(t)$ is the volume-averaged fuel temperature in region n and $\bar{P}_n(t)$ is the volume-averaged coolant density in region n.

1.5. Primary Loop Model

1.5.1. Thermal Model

The primary coolant loop thermal model in TART considers nodes in the core outlet plenum, in each IHX (intermediate heat exchanger) primary side, tube wall, and secondary side, and in the pot (see Figure A-2). The coolant flow out of the core is assumed to mix and then to flow into the outlet plenum. The bulk reactor outlet temperature is determined by the energy balance

$$T_{out}(t) = \frac{\sum_n W_n \, c(T_{out}^n) \, T_{out}^n}{W_T \, c(T_{out})} \qquad (29)$$

where W_n is the coolant flow rate in thermal-hydraulic region n, T_{out}^n is the outlet temperature in region n, c is the specific heat, W_T is the total coolant flow rate, and T_{out} is the bulk outlet temperature.

The average temperature in the core outlet plenum is given by

$$(\rho c V)_{cp} \frac{dT_{cp}}{dt} = W_T[c(T_{out})T_{out} - \frac{\rho(T_{cp})c(T_{cp})}{\rho(T_{out})} T_{cp}]. \qquad (30)$$

Figure A-2. Pot-Type — Primary System Schematic Representation
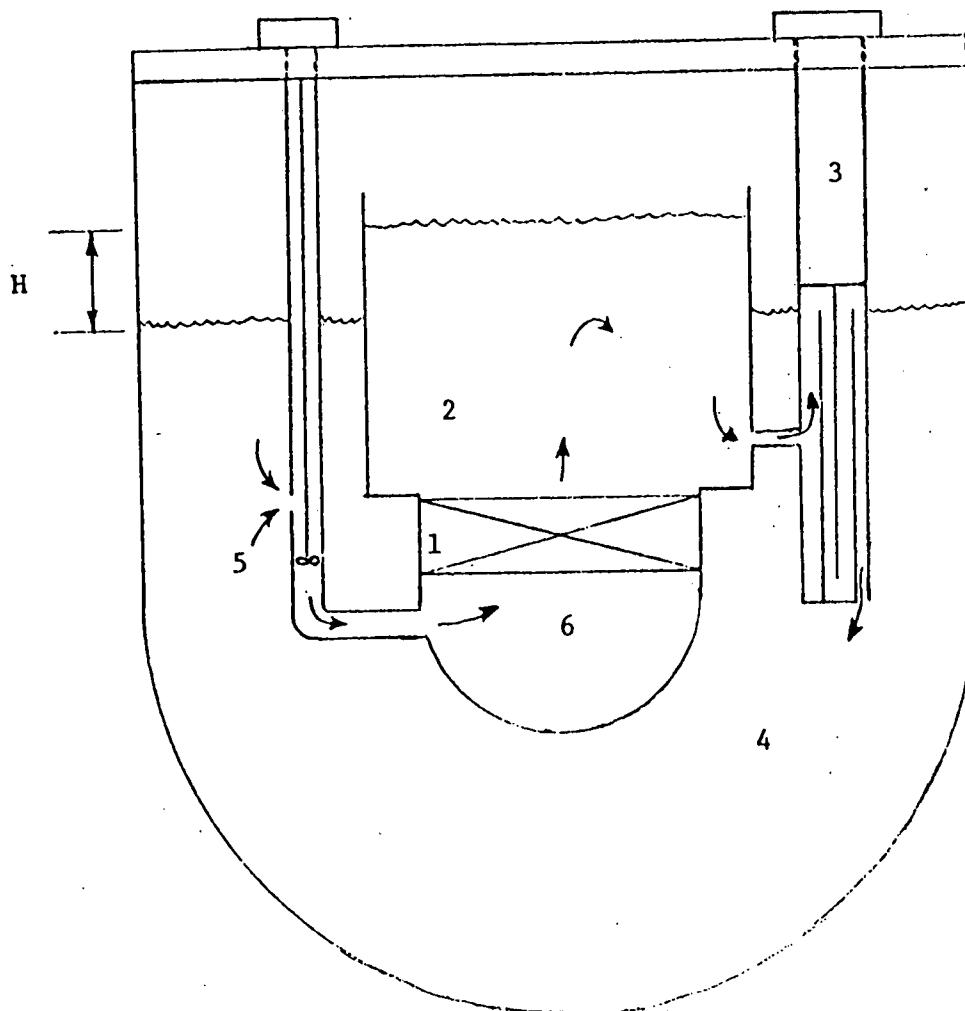
Key

1 - Core
2 - Core Outlet Plenum
3 - IHX
4 - Pot
5 - Primary Pump
6 - Core Inlet Plenum

The primary coolant temperature is assumed to vary linearly in the IHX, and the average, $\overline{T}_i^P$, is then given by

$$(\rho c V)_i \frac{d\overline{T}_i^P}{dt} = W_i \{ [c(T_{cp}) + c(\overline{T}_i^{OP})]T_{cp} - 2c(\overline{T}_i^{OP}) \overline{T}_i^P \}$$
$$- (UA)_i^P (\overline{T}_i^P - \overline{T}_i^W)$$

where W_i is the coolant flow rate through each IHX, $\overline{T}_i^W$ is the average tube wall temperature, $\overline{T}_i^{OP}$ is the IHX primary coolant outlet temperature, and $(UA)_i^P$ is the overall conductance from the primary coolant to the center of the tube wall.

The average tube wall temperature is given by

$$(\rho c V)_w \frac{dT_i^W}{dt} = (UA)_i^P (\overline{T}_i^P - \overline{T}_i^W) - (UA)_i^S (\overline{T}_i^W - \overline{T}_i^S)$$

where $(UA)_i^S$ is the overall conductance from the center of the tube wall to the secondary coolant and $\overline{T}_i^S$ is the average secondary coolant temperature. $\overline{T}_i^S$ is given as a fixed input quantity or as an input time table.

The average temperature of the coolant in the pot (the core inlet temperature) is calculated from

$$(\rho c V)_{pot} \frac{dT_{in}}{dt} = \sum_i W_i c(\overline{T}_i^{OP}) \overline{T}_i^{OP} - \rho(T_{in}) c(T_{in}) T_{in} \sum_i \frac{W_i}{\rho(\overline{T}_i^{OP})} .$$

Equations for the core outlet plenum temperature and core inlet temperature are solved using forward differences in time, and the equations for the IHX primary coolant and tube wall temperatures are solved using trapezoidal rule integration or central differences in time.

The initial steady state temperatures for the IHX primary coolant and tube wall are given as input quantities, and the over-all conductances $(UA)_i^P$ and $(UA)_i^S$ are calculated from these temperatures.

An option is also provided so that $(UA)_i^p$ for a given number of IHXs may be set to zero before the transient calculations begin in order to simulate loss of heat sink conditions.

1.5.2.   Flow Coastdown Model

The flow coastdown model in TART is based on a simplified model of the open loop pot system used in B&W's 1000-MWe LMFBR reference design. The only pressure drops considered are those due to frictional losses in the core and the IHXs. These are assumed to be given by

$$\Delta P_c = K_c W_c^2 \tag{31}$$

for the core, and

$$\Delta P_x^m = K_x (W_x^m)^2 \tag{32}$$

for each IHX; W_c is the total flow rate through the core, W_x^m is the flow rate through an IHX, and K_c and K_x are constants determined from critical values. The head H(t) (see Figure A-2) driving the flow through the IHXs is due to the difference in elevation between the sodium in the core vessel and the sodium in the reactor vessel. H(t) can be obtained by a mass balance on the sodium in each vessel; it is given by

$$H(t) = H(0) + \left(\frac{1}{\rho_c A_c} + \frac{1}{\rho_p A_p} \right) \int_0^t [W_c(\tau) - W_x(\tau)] d \tag{33}$$

where ρ_c and ρ_p are the sodium densities in the core and reactor (pot) vessels, respectively, A_c and A_p are the cross-sectional areas of the core and reactor vessels, and $W_x(\tau)$ is the total flow through the IHXs. Since H(t) is equal to the pressure drop across the IHXs, the flow through each IHX is given by equation 32 as

$$W_x^m(t) = [H(t)/K_x]^{1/2}. \tag{34}$$

The head ΔP_p developed by the pumps must be equal to the total pressure drop in the system; thus

$$\Delta P_p(t) = K_c W_c^2 + H \tag{35}$$

or

$$\Delta P_p = K_c \left\{ \sum_\ell W_\ell \right\}^2 + H. \tag{36}$$

After power to a pump is lost, the impeller rotational speed ω_ℓ is given by

$$\frac{d\omega_\ell}{dt} = - \frac{g W_\ell \Delta P_p}{I \omega_\ell} \tag{37}$$

where g is the gravitational constant and I is the pump moment of inertia. The characteristic relations for the pumps provide the final necessary equation in the form

$$W_\ell(t) \big/ \omega_\ell(t) = f\left(\Delta P_p \big/ \omega_\ell^2\right). \tag{38}$$

Equations 33, 34, 36, 37, and 38 must be solved as a function of time. The solution technique in TART uses a forward-difference method for equations 33 and 37 to obtain at time t_{n+1},

$$H^{n+1} = H^n + \Delta t \left\{ \left(\frac{1}{\rho_c A_c} + \frac{1}{\rho_p A_p} \right) [W_c^n(t) - W_x^n(t)] \right\} \tag{39}$$

and

$$\omega_\ell^{n+1} = \omega_\ell^n - \Delta t \frac{g W_\ell^n \Delta P_p^n}{I \omega_\ell^n} . \tag{40}$$

A temporary estimate of the pump pressure rise at time t_{n+1} is given by

$$\Delta P_p^{n+1} = (H^{n+1} - H^n) + \Delta P_p^n . \tag{41}$$

An input table is used for the pump characteristic function (equation 38). Rather than solving 36 and 38 iteratively, a linear function giving the flow through each pump as a function of ΔP_p is found from the table; i.e.,

$$W_\ell^{n+1}(\Delta P_p) \cong a_\ell^{n+1} + b_\ell^{n+1} \Delta P_p^{n+1} . \tag{42}$$

The coefficients a_ℓ^{n+1} and b_ℓ^{n+1} are found using the points in the table on either side of the point given by $W_\ell^n / \omega_\ell^{n+1}$ and $\Delta P_p^{n+1} / (\omega_\ell^{n+1})^2$. Equation 42 is substituted into 36 to obtain

$$\Delta P_p^{n+1} = K_c \left\{ \sum_\ell [a_\ell^{n+1} + b_\ell^{n+1} \Delta P_p^{n+1}] \right\}^2 + H^{n+1} . \tag{43}$$

This results in a quadratic equation in ΔP_p^{n+1}, and the smaller root gives the correct solution for ΔP_p^{n+1}. The values of W_ℓ^{n+1} are then found from the table using ΔP_p^{n+1} and ω_ℓ^{n+1}, and the IHX flow rates $(W_x^m)^{n+1}$ are calculated from equation 34.

1.6. Control System Simulation

1.6.1. Reactivity Control

The control system incorporated into TART corresponds roughly to that in B&W's 1000-MWe LMFBR. Both safety and shim-regulating control rods are included, and a bank of either type rod is allowed in any temperature-hydraulics region. Two rod speeds are permitted, thus allowing one speed for normal control movement and another for scrams. A delay time between the scram command from a monitor and the beginning of rod insertion is allowed.

In general, the control system logic follows this pattern:

1. Monitor all necessary system variables.

2. Determine correct mode of action according to preset conditions on the system variables.

3. Follow this mode of action until all conditions for action are satisfied or until all rods are completely inserted.

The details of control action for the three modes of action in TART are given below.

Normal Control Mode

Monitor	Condition for action	Action
(1) Total reactor power	Deviation greater than $\pm x\%$[a] from demand power	Normal speed insertion or withdrawal of one bank of shim-reg rods (in order of bank number)
(2) Bulk outlet temperature	Deviation greater than $\pm x\%$[a] from demand temperature	
(3) --	External demand[b]	

Fast Setback Mode

Monitor	Condition for action	Action
(1) Power to flow ratio	Greater than x[a] times initial power to flow ratio	Simultaneous normal speed insertion of all shim-reg rod banks until a power level of x[a] is reached. Return to normal control.
(2) --	External demand[b]	

Scram Mode

Monitor	Condition for action	Action
(1) Reactor power	Exceeds maximum	Simultaneous high speed insertion of all rods
(2) Instantaneous period	Less than minimum	
(3) Bulk outlet temperature	Exceeds maximum	
(4) Rate of increase of (3)	Exceeds maximum	
(5) --	External demand	

[a] Input quantity.

[b] "External demand" implies that an action command is sent from a monitor not included above, or from an external operator or controller.

The priority of action commands is as follows:

1. Scram commands have priority over all other commands.

2. Fast setback commands have priority over normal control commands.

3. Normal control insertion commands have priority over withdrawal commands.

1.6.2. Flow Control

In the flow control model[6] provided as an option in TART, the speeds of the primary coolant pumps are varied to hold the reactor inlet temperature constant. The demand change in pump speeds is given by a two-mode controller as

$$\Delta\omega_d = -K_1[T_{in}(t) - T_{in}(0)] - K_2 \int_o^t [T_{in}(\tau) - T_{in}(0)]d\tau$$

wher K_1 and K_2 are input gain constants. The time response of the coolant pump eddy current coupling is described by a first-order equation; that is,

$$\frac{d\Delta\omega}{dt} = \frac{\Delta\omega_d - \Delta\omega}{\tau_\omega}$$

where τ_ω is an input time constant and $\Delta\omega = \omega(t) - \omega(C)$. This equation is time-differenced using a forward-difference to obtain

$$\Delta\omega^{j+1} = \Delta\omega^j + \frac{h_j}{\tau_\omega}[\Delta\omega_d^j - \Delta\omega^j];$$

then

$$\omega^{j+1} = \Delta\omega^{j+1} + \omega^o.$$

Once the pump speeds are known, the system flows can be calculated using the same technique as in the flow coastdown solution (section 1.4.2).

2. FARED System

2.1. Introduction

For the next several years, industrial fast reactor activities will involve the analysis of a wide variety of conceptual or preliminary designs, and optimization and parametric studies involving these designs will be continued even through the demonstration phase. This search for systems with acceptable safety and economic characteristics requires an unusually large number of routine static physics calculations, many of which can be performed with a one-dimensional geometrical model of the system. It is important, however, for the calculational models used in these studies to admit a reasonably realistic physics model of the assembly and still be flexible enough to require little or no user intervention during wide-ranging criticality and depletion studies. In addition, the models should be economical enough to be used routinely with good throughput and turnaround time, and accurate enough to permit the calculation of reliable safety parameters. The FARED code was designed to these specifications with the added constraint that it be as nearly machine-independent as possible and require no more than $50,000_{10}$ words (60 bits/word) of core storage.

The basic FARED package comprises two codes:

1. RETAP — A code for preparing a microgroup library for use by the cross section averaging and depletion routines. Free-format input is used for library generation and updating.

2. FARED — A one-dimensional static physics design code with an internal cross section collapse program; criticality, depletion, and search routines; fuel management capability; and a variety of edits including an extensive perturbation edit. Execution of the various routines in FARED is controlled by user directives, and all input is free-format.

The cross section averaging in FARED is performed in program REGA which computes a fundamental-mode (B_1) flux and current in up to 20 reactor block compositions for use as weighting functions in the cross section collapsing calculation. REGA will collapse the RETAP group structure (100 or less) to no more than 30 polygroups with up to 15 groups of

Table A-1. RETAP Data Files

FILE ONE

  Tape Description
  Fine Group Bounds

FILE TWO

  Decay Chains
  (including fission product and control materials)

FILE THREE

  Resolved Resonance Data
  Potential Scattering Xsection

FILE FOUR

  Unresolved Resonance Data

FILE FIVE

  Capture, Fission, N2N, EXAB Xsections
  NU
  P_0 Matrix (elastic + inelastic + 2 N2N)
  P_1 Matrix

FILE SIX

  Sources

FILE SEVEN

  Fission Products and Yields
  Decay Constants
  Delayed Neutron Data

downscatter. A microscopic cross section set will be generated for each reactor block for use by the criticality and depletion routines. A reactor block may be a single zone or a combination of zones of similar material content (e.g., core, blanket, reflector), and each block may contain up to 30 different nuclides. A homogeneous or heterogeneous resolved and unresolved resonance treatment is provided to compute effective microgroup resonance cross sections for the block mixture or for up to two cell types per block.

The criticality, depletion, search, and edit calculations are performed in the RAIM routine. A variety of directives is available to the user for controlling the execution of a criticality-search-depletion fuel management problem. For example, after a depletion command, tests may be specified for k_e, isotope concentration, and burnup of various material units to limit the specified depletion time and maintain a fixed k_e during burnup. A command to REGA for recalculation of the block cross section sets may be made at any time. The fuel management directive permits the user to shuffle material units (called "zone materials") within the core and move units out and others in as feed material. FARED automatically displays the material configuration of the reactor after a fuel management directive, summarizing the status of each zone material. Depletion is performed by zones in the same number of groups specified for the polygroup cross section set.

2.2. Preparation of FARED Library Tape

The RETAP program processes basic cross section, resonance parameter, decay chain, fission product, source, and delayed neutron data to produce a 100 fine-group or less library tape for use by the REGA routine. Table A-1 summarizes the contents of the tape. At the beginning of the project, the source of the P_0 and P_1 matrices and smooth (nonresonance) cross sections was to be the MC^2 code, since it was felt that these cross sections should reflect ultrafine spectrum weighting over the resonance scattering structure in the range of high anisotropy in the CM system. The data processing complex shown in Figure A-3 was implemented on the CDC-6600 at New York University for this purpose. In addition, a special 68 broad-group version of MC^2

was produced with improved binary record handling capability.[*] Since
this work was being done during the early days of the ENDF/B project,
the work of implementation was laborious and expensive. Inconsistencies
and errors would often be uncovered only after execution of MC^2 itself,
and correction would require a new series of runs involving CRECT,
DAMMET, and ETOE. The processing complex is operational, but
little use of its capability has been made, since the implementation
process took longer then originally anticipated and some calculational
algorithms in MC^2 are still suspect.[**] However, a 68-group FARED
library has been produced for 50 nuclides using ENDF/B data for all
but the elastic transfer matrices, which were taken from an ORNL
GAM-I set. The library appears fully satisfactory for production test-
ing and initial design use of the code. Since RETAP permits directive-
controlled, free-format updating, the replacement of nuclide data on
any file is very simple.

2.3. FARED Code

The logic flow in the FARED code is illustrated in Figures
A-3 through A-9. Through the CONFIGURATION directive, the user
supplies secondary directives and associated data sets which permit
the following material and configuration information to be generated:

1. The homogeneous composition of each zone.

2. The homogeneous composition of each BLOCK. In FARED,
zones are assigned to blocks to identify spatial regions of the reactor

- - - - -

[*]These improvements were suggested by a graduate student working
under M. Becker at RPI. Using the ANL test case, the following
run times were observed:

	Fine group	Ultrafine group
MC^2((Standard)	cp 539.8	--
	pp 364.1	--
MC^2 (B&W-RPI)	cp 398.4	cp 315.7
	pp 375.2	pp 867.6

[**]For 0.25 lethargy width fine groups, MC^2 will generate negative diagonal
elastic transfer elements in the resonance region.

whose material content is similar, permitting the use of a single poly-group microscopic cross section set (generated by REGA) for nuclides in these zones.

3. The heterogeneous composition of one or two lump mate-rials per block which are to be used for preparing effective resolved and unresolved resonance cross sections for resonance nuclides appear-ing in the problem. A homogeneous resonance treatment will be used if no CELLS are defined by the user.

4. Zone and block geometry.

5. Identification of unique materials units ("zone materials"), such as a nuclide list occupying a given volume of a zone, which are used to specify desired fuel shuffle patterns, searches, worth calculations, etc.

Material specification begins with bulk materials (BM), usually pellet, cladding, control, and coolant compositions which are used with two levels of mixing fractions to form the zone materials (ZM) and other homogeneous and heterogeneous compositions. A typical CONFIGURA-TION deck for a five-zone, 1000-MWe LMFBR is shown in Table A-2. The FUELMGMT directive is used to process commands relating to the movement of zone materials, or fractions of zone materials, into, out of, or within the reactor at any time during a depletion cycle.

The REGA directive causes the formation of homogeneous block compositions (by volume averaging) and the formation of "average" resonance lump compositions (by appropriate indexing and volume aver-aging of pellet materials). The resolved and unresolved resonance cal-culations are then performed followed by the fine group cross section collapse calculation using the fundamental mode spectrum for each block. The unresolved resonance calculation is similar to that used in the GANDY code.[7] In the resolved resonance range, a multigroup collision probability procedure is used to compute the average flux in the lump or mixture for each group in an ultrafine group mesh which spans the entire resolved resonance range; the boundary for each such group is computed by a special algorithm[8] in REGA as the calculation proceeds down the energy range. Polygroup cross section sets for each block are generated for up to 30 groups with 15 downscatter groups.

Table A-2. Sample CONFIGURATION Deck

FARED TEST CASE – BABCOCK AND WILCOX REFERENCE LMFBR

```
CONFIGURATION
GDATA  CYL  17  5  2342.2  88.222  3  1  5  1  .1-3  40  .0  .2
BULK   BM1  1  FUEL      PU239  .2016-2   PU240  .7823-3
                         PU241  .1504-3
               DILUENT   U238   .1785-1
               MIX       016    .4182-1
               0.5398    ZM1
       BM2  1  FUEL      PU239  .2172-2   PU240  .8429-3
                         PU241  .1621-3
               DILUENT   U238   .1762-1
               MIX       016    .4184-1
               0.5398    ZM2
       BM3  1  FUEL      PU239  .2524-2   PU240  .9794-3
                         PU241  .1884-3
               DILUENT   U238   .1712-1
               MIX       016    .4188-1
               0.5398    ZM3
       BM4  1  U238  .2196-1    016  .4404-1
               0.7341    ZM4
       BM5     NA23  .2159-1
               0.3510    ZM5
               0.1991    ZM6
               1.0       ZM7
       BM6     SS304  .8613-1
               0.1092    ZM8
               0.0668    ZM9
               1.0       ZM10
ZONE   Z1  CORE   90.426   20  0.7836  ZM1  ZM5  ZM8  0.1398  ZM7
                                0.0766  ZM10
       Z2  CORE  122.282   10  0.8304  ZM2  ZM5  ZM8  0.0930  ZM7
                                0.0766  ZM10
       Z3  CORE  153.359   10  0.8429  ZM3  ZM5  ZM8  0.0805  ZM7
                                0.0766  ZM10
       Z4  BLANKET  184.088  10  0.8767  ZM4  ZM6  ZM9  0.0467  ZM7
                                 0.0766  ZM10
       Z5  REFLECTOR  214.088  10  0.5  ZM7  0.5  ZM10
BLOCK  B1  Z1  Z2  Z3  0.950-3  1   01
       B2  Z4  0.950-3  1   C2
       B3  Z5  0.950-3  1
CELL   C1  1  HEX  0.66040  0.85598  1643.3  0.2657
       C2  1  HEX  1.45796  1.62052  1366.4  0.2774
```

The RAIM directive causes the processing of a number of important secondary commands which initiate (1) flux and eigenvalue calculations, (2) searches, including special power flattening searches which permit zone enrichments to be determined, yielding a prespecified eigenvalue and degree of power flattening, (3) depletion, with automatic control material composition search and termination tests based on zone material burnup, control depletion, and eigenvalue, and (4) all edit calculations. Simple edit directives permit a high degree of selectivity in output information and include an extensive list of special perturbation calculations. A sample REGA-depletion-fuel management deck is shown in Table A-3.

The code and operating manual are described in reference 9. The code is now undergoing "experimental" testing at three installations and will be released to the Argonne Code Center by October 15, 1969.

2.4. Production Tests and Sensitivity Studies

Two CSEWG benchmark cases (ZPR-3 Assembly 48 and ZPR-3 Assembly 11) described in CSEWG Newsletter 18[10] have been calculated using the FARED program and 27 collapsed groups (collapsed from 68 groups with B1 spectra). The results for Assembly 48 are compared with reported measured data in Table A-4. Two ANL calculations are also given for comparison. The ANL calculations are based on the ENDF/B-ETOE-MC^2-MACH 1 calculational scheme. In general, the calculated results of Assembly 48 and Assembly 11 are in good agreement with experiments.

In addition, sensitivity studies were made using B&W's 1000-MWe Follow-On reference design. Preliminary results of these calculations show that:

1. Criticality, breeding ratios, external breeding ratios and final masses (100,000 MWd/tonne) are insensitive to cross section re-averaging during depletion, and are insensitive to the buckling values used for spectrum generation. The conclusions may be altered for a finer spectrum calculation.

2. A homogeneous versus heterogeneous resonance treatment resulted in an initial k_{eff} difference of 0.8% with the heterogeneous resonance treatment giving the higher k_{eff}. After a burnup of 100,000

MWd/tonne, the final core masses were in good agreement. The final blanket masses for the higher plutonium isotopes, however, were considerably different. The final differences in k_{eff} was 0.2% Δk.

3. FIRE

The FIRE program is a modified version of SOFIRE B. Two major modifications were incorporated: reactor building fires and a reactor building spray fire. Both modifications were extensions of the SOFIRE B computer program. The overall flow of the FIRE program is given in Figure A-10.

The spray fire subroutine is based on the experimental data that are available. The curves used for the pressure and temperature change in the reactor building are illustrated in Figures A-11 and A-12. These curves are applicable only up to a mole ratio, Na/O_2, of 5. This covers the cases studied to date. Should we exceed this limit, then corrective programming will be needed. It should be pointed out that the experimental systems were much smaller than the reactor building, so that the analyses using this approach will be conservative since mixing will not be as good. As more experimental data become available, the evaluation curves will be updated and extended as needed.

The reactor building fire uses essentially the same burning rate evaluation as in the SOFIRE B program. However, the heat transfer model has been modified to extend the calculation to relatively thin sodium pools or films since the pool depths are expected to be small. This modification has not been completely checked out.

The reactor vessel fire was modified to permit the inclusion of a burning rate constant. This will permit one to study the effects of various burning rates on the system pressures and temperatures.

The heat conduction coefficient between the sodium and the sodium flame needs to be examined. The calculation in SOFIRE B may need some modification based on the atmospheric components in the reactor building and reactor vessel.

Table A-3. Sample RAIM Deck

```
REGA    REGRES    REGMICRO
RAIM
SEARCH    COMPOSITION    ZM11    ZM12    ZM13    1.0    .00001
EDIT    BALANCE    REACTOR
ADJOINT
EDIT      VPERT    Z1    NA23    MO.
          VPERT    Z2    NA23    MO.
          VPERT    Z3    NA23    MO.
DEPLETE    0.0    3    100.0    1    ZONEMAT
TEST    BMAXIMUM    3.3+4    ZM1    ZM2    ZM3
        CONTROL    ZM11    ZM12    ZM13    1.0    .00001
DEPLETE    TIME    10    50.0    1    SETEDIT    SETTEST
FUELMGMT
MOVE    ZM1    Z1    .666667    ZM31
                    .333333    OUT
        ZM2    Z2    .666667    ZM32
                    .333333    OUT
        ZM3    Z3    .666667    ZM33
                    .333333    OUT
        ZM21   Z1    .2612      IN
        ZM22   Z2    .2768      IN
        ZM23   Z3    .28097     IN



EDIT    BALANCE    REACTOR
ADJOINT
EDIT    VPERT    Z1    NA23    MO.
        VPERT    Z2    NA23    MO.
        VPERT    Z3    NA23    MO.
FINIS
```

Table A-4. Assembly 48 Results

	Calculated			Measured
	B&W	ANL(1)*	ANL(2)	
K_{eff}	0.9949	0.9872	0.9730	1.000

Spectral Indices at Core Center
Assembly 48

	B&W	ANL(1)	ANL(2)	Measured
$\sigma_f(U238)/\sigma_f(U235)$	0.0295	0.0303	0.0304	0.0307
$\sigma_f(U233)/\sigma_f(U235)$	1.418	1.422	1.421	1.480
$\sigma_f(Pu239)/\sigma_f(U235)$	0.910	0.928	0.919	0.976
$\sigma_f(Pu240)/\sigma_f(U235)$	0.222	0.225	0.226	0.243
$\sigma_{n,\gamma}(U238)/\sigma_f(U235)$	0.134	0.142	0.142	0.138

Material Worths at Core Center
Assembly 48
x 10^5 $\Delta K/K$ mole

	B&W	ANL(1)	ANL(2)	Measured
Pu-239	128.5	126.6	134.2	106.1
Pu-240	17.2	19.0	20.7	19.4
U-235	99.1	94.22	101.9	79.3
U-238	-7.6	-7.8	-7.9	-5.9
Fe	-0.79	-0.79	-0.84	-0.69
Cr	-0.93	-1.03	-1.11	-0.49
Ni	-1.35	-1.01	-1.10	-1.07
Mn	-2.40	-2.96	-2.26	-1.18
Al	-0.46	-0.38	-0.42	-0.42
Na	-0.04	-0.03	-0.07	-0.14
C	-0.06	-0.07	-0.02	-0.05
O	-0.05	-0.04	-0.10	-0.11

*Based on experimental eigenvalue of 1.013.

Figure A-3.   ENDF/B System for Fast Reactor Data Processing
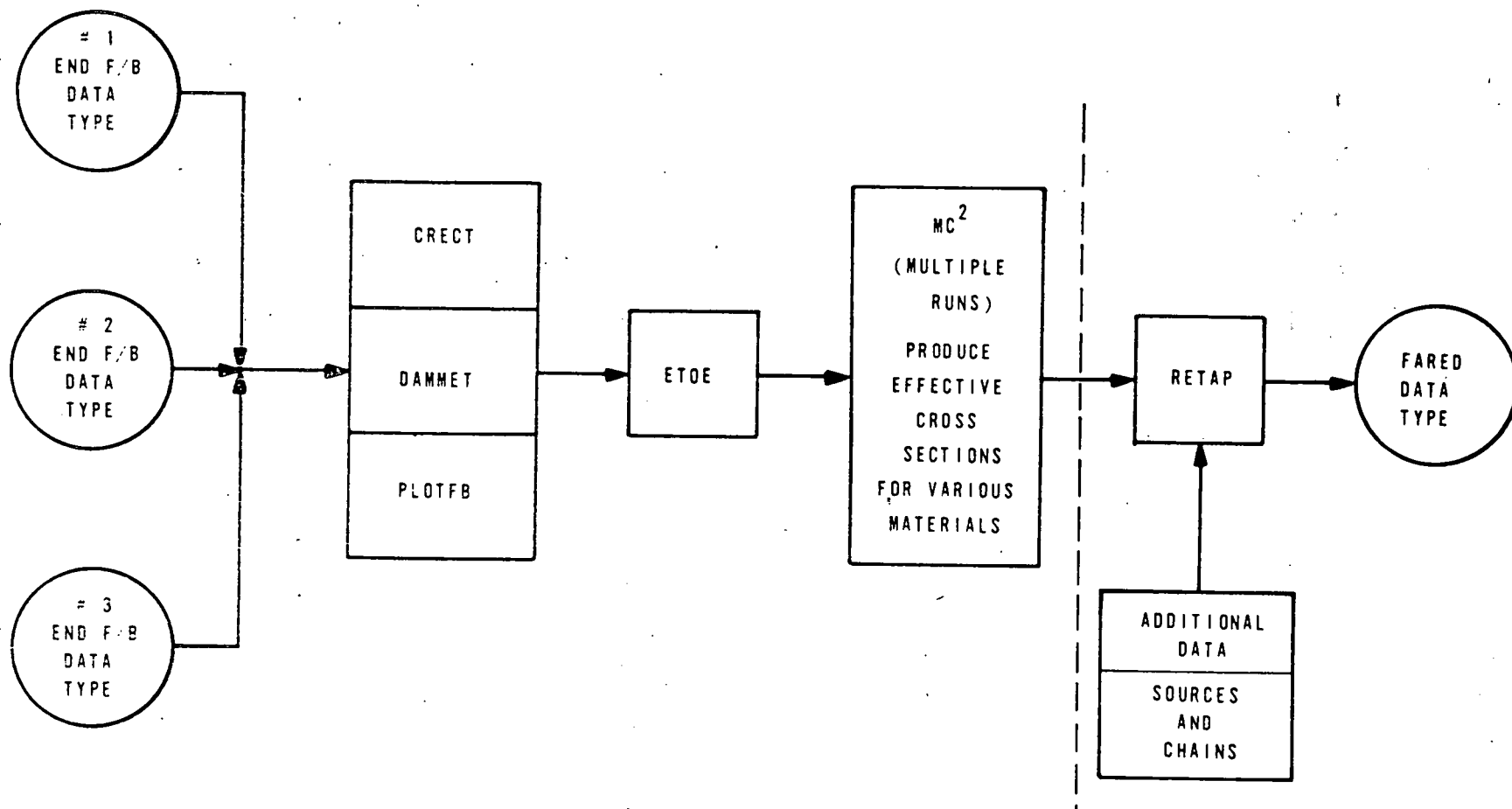
Figure A-4. Overlay (0,0) Program FARED
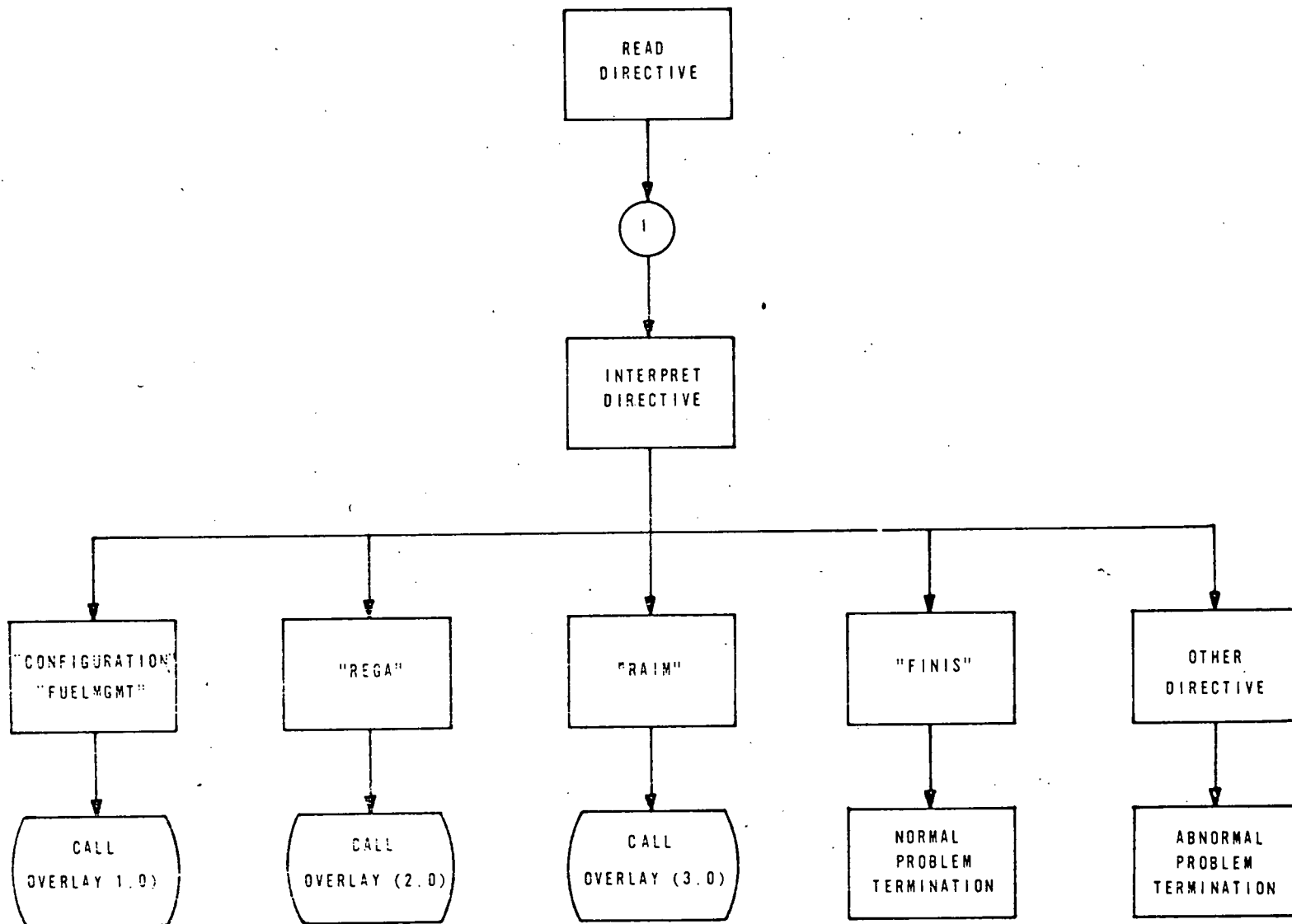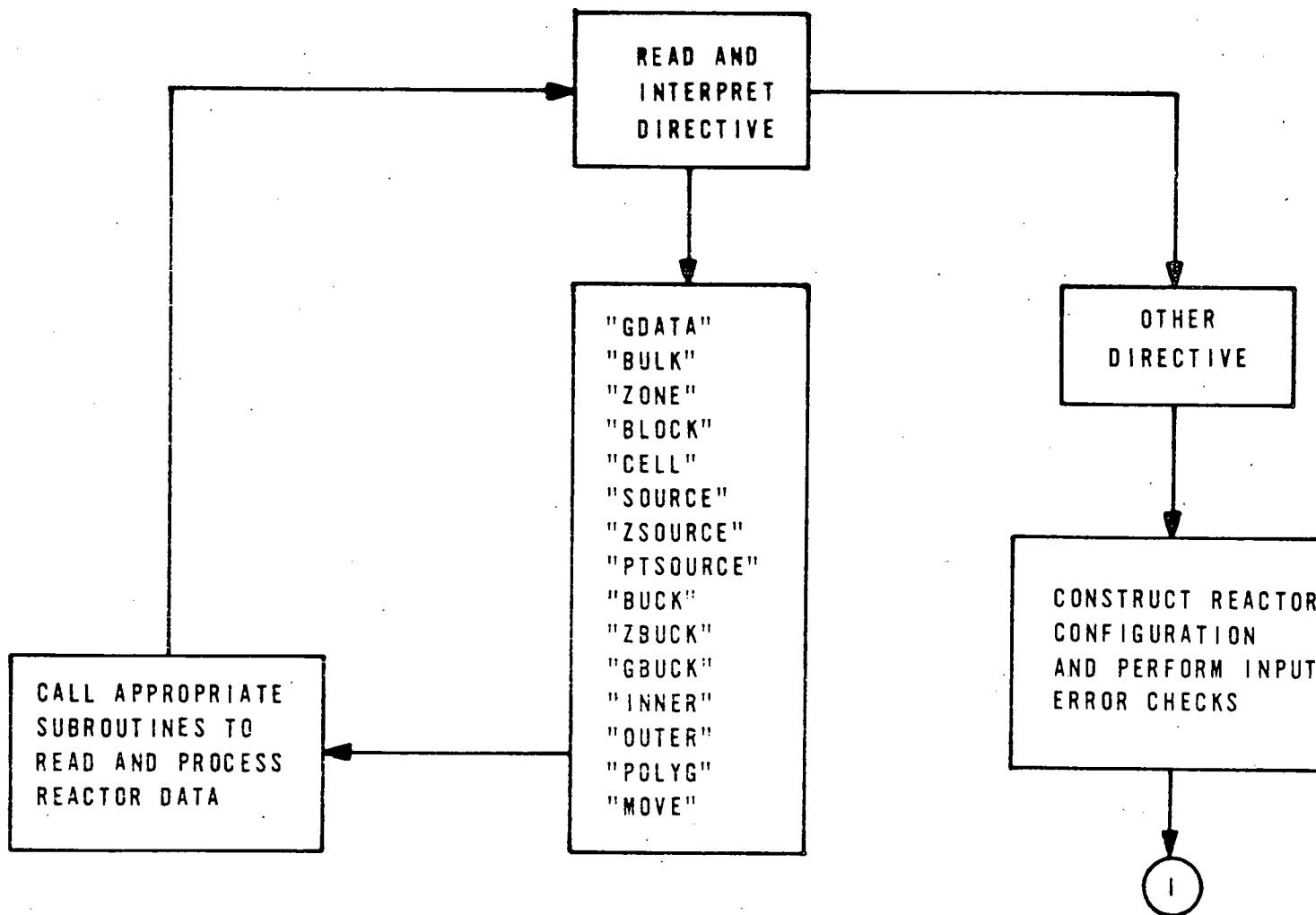
Figure A-5. Overlay (1, 0) Program INPUT

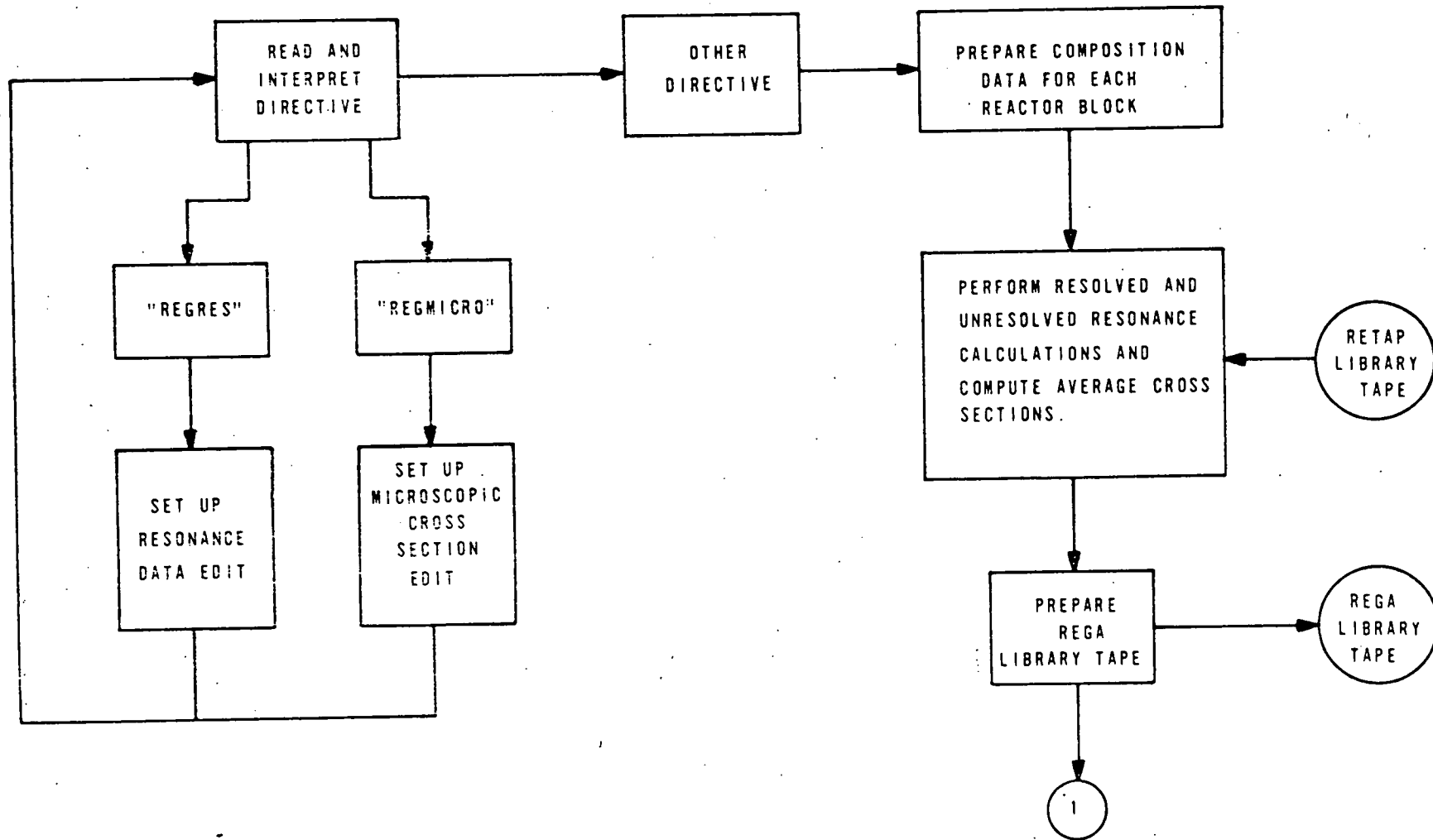Figure A-6.   Overlay (2, 0) Program REGA

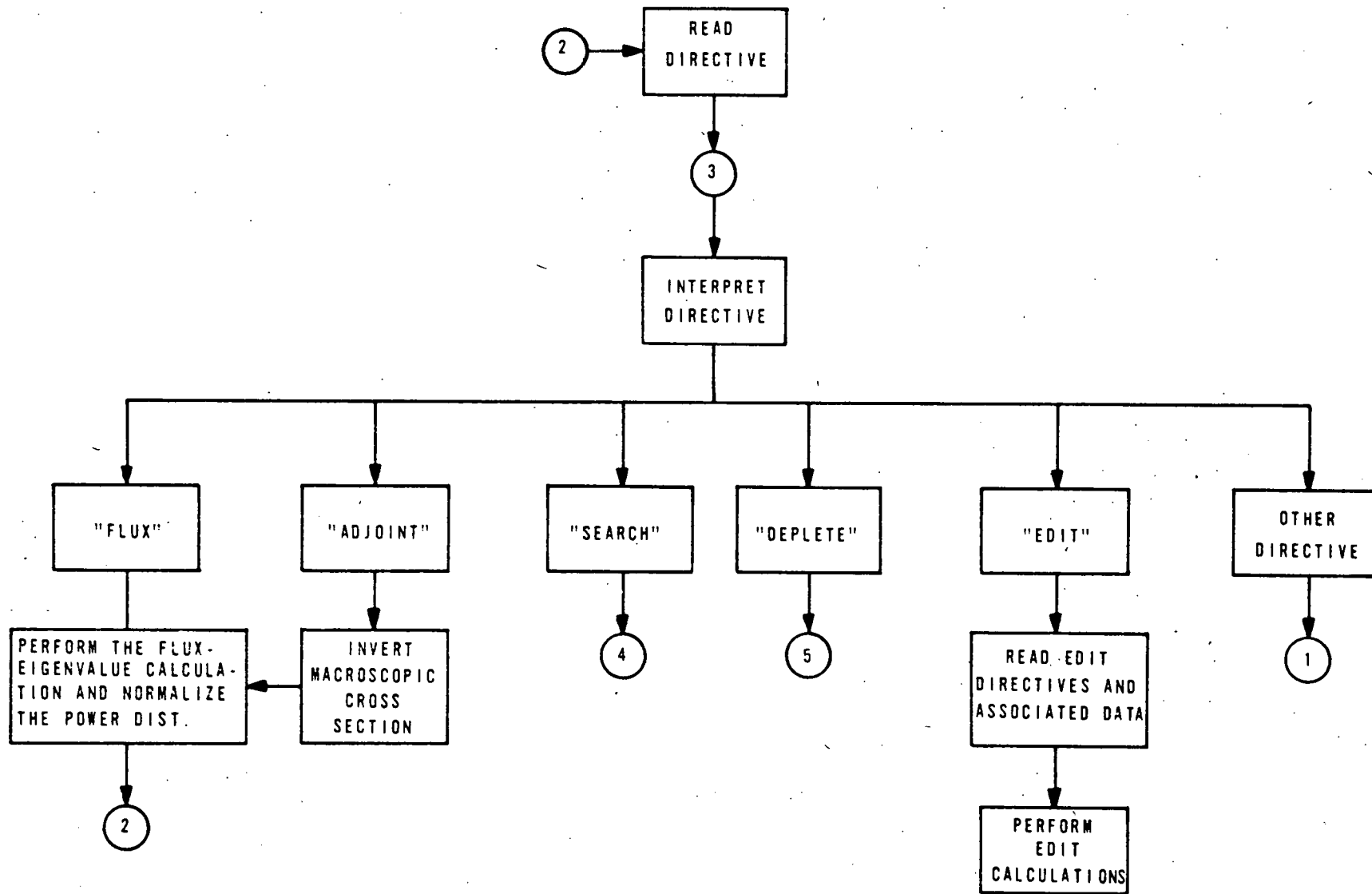Figure A-7. Overlay (3,0) Program RAIM (Cont'd)

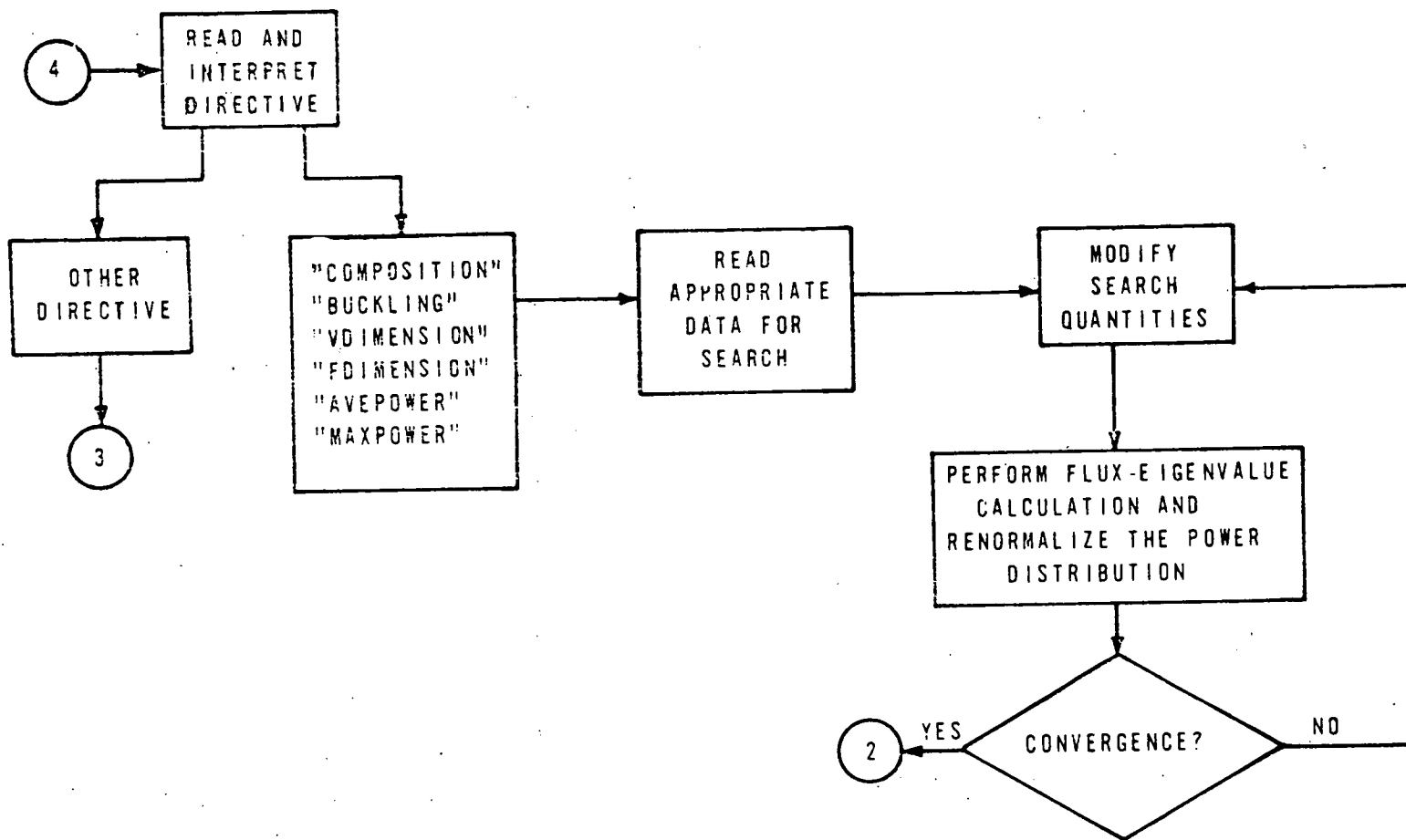Figure A-8.   Overlay (3,0) Program RAIM (Cont'd)
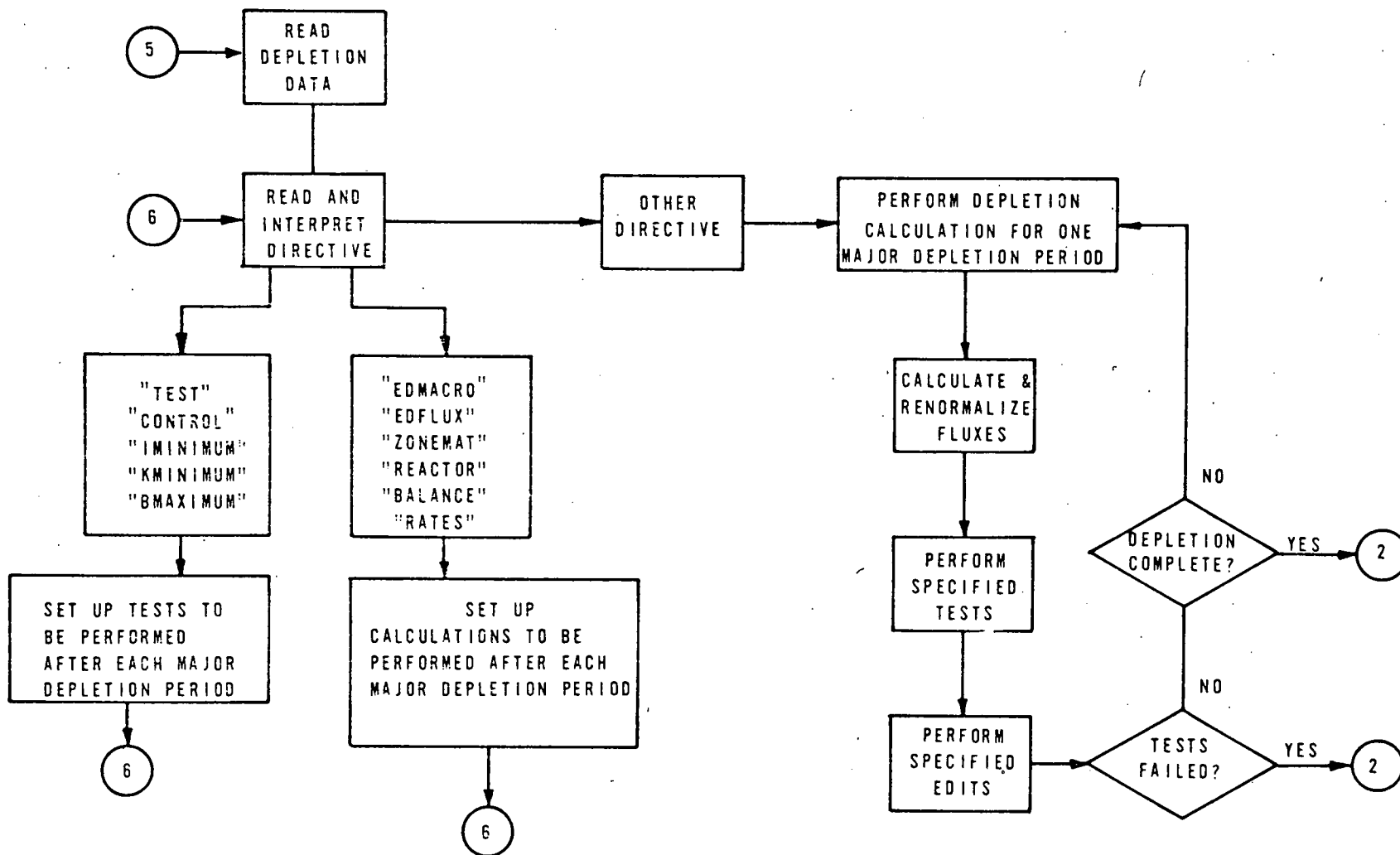
Figure A-9. Overlay (3,0) Program RAIM (Cont'd)
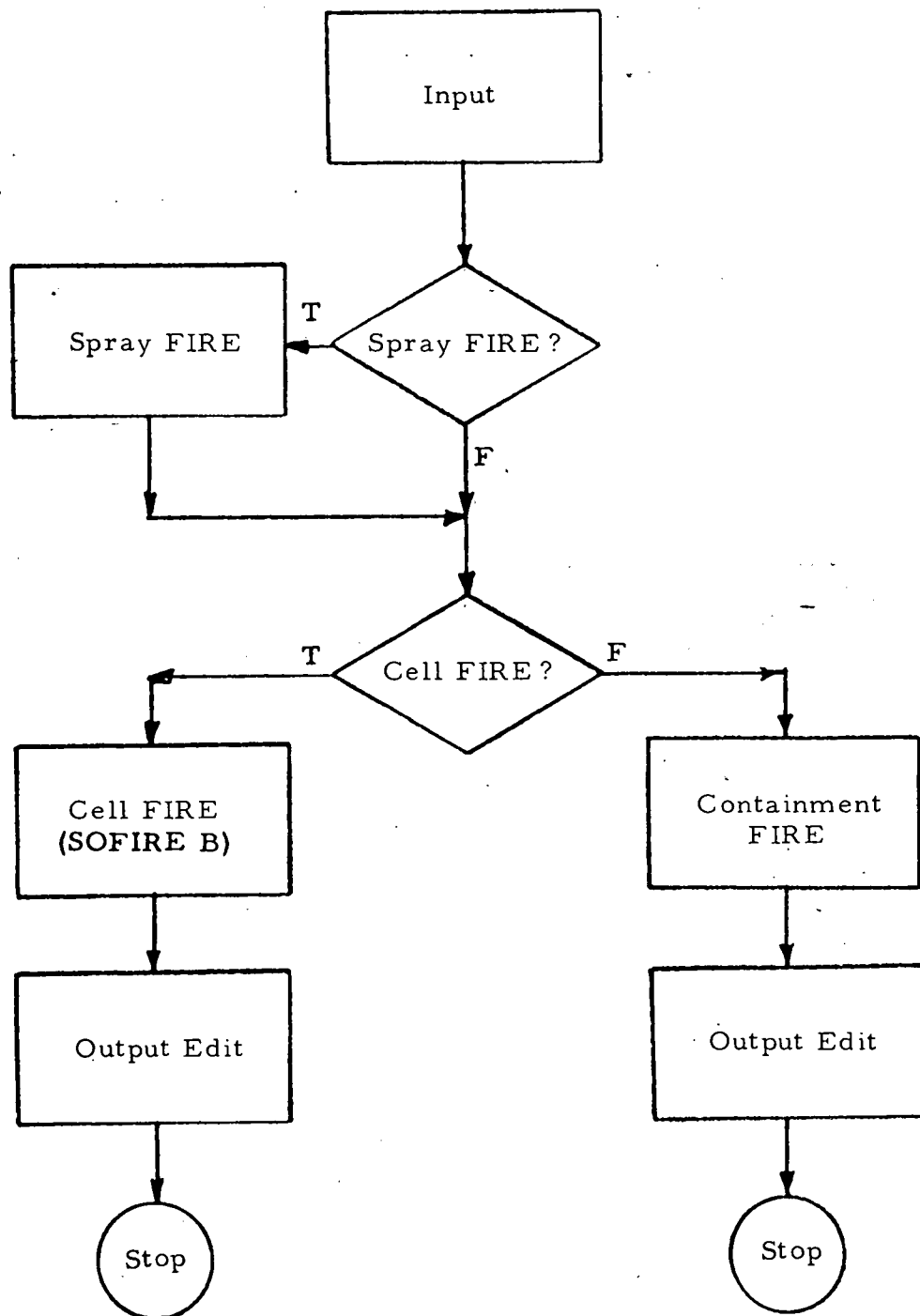
Figure A-10. FIRE — Sodium Fire Evaluation Program

Figure A-11. Spray Fire Pressure Evaluation Curve and Experimental Data Comparison
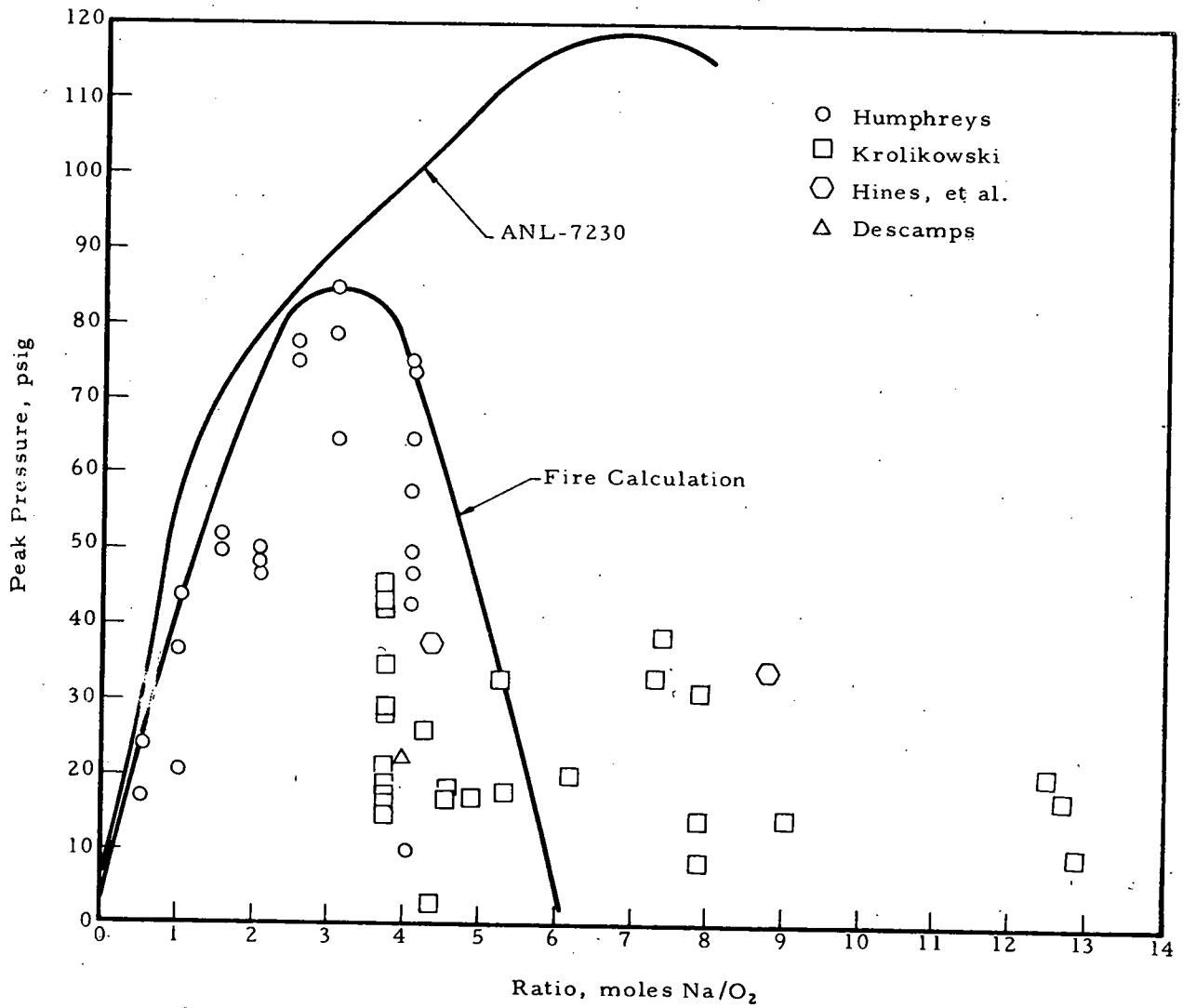

Ratio, moles Na/O_2

Peak Pressure, psig

O Humphreys
□ Krolikowski
⬡ Hines, et al.
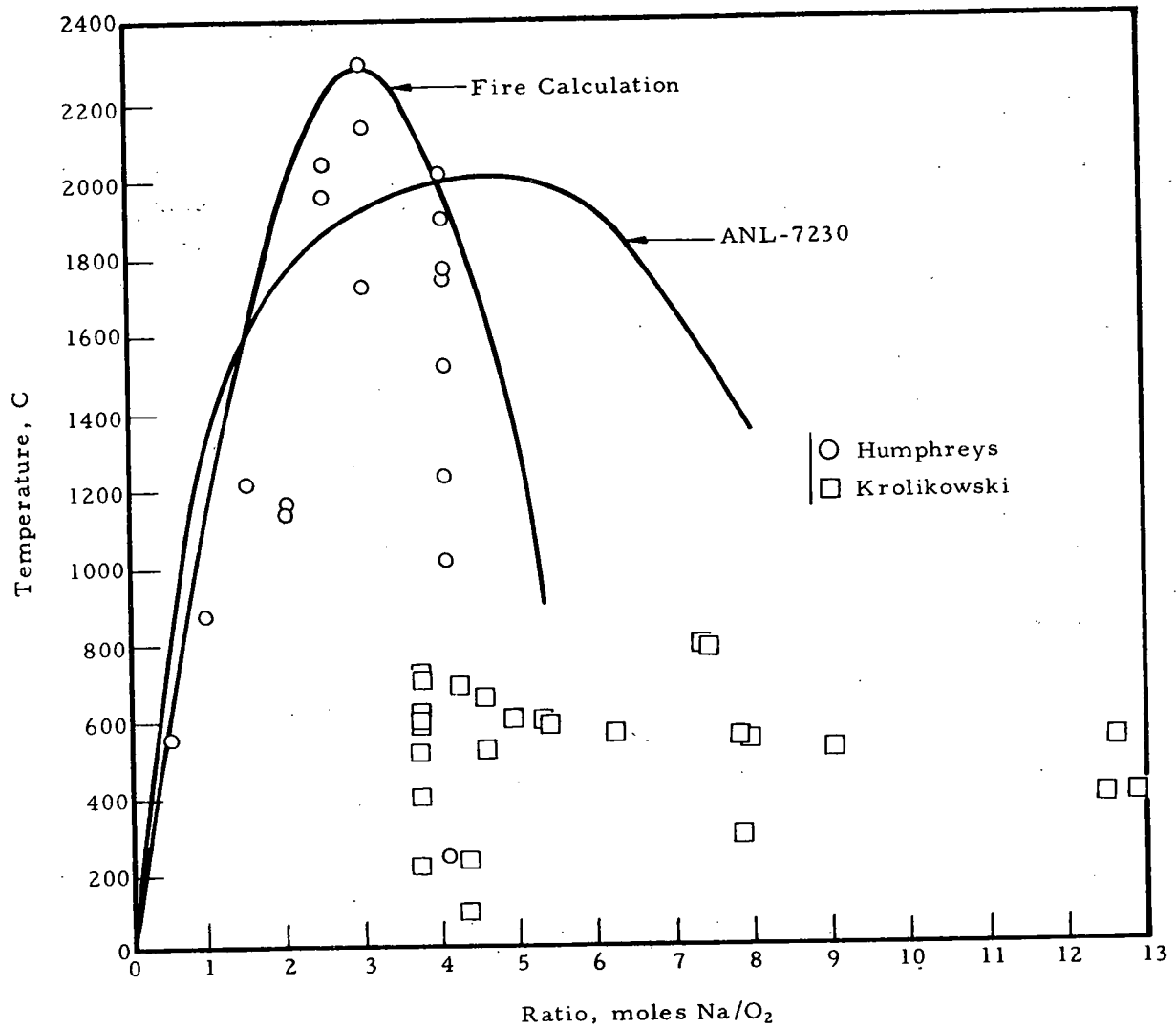△ Descamps

ANL-7230

Fire Calculation

Figure A-12. Spray Fire Temperature Evaluation Curve and Experimental Data Comparison

4. CLOUD

The CLOUD program as obtained from the Argonne Code Center is described in the CLOUD manual. For convenience, the abstract and introduction are reproduced here and followed by a discussion of limitations and a description of some modifications; results of test cases are discussed.

CLOUD is an IBM 709 code which calculates the external gamma-ray dose rate and total integrated dose resulting from the continuous release of radioactive materials to the atmosphere. The code was programmed in FORTRAN II for a 32 K machine. Considered are such meteorological parameters as wind velocity, lateral and vertical diffusion coefficients, stability parameters, and the presence of physical boundaries such as a ground surface and a temperature inversion layer. Depletion of the cloud due to washout and fallout has also been included. A two-compartment continuous release model is assumed. Decay of the source material is described by the use of a simple parent-daughter decay scheme or by a Way-Wigner type relationship.

In evaluating the potential radiological hazards associated with the design of a nuclear power plant, the possibility of an accidental release of radioactive aerosols or gases to the atmosphere must be considered. The degree of hazard to individuals in or near the resultant cloud formation must be estimated from the standpoint of both internal and external exposure. This report deals with a method for calculating the external gamma-ray exposure resulting from the continuous release of radioactive matter to the atmosphere.

The radiological hazard from inhalation is generally more severe than that resulting from external gamma exposure, particularly when considering the release of gross fission product inventories. However, situations often arise in which external exposure from a radioactive cloud is more important.

For example, a "breathing receptor" may be located at a position downwind from the release point where it will not be subjected to inhaling or ingesting the released material. Furthermore, the biological effects associated with the radioactive material (e. g. , the effective body intake, the radioactive half-life, the type of decay, etc.) may result in a predominance of external exposure even when the receptor is located within the cloud.

Hand calculational techniques based on an instantaneous release model are available[11] for calculating the external exposure from a cloud; however, these techniques are quite tedious and require the use of many simplifying assumptions that are not necessary when using a high-speed computer. Furthermore, calculations designed to accommodate an instantaneous release may be used to a fair degree of approximation only when the period of time over which the release takes place is short. Since hazards evaluations involving continuous release often play an important role in determining site or facility locations, site boundaries, containment reliability, etc., the need for accurate and rapid methods of calculation becomes obvious. Consequently, CLOUD was developed for calculating the external gamma-ray dose rate and the total integrated dose resulting from a continuous release of radioactive materials to the atmosphere.

The analytical expressions used and the input data are described in the reference document[12] and are not discussed here. However, corrections to the document concerning our version of CLOUD are discussed. Two errors discovered in the input data description would affect only those cases where the parent-daughter source decay option was selected (not selected in the sample problem). The original and corrected input quantities are as follows:

	Symbol	Definition
Original	$DE_{p,s}$; $DE_{D,s}$	Decay energies associated with the parent and daughter isotopes, respectively, of the sth chain, MeV.
Corrected	$DE_{p,s}$; $DE_{D,s}$	Decay energy group number associated with the parent and daughter isotopes, respectively, of the sth chain.
Original	V_i	Flux to dose rate conversion factor for the ith energy group, R/h/MeV/cm^2-s.
Corrected	V_i	Flux to dose rate conversion factor for the ith energy group, R/h/MeV/cm^2-s.

An obviously incorrect program statement was also changed. This statement is an expression for the source activity for the daughter isotope

as a function of time. Statement number 2W137378 in subroutine STCAL was changed from $E(NZ) = (DN(NX)*DLT)+OP*(PLT-DLT)*A4PI$ to $E(NZ) = ((DN(NX)*DLT)=OP*(PLT-DLT))*A4PI$. The constant A4PI obviously should have been multipied by both terms in the expression for the daughter activity, not merely the last.

Certain other limitations of the code were also discovered as discussed below.

Region boundaries: Dose points should not lie on region boundaries. This can cause numerical instabilities. The number of regions and therefore the number of mesh points in the X-direction should be as large as possible (≤ 10) for reasonable accuracy.

Time considered: The number of times considered must be greater than one to get the integrated dose rate calculation.

Division by zero: The following values for input parameters or combinations thereof (consult CLOUD manual) result in division by zero, which is a fatal error on the CDC:

$$K_2 - K_i = 0, C_z = 0, X = 0, \lambda_D - \lambda_P = 0.$$

4.1. Test Cases

Two test cases were set up to check out the CLOUD version currently available. The first was a check of the integrated 2-hour whole body dose at the exclusion boundary of the Duke site following a maximum hypothetical accident. These hand calculations employed a "semi-infinite" cloud model whereby all energy generated in a cm^3 of air was assumed to be absorbed instantaneously. This assumption is overly conservative, and as expected the CLOUD result was roughly a factor of four smaller than the hand calculation. CLOUD yielded a 2-hour integrated dose of 0.41 Rem compared to the 1.47 Rem value from the hand calculation.

A second test case was set up in an effort to duplicate Nuclear Merchant Ship Reactor (NMSR) maximum credible accident calculations. These calculations employed a finite cloud model using Sutton's equation and an r-Z point source summation shielding code. Direct dose rates

Figure A-13. Direct Dose Rate From Sutton Plume Assuming 1 Curie/Second Release Rate per Isotope (^{133}Xe) — 700 m Cloud
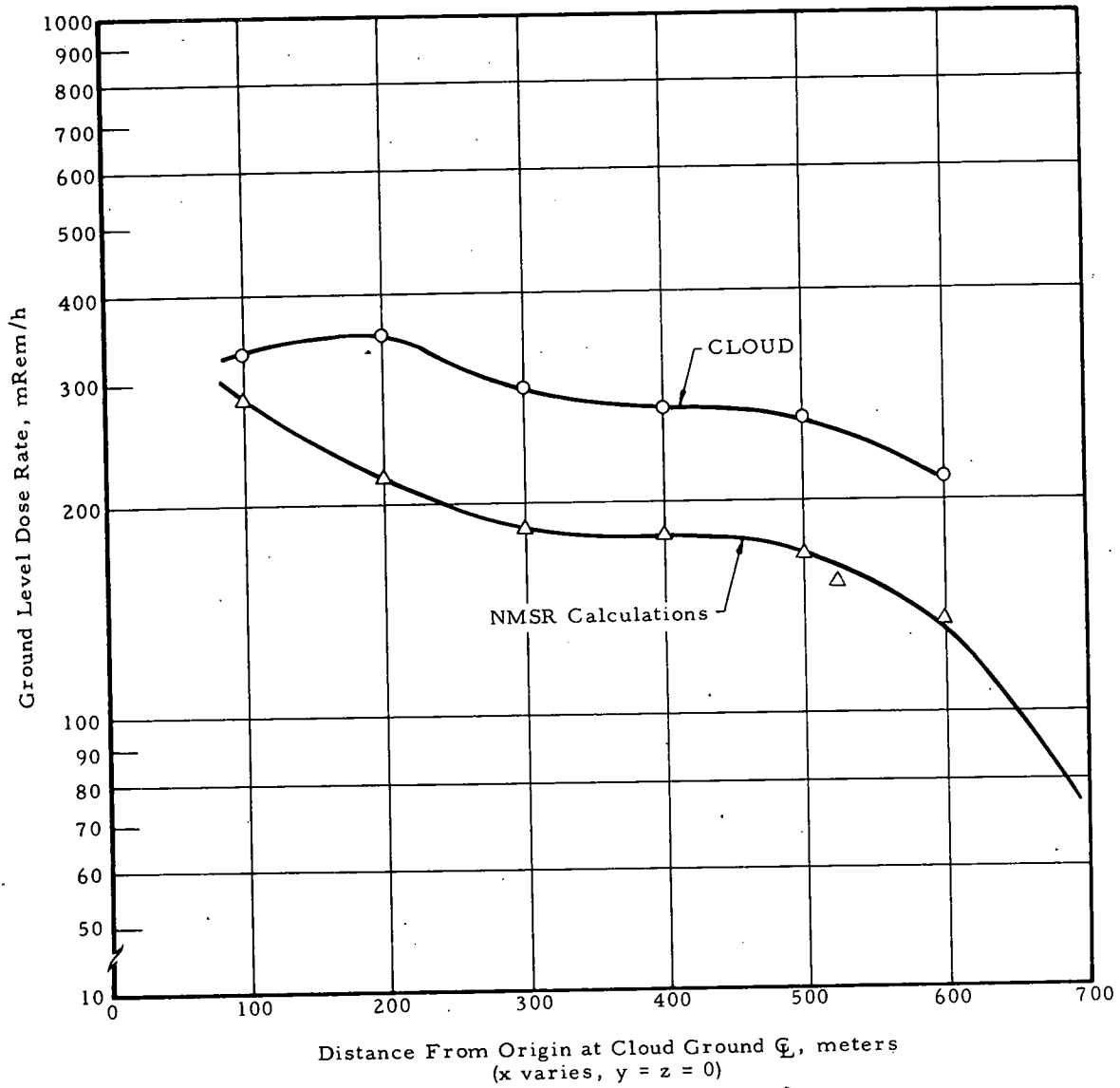
were calculated by isotope from a 700 M/plume of radioactive fission products. In the test case, the ^{133}Xe dose rate was calculated.

The CLOUD results are compared with the previous calculations in Figure A-13. Beyond 200 meters downwind, the shapes of the two curves are almost identical, the CLOUD results being 50 to 60% higher. The point at 100 meters is questionable although it is well known that the accuracy of Sutton's equation is marginal near the source. The overall agreement is considered to be within the limitations of the method, at least good enough to be reasonably certain that the code is working properly. The user should, however, acquaint himself with the limitations of the method for proper utilization of the code.

4.2. Auxiliary Programs

A digital computer program has been prepared for determining the space-time atmospheric concentration of radioactive materials resulting from continuous release of radioactive material from a ground level or elevated source. The code was written to aid in evaluating biological hazards associated with the inhalation of radioactive material released following major LMFBR accidents. The equations programmed are those available in the CLOUD code description in x, y, z, t coordinates. These equations were programmed since the desired functions are not available for output from the CLOUD code in the desired form.

The basic assumptions underlying the following equations and the derivations are discussed in detail in reference 12. Therefore the equations programmed are briefly discussed here. Basically, three functions are required to describe the time-dependent concentration of a radioisotope at a given space point. These are a source activity function describing the time-dependent activity of the source isotope, a leak function describing the rate of escape of the isotope from the containment, and a concentration function indicating the degradation of the isotopic density due to atmospheric dispersion. The latter two functions were programmed for the CDC-6600. The source activity function has not been programmed since it can be calculated by CLOUD, or more accurately, by BURP and RIBD. The leak function is $L(t - \frac{x}{u})$.

A one- or two-compartment release model is available. For a two-compartment release

$$L\left(t - \frac{x}{u}\right) = \frac{K_1 K_2}{K_2 - K_1} \left\{ \exp\left[-K_1\left(t - \frac{x}{u}\right)\right] - \exp\left[-K_2\left(t - \frac{x}{u}\right)\right] \right\}$$

and, for a one-compartment system,

$$L\left(t - \frac{x}{u}\right) + K_1 \exp -K_1\left(t - \frac{x}{u}\right)$$

where

$L\ t - \frac{x}{u}$ = release function of material located at x at a time t in a mean wind velocity u, s^{-1},

K_1, K_2 = compartment release constants, s^{-1},

x = downwind distance from source release point, m,

t = time after release, s,

u = mean wind velocity, m/s.

The concentration function is given by

$$\chi(x, y, z) = \exp - \frac{(y^2/C_y^2 \times \omega_2)}{(\Pi C_y C_z u \times \omega_1)} \exp - \frac{(z - h)^2}{(C_z^2 \times \omega_3)} + \exp - \frac{(z + h)^2}{(C_z^2 \times \omega_3)}$$

If a temperature inversion boundary is introduced that is to be of an impervious nature, and further, to act as a perfect reflector, a series of imaginary source points may be located along the z-axis to account for this additional effect. Using this technique or, more directly, using a one-dimensional solution to the wave equation, the concentration function becomes

$$\chi(x, y, z) = \exp \frac{\left[-y^2/C_y^2 \times \omega_2\right]}{\Pi C_y C_z u \times \omega_1} \left\{ \sum_{m=1}^{\infty} \exp\left[-\frac{(z - \Psi_m)^2}{C_z^2 \times \omega_3}\right] + \sum_{m=1}^{\infty} \exp\left[-\frac{(z + \Psi_m)^2}{C_z^2 \times \omega_3}\right] \right\}$$

where

$$\Psi_m = \left(m - \left| \sin \frac{(m-1)}{2}\Pi \right|\right)h + \left(m - \left| \sin \frac{m\Pi}{2} \right|\right)(H-h),$$

$H \equiv$ height of inversion lid above groud, m;

$h \equiv$ height of release above ground, m,

$n_y, n_z \equiv$ lateral and vertical stability parameters, respectively,

$$\omega_1 \equiv 2 - \frac{n_y + n_z}{2},$$

$$\omega_2 \equiv 2 - n_y,$$

$$\omega_3 \equiv 2 - n_z,$$

$C_y \equiv$ lateral diffusion coefficient, $(m)^{n_y}/2$,

$C_z \equiv$ vertical diffusion coefficeint, $(m)^{n_z}/2$.

Usually $m \leqq 10$ for good accuracy.

The mean wind speed, stability parameters and diffusion coefficients describe the meteorological conditions of the site. C_y and C_z can be further described by

$$C_y^2 = \frac{2\sigma_y^2}{x^{2-n_y}} \quad \text{and} \quad C_z^2 = \frac{2\sigma_z^2}{x^{2-n_z}}$$

where σ_y and σ_z are called the lateral and vertical dispersion coefficients, respectively. These coefficients vary with x and also with the meteorological condition. Pasquill and Meade have defined six meteorological conditions. For each of these conditions, plots are available for σ_v and σ_z versus x.

5. BANGO

The BANGO program was designed to automate the study of the cover-structure loading following a major meltdown accident in which molten fuel is released into the sodium. The computational model in its present form assumes several things:

1. All the molten fuel is released to and intimately mixed with the coolant in the same region of the core, so that the temperature of the fuel and the coolant is the same. This assumption eliminated the need

Figure A-14.   BANGO — Sodium-Fuel Pressure Relief
Program
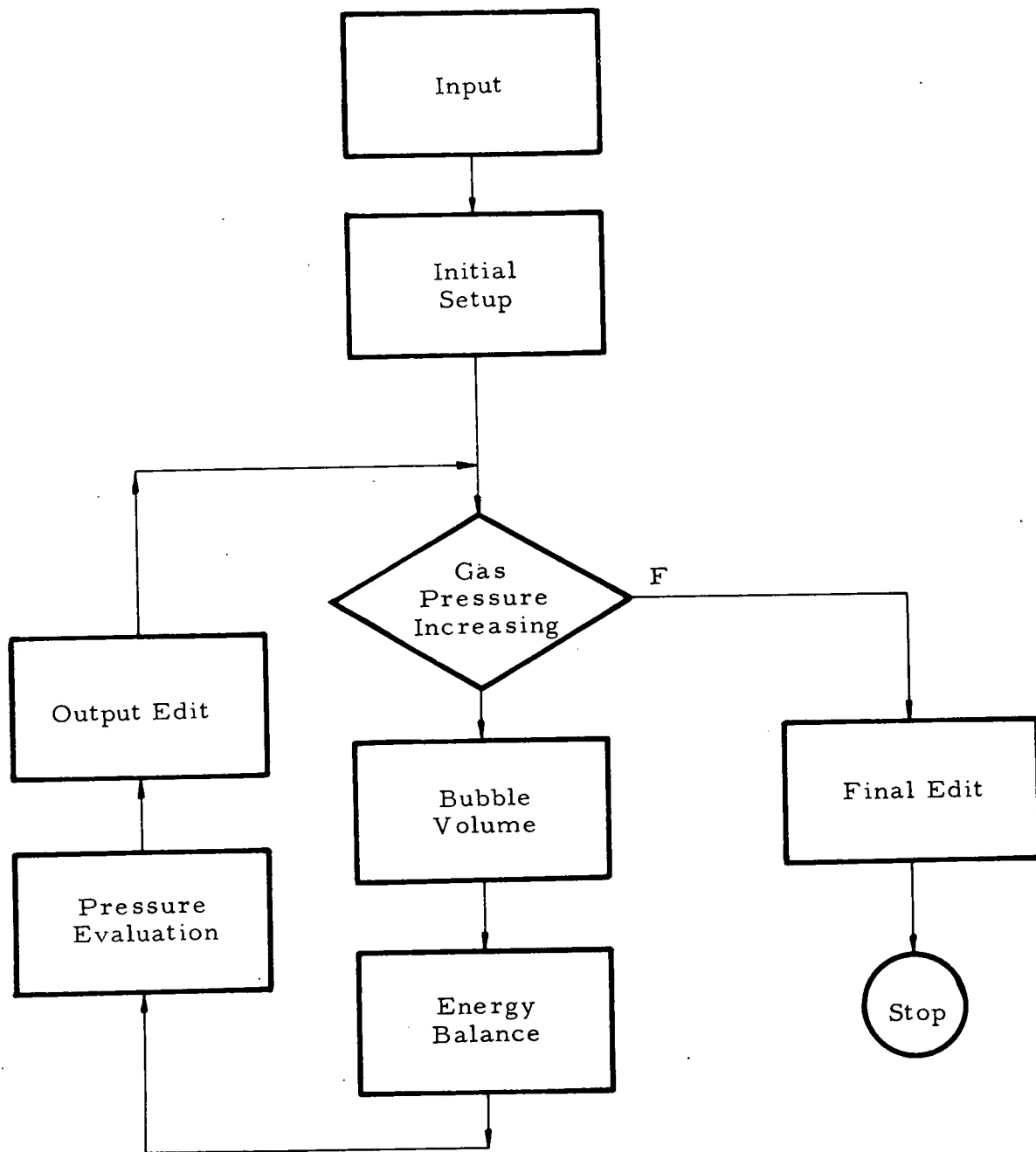
for heat transfer calculations from the dispersed fuel to the sodium. The pressure of the sodium is then evaluated from the specific energy and specific volume. Since the development of this model, information on the size of the resultant fuel particles has been released, permitting incorporation of the heat transfer mechanisms. This should be included for use on the present contract.

2. Sodium pressure is relieved by the upward acceleration of the column of sodium above the core. No credit is taken for the energy absorbed owing to deformation of the materials within the sodium pool.

3. The heat transfer from the sodium-fuel vapor bubble to the surrounding sodium is governed by

$$q = A\ 22,000\,(T - T_s) - 36,000$$

where
q = heat removal rate, Btu/h,

A = bubble surface area (assumes bubble to be spherical), ft^2,

T = sodium-fuel bubble temperature, F,

T_s = sodium pool temperature, F.

4. The gas above the core is compressed according to the ideal gas laws, using adiabatic compression. The calculations continue until this pressure in the gas space peaks.

The flow diagram for the computations is given in Figure A-14. The program should be upgraded to use the equation-of-state fit developed by B&W when it becomes available.

6. DEFLECT

6.1. Introduction

In most reactors the radial power distribution is such that the peak power exists near the center of the core and decreases radially outward. This nonuniform power distribution within the core will produce variations in component temperatures which lead to thermal bowing of the individual components. This tendency has been clearly demonstrated in EBR-I, where inward thermal bowing of fuel assemblies has

been shown to produce core reactivity insertions. In addition, fast flux damage to stainless steels has been found to lead to an additional volumetric expansion and will result in an irradiation-induced bow quite similar to that resulting from thermal effects.

Since any type of unintentional reactivity insertion is considered to be detrimental to reactor safety, mechanical means are generally included in the design to prevent or retard these deflections. This is done by placing various restraints, clamps, and support grids around the fuel assemblies. The design of these mechanisms is somewhat of a problem because of the length of the calculations involved; consequently, a computer code is generally used for analyses of this kind. In this particular case, where bowing of LMFBR hexagonal fuel assemblies is to be considered, it has been decided to use the methods originally developed for the ELBOW[13] code. This code, originally written by GGA for the HTGR, is of interest because it is one of the few that adequately consider thermal, irradiation-induced and creep-induced deflections. In addition, it considers the same basic type of core restraints used in the present LMFBR reference design, so that only minimum modification is required.

As written, the ELBOW code considers the case of a fuel element, orginally deflected as a result of temperature and irradiation effects, and its interactions with adjacent assemblies or supporting structures. The problem, then, is to determine assembly deflections, restraint forces, and the distribution of stresses within the assembly. The problem is restricted to an analysis of a given fuel element under reactor steady state conditions. The fuel element is considered to be a beam which deflects because of an unsymmetrical strain distribution and is restrained by forces imposed by the surroundings (assumed to be completely rigid). Any column loads imposed by the core holddown device are not considered. The only stresses to be considered are flexural (axial), which are calculated from simple beam theory. The stresses resulting from the symmetrical temperature and fast flux damage are ignored in this problem.

6.2. Methods

The DEFLECT code, which is similar to the ELBOW code[13] originally developed for the HTGR, contains modifications necessary to

adequately model the hexagonal fuel assemblies used in most advanced fast reactor concepts. Single-beam theory is used in the analysis, so that the assumptions of coplaner forces and relatively small deflections are implicit. Additionally, it is assumed that both Young's modulus and the creep strain are the same in both tension and compression.

The analysis incorporates a superposition technique in which the thermal and fast flux deflections are determined first. We then determine forces at the restraint points which will restore the element to the proper deflections at these points. The calculations are time dependent since the irradiation-induced bow is a function of exposure. Provisions are included to allow for clearances at the restraint points. This method involves an iterative procedure since the number and the direction of resultant forces are not immediately known. For example, in some cases a fuel assembly may deflect so that there is no contact between the support and the fuel assembly. In such a case the support is neglected, and the deflection curve will reflect the reduced number of support points.

6.2.1.   Unrestrained Deflections

The fuel element is modeled as a cantilever beam with constant cross section and coplaner forces. For the case of unrestrained deflection, the following equation is valid:

$$\frac{d^2 y_2}{dx} = \frac{\alpha(x) Tm(x)}{DF}$$

where
  DF = distance across flats of hexagon, in.,
  Tm = temperature moment, F,
  x = distance from cantilever support, in.,
  y = deflection of beam, in.,
  α = coefficient of thermal expansion, in./in.-°F,

$$Tm \equiv \frac{DE}{2I} \int_A TzdA.$$

The temperature moment is derived as follows: Assume a straight line function for the temperature distribution:

$$T = \left(\frac{TH - Tc}{DF}\right) z + \left(\frac{TH + Tc}{2}\right)$$

where
TH = hot side temperature, F,

Tc = cold side temperature, F,

z = distance from geometrical center of assembly (assumed positive in the hot side direction), in.

Then, substituting this temperature distribution into the generalized equation

$$
TM = \frac{DF}{\sqrt{3I}} \left\{ \int_0^{DF/2} (DF - z)\left[\left(\frac{TH - Tc}{DF}\right) z^2 + \left(\frac{TH + Tc}{2}\right) z\right] dz \right.
$$

$$
- \int_0^{DIF/2} (DIF - z)\left[\left(\frac{TH - Tc}{DF}\right) z^2 + \left(\frac{TH + Tc}{2}\right) z\right] dz
$$

$$
+ \int_{-DF/2}^{0} (DF + z)\left[\left(\frac{TH - Tc}{DF}\right) z^2 + \left(\frac{TH + Tc}{2}\right) z\right] dz
$$

$$
\left. - \int_{-DIF/2}^{0} (DIF + Z)\left[\left(\frac{TH - Tc}{DF}\right) z^2 + \left(\frac{TH + Tc}{2}\right) z\right] dz \right\}.
$$

Then intregrating, simplifying, and inserting constants,

$$
TM = \frac{5(TH - Tc)(DF^4 - DIF^4)}{96 \sqrt{3} \, DF}.
$$

The irradiation-induced deflection is also determined from basic beam equations. Assume that the neutron irradiation produces a bow in the assembly. Then, since in simple beam theory plane sections remain plane, the irradiation-induced growth is assumed to be linear:

$$
\Delta L = my = \left(\frac{\epsilon_H - \epsilon_c}{DF}\right) y.
$$

The geometrical relation can be obtained from

$$\frac{R}{dx} = \frac{R + y}{dx + my\ dx}.$$

Rearranging and simplifying,

$$\frac{1}{R} = m = \frac{\epsilon_H - \epsilon_c}{DF}.$$

Again, from basic beam theory

$$\frac{d^2y}{dx^{-2}} = -\frac{1}{R} = \frac{\epsilon_c - \epsilon_H}{DF}.$$

Intregrating and substituting the boundary conditions,

$$\textcircled{a}\ x = 0, y'(0) = y'(0),\ y = y(0),$$

the following equations are derived:

$$\frac{dy}{dx} = \frac{\epsilon_c - \epsilon_H}{DF} x + y'(0).$$

$$y = \left(\frac{\epsilon_c - \epsilon_H}{DF}\right)\frac{x^2}{2} + y'(0)x + y(0).$$

The linear expansion of stainless steel cladding is determined in accordance with data developed for the FFTF:

$$\frac{\Delta V}{V} = 5.0 \times 10^{-38}(\phi t)^{1.66}[\exp(-6800/RT) - 1.87 \times 10^4 \exp(-2700/RT)]$$

where
ϕ = neutron flux, n/cm^2-s,

t = time, s,

R = universal gas constant, cal/gmol-$^\circ$K,

T = temperature, K.

The change in length is found from

$$\frac{\Delta V}{V} = \frac{(L + \delta)^3 - L^3}{L^3} .$$

Multiplying through and neglecting higher order terms, the equation reduces to the form

$$\frac{\Delta V}{V} = \frac{3\epsilon}{L}$$

or

$$\epsilon = \frac{L}{3} \frac{\Delta V}{V} .$$

REFERENCES

[1] 1000-MWe LMFBR Follow-On Study, Babcock & Wilcox, BAW-1328, Vol 2, Lynchburg, Virginia (1968).

[2] Hansen, K. F., Koen, B. V., and Little, W. W., "Stable Numerical Solutions of the Reactor Kinetics Equations," Nucl. Sci. Engr., 22, 51-59 (1965).

[3] Andrews, J. B., II and Hansen, K. F., "Numerical Solution of the Time-Dependent Multigroup Diffusion Equations," Nucl. Sci. Engr., 31, 304-313 (1968).

[4] Birkhoff, C. and Kimes, T. F., CHIC Programs for Thermal Transients, Westinghouse, WAPD-TM-245 (1962).

[5] Wahle, H. W., Transient 1-Dimensional Thermal Model of an LMFBR Fuel Pin, Babcock & Wilcox, Alliance Research Center, ARC-4589, Alliance, Ohio (1969).

[6] 1000-MWe LMFBR Follow-On Study, Control Study, Babcock & Wilcox, BAW-1330, Lynchburg, Virginia (1968).

[7] Cohen, S. C. and Koch, P. K., GANDY — A Computer Program for the Evaluation of Effective Cross Sections in the Unresolved Resonance Region, GA-8003, General Atomic (1967).

[8] Helholtz, J. and Roy, D. H., STRIP — Resonance Absorption Program Treating Overlap and Interference, Babcock & Wilcox, TP-332, Lynchburg, Virginia (1967).

[9] Roy, D. H., et al., FARED: A One-Dimensional Fast Reactor Physics Design and Analysis Code, Babcock & Wilcox, BAW-3867-9, Vol 1, Lynchburg, Virginia (1969).

[10] Pearlstein, S., CSEWG Newsletter 18, March 1969.

11 Leonard, B. P., "Hazard Associated With Fission Product Release, International Conf. on Peaceful Uses of Atomic Energy," A/Conf., 15/P/428, June 1958.

12 Duncan, D. S., et al., CLOUD — An IBM 709 Program for Computing Gamma-Ray Dose Rate From a Radioactive Cloud, Atomics International, NAA-SR-MEMO-4822, June 1959.

13 Katz, R., Gerber, M. J., and Hamrick, J. R., ELBOW, Fuel Element Bowing Code, GAMD-6334 (to be released).

ARGONNE ·NATIONAL· LABORATORY

February 19, 1971

PRO:K:029

Mr. Robert L. Shannon, Director
Division of Technical Information Extension
U.S. Atomic Energy Commission
P.O. Box 62
Oak Ridge, Tennessee   27830

> Subject: 1000-MWe LMFBR Safety Studies –
> Publication of Babcock & Wilcox Topical Reports

> Reference: Letter, L. W. Fromm to R. L. Shannon, "1000-MWe LMFBR
> Safety Studies – Publication of Contractors' Phase and
> Topical Reports," October 16, 1970

Dear Mr. Shannon:

    In the reference letter I advised you that we would be transmitting
to you for publication a total of twelve Babcock & Wilcox Company Phase and
Topical Reports, and possibly three reports from other contractors, generated
under the AEC-sponsored 1000-MWe LMFBR Safety Analysis Studies program.
With that letter I enclosed one B&W report (BAW-1344, which you have since
published), and advised that the remainder would be transmitted to you for
publication when received and patent-cleared.

    I am enclosing herewith one copy of each of the eight B&W Topical Reports
listed below, all of which are now patent-cleared and ready for publication.
The covers for these reports should be that used for the previously-issued
BAW-1344, except for the changes noted in the table below. The letters
heading   the columns of the table are keyed to the markings on the attached
xerox copy of the cover for BAW-1344.

OK
pwR
2.-25-71

"A"	"B"	"C"
BAW-1342	TOPICAL REPORT	Accident Analysis Methods
BAW-1349	TOPICAL REPORT	Candidate Secondary Containment Support Systems
BAW-1350	TOPICAL REPORT	Accident Initiating Conditions Part 1 - Flow Abnormalities
BAW-1351	TOPICAL REPORT	Candidate Emergency Decay Heat Removal Systems
BAW-1352	TOPICAL REPORT	Candidate Primary Containment Safety Features
BAW-1354	TOPICAL REPORT	Candidate Protective Features
BAW-1355	TOPICAL REPORT	Effects of Irradiation-Induced Metal Swelling on the Reference Design
BAW-1360	TOPICAL REPORT	Accident Initiating Conditions Part 2 - Reactivity Insertions

All other parts of the front covers for these reports should remain the same as the cover for BAW-1344.

Binding edge captions for the reports should read:

BAW-1342	1000-MWe LMFBR Safety Studies	B&W	Acc. Anal. Methods	USAEC
BAW-1349	1000-MWe LMFBR Safety Studies	B&W	Sec. Containment	USAEC
BAW-1350	1000-MWe LMFBR Safety Studies	B&W	Init. Cond. - 1. Flow	USAEC
BAW-1351	1000-MWe LMFBR Safety Studies	B&W	Decay Heat Removal	USAEC
BAW-1352	1000-MWe LMFBR Safety Studies	B&W	Pri. Containment	USAEC
BAW-1354	1000-MWe LMFBR Safety Studies	B&W	Protective Features	USAEC
BAW-1355	1000-MWe LMFBR Safety Studies	B&W	Eff. of Metal Swelling	USAEC
BAW-1360	1000-MWe LMFBR Safety Studies	B&W	Init. Cond. - 2. Reactivity	USAEC

I note that for BAW-1344 you used a two-piece cover with staple binding, and the "binding edge caption" actually appeared on the back of the report. If this is to be the case with the reports enclosed, then the binding edge captions may be omitted. However, if any of the reports will actually have binding edges upon which printing can appear (and be visible with the reports on a library shelf), then the above captions should be used.

The distribution of all of these reports should be our "Distribution A" plus Category UC-80, Reactor Technology, as before. For your convenience I am enclosing another copy of the "Distribution A" list previously supplied to you.

In the reference letter I stated that there would be twelve B&W reports, and possibly three from other contractors. This has now been revised downward to eleven B&W reports and one report from Atomics International. The single remaining B&W report and the AI report will be transmitted to you when received and patent-cleared.

Thank you again for your excellent cooperation in publishing these reports. If there are any questions, please contact me on FTS extension 312/739-2971 or 312/739-4844.

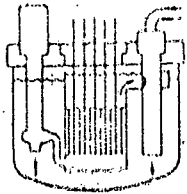Very truly yours,

L. W. Fromm, Manager
1000-MWe Studies
LMFBR Program Office

LWF:el
encls.

cc: (w/o encl.)
     AEC-RDT: Director
                Asst. Dir. for Project Mgt.
                Chief, Liquid Metal Proj. Br.
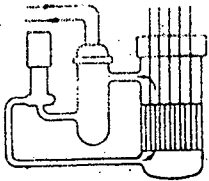   LMFBR Program Manager
                Sr. Site Representative - ANL

     Manager, AEC-CH
     Director, LMFBR Program Office - ANL (2 copies)
     R. C. Dreyer, DTIE
     C. R. Bruce, DTIE
     P. W. Rosser, DTIE

1000 MWe
L M F B R
Liquid Metal Fast Breeder Reactor
SAFETY ANALYSIS STUDIES

BABCOCK & WILCOX

Accident Analysis and Safety System Design Study

PHASE I REPORT "B"

Fault Trees and Malfunction Catalog "C"

Prepared for ARGONNE NATIONAL LABORATORY

DISTRIBUTION "A"

(1 copy to each addressee unless otherwise noted)

Division of Reactor Development and Technology.
U. S. Atomic Energy Commission
Washington, D. C. 20545

Milton Shaw, Director
Assistant Director for Project Management
Chief, Liquid Metal Projects Branch (2 copies)
LMFBR Program Manager
Assistant Director for Plant Engineering
Chief, Applications and Facilities Branch
Chief, Components Branch
Chief, Systems Engineering Branch
Assistant Director for Reactor Engineering (2 copies)
Chief, Core Design Branch
Chief, Fuel Handling Branch
Assistant Director for Reactor Technology
Assistant Director for Nuclear Safety
Assistant Director for Program Analysis
Project Manager, FFTF

Director, LMFBR Program Office - ANL (2 copies)
Argonne National Laboratory
9700 South Cass Avenue
Argonne, Illinois 60439

Office of Senior RDT Site Rep. - AI
U. S. Atomic Energy Commission
P. O. Box 309
Canoga Park, California 91304

Office of Senior RDT Site Rep. - APDA
U. S. Atomic Energy Commission
1911 First Street
Detroit, Michigan 48226

Office of Senior RDT Site Rep. - GE
U. S. Atomic Energy Commission
310 DeGuigne Drive
Sunnyvale, California 94086

Office of Senior RDT Site Rep. - PNL
U. S. Atomic Energy Commission
Federal Building
Richland, Washington 99352

Office of Senior RDT Site Rep. - ID
U. S. Atomic Energy Commission
P. O. Box 2108
Idaho Falls, Idaho 83401

Office of Senior RDT Site Rep. - GGA
U. S. Atomic Energy Commission
P. O. Box 2325
San Diego, California 92112

Office of Senior RDT Site Rep. - ORNL
U. S. Atomic Energy Commission
P. O. Box X
Oak Ridge, Tennessee 37830

Office of RDT Site Rep. - CE
U. S. Atomic Energy Commission
P. O. Box 500
Windsor, Connecticut 06095

Office of RDT Site Rep. - UNC
U. S. Atomic Energy Commission
Grasslands Road
Elmsford, New York 10523

Reactor Systems and Performance Branch
Division of Reactor Standards - BETH - 010
U. S. Atomic Energy Commission
Washington, D. C. 20545

Atten: Mr. C. L. Allen

Division of Reactor Licensing - BETH - 010
U. S. Atomic Energy Commission
Washington, D. C. 20545
Atten: Dr. P. Morris, Director (1 copy)
         Mr. S. Levine (1 copy)

Chief, Foreign Activities Staff
Office of Assistant General Manager for Reactors
U. S. Atomic Energy Commission
Washington, D. C. 20545

Mr. Carl R. Malmstrom
U. S. Atomic Energy Commission
Scientific Representative - London
American Embassy Box 40
F.P.O., New York 09510

Mr. Joseph DiNunno
U. S. Atomic Energy Commission
Scientific Representative - Paris
American Embassy
A.P.O., New York 09777

Mr. Dickson B. Hoyle
U. S. Atomic Energy Commission
Senior Scientific Representative
U. S. Mission to the European Communities
U. S. Embassy
A.P.O., New York 09667

Dr. William H. Hanum
Fast Reactor Physics Division
Atomic Energy Establishment, Winfrith
Dorchester, Dorset, England

Mr. Robert E. Macherey
Metallurgical Specialist
Fast Reactor Fuels
Gesellschaft fur Kernforschung M.B.H.
Postfache 947
75 Karlsruhe, Germany

Dr. Stanley J. Stachura
Commissariat a l' Energie Atomique
Centre d' Etudes Nucleaires de Cadarache
Boite Postale 1
St. Paul Les Durance (B. Du. Rh.), France

Brookhaven National Laboratory
Upton, New York 11973
Attn: M. Goldhaber, Director (2 copies)

Los Alamos Scientific Laboratory
Post Office Box 1663
Los Alamos, New Mexico 87544
Attn: Dr. David B. Hall (2 copies)

Oak Ridge National Laboratory
Union Carbide Corporation
AEC Operations - Post Office Box X
Oak Ridge, Tennessee 37831
Attn: Dr. Floyd L. Culler (2 copies)

Oak Ridge National Laboratory
Building 9201-2, Y-12
Post Office Box Y
Oak Ridge, Tennessee 37830
Attn: Mr. R. E. MacPherson, Jr.

Atomics International
A Division of North American Rockwell Corporation
Post Office Box 309
Canoga Park, California 91304
Attn: Mr. J. J. Flaherty, President

Liquid Metal Engineering Center
P. O. Box 1449
Canoga Park, California 91304
Attn: Mr. R. W. Dickinson, Director (3 copies)

General Electric Company
Advanced Products Operation
310 DeGuigne Drive
Sunnyvale, California 94086
Attn: Mr. Karl P. Cohen, Manager (3 copies)

Pacific Northwest Laboratory
Battelle Memorial Institute
Post Office Box 999
Richland, Washington 99352
Attn: Dr. F. W. Albaugh, Director (1 copy)
       Dr. E. R. Astley, Project Mgr., FFTF (4 copies)

Westinghouse Electric Corporation
Advanced Reactors Division
Waltz Mill Site - P.O. Box 158
Madison, Pennsylvania 15663
Attn: Dr. J.C.R. Kelly, Jr., General Manager (2 copies)

Combustion Engineering, Inc.
Nuclear Power Department
P.O. Box 500
Windsor, Connecticut 06095
Attn: Dr. Walter H. Zinn (2 copies)

MSA Research Corporation
Callory, Pennsylvania 14024
Attn: Mr. C. H. Staub, Director, Marketing Division

Atomic Power Development Associates, Inc.
1911 First Street
Detroit, Michigan 48226
Attn: Mr. Alton P. Donnell, General Manager (2 copies)

Power Reactor Development Company
1911 First Street
Detroit, Michigan 48226
Attn: Mr. Arthur S. Griswold, General Manager

United Nuclear Corporation
Post Office Box 1583
365 Winchester Avenue
New Haven, Connecticut 06511
Attn: Dr. A. Strasser (1 copy)
       Dr. K. Goldman (1 copy)

The Babcock & Wilcox Company
Atomic Energy Division
Technical Library
5061 Fort Avenue - P.O. Box 1260
Lynchburg, Virginia 24505
Attn: Mr. S. H. Esleeck (3 copies)

General Atomics
Division of General Dynamics Corporation
Post Office Box 608
San Diego, California 92115
Attn: Dr. Frederic de Hoffmann

Nuclear Materials & Equipment Corporation
Apollo, Pennsylvania 15613
Attn: Dr. Z. M. Shapiro, President

Baldwin-Lima-Hamilton Corporation
Industrial Equipment Division
Eddystone, Pennsylvania 19013
Attn: Mr. John Gaydos, Senior Engineer (1 copy)
       Mr. R. A. Tidball (1 copy)

M. W. Kellogg Company
711 Third Avenue
New York, New York 10017
Attn: Mr. D. W. Jesser, Vice President of Engineering

Southwest Atomic Energy Associates
Post Office Box 1106
Shreveport, Louisiana 71102
Attn: Mr. J. Robert Welsh, President

U. S. Atomic Energy Commission
Technical Information Extension
Post Office Box E
Oak Ridge, Tennessee 37830
Attn: Mr. Robert L. Shannon, Manager (3 copies)

Professor W. Haefele
Kernforschungszentrum Karlsruhe
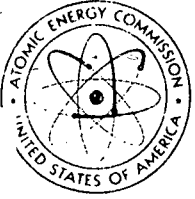7500 Karlsruhe, Germany (10 copies)

Mr. C. Vendryes
CEN Saclay
Boite Postale 2
Gif-Sur-Yvette (S at O), France (10 copies)

Mr. A. deStordeur
Euratom
53 Rue Belliard
Brussels 4, Belgium (10 copies)

Dott, Ing. F. Pierantoni
CNEN
Via Mazzini 2
Bologna, Italy (4 copies)

United Kingdom Atomic Energy Authority
Reactor Group Headquarters
Kisley, Warrington; Lancashire
England
Attn: Mr. Robin Nicholson, Head of Commercial and Overseas
                           Relations Dept. (12 copies)

Argonne National Laboratory
9700 S. Cass Avenue
Argonne, Illinois 60439
Attn: Mr. L. W. Fromm (40 copies)

In Reply Refer To: TDD:PWR   October 20, 1970

Files

PROCESSING OF 1000-MWe LMFBR SAFETY STUDIES

We have been asked by L. W. Fromm, Manager, 1000-MWe
Studies LMFBR Program Office, ANL, to print and dis-
tribute subject reports as a logical continuation of
our involvement in the Follow-on Study Program.
A total of 12 reports have been generated by BAW.
There may also be a single report from each of 3
contractors, AI, GE and Westinghouse. Each report
will be cleared for publication before being sent to
DTIE.

Distribution is to be as follows:

UC-80	- 225	copies
NTIS	- 25	extra cys.
Stock	- 50	copies
1000 MWe Dist.	- 165	copies
	465	copies

Phillip W. Rosser

cc: Dreyer
     Masters (12)